Modelling *Chlamydia* infection of the cardiovascular system and the gastrointestinal tract

Ph.D. Thesis

Ildikó Ilona Lantos

Supervisor: Valéria Endrész Ph.D.

Department of Medical Microbiology and Immunobiology

Faculty of Medicine

University of Szeged

Szeged

2018

Publications related to the subject of the Thesis:

I. **Lantos I**, Endrész V, Virok DP, Szabó A, Lu X, Mosolygó T, Burián K: *Chlamydia pneumoniae* infection exacerbates atherosclerosis in ApoB100only/LDLR$^{-/-}$ mouse strain Biomed Res Int. 2018, Article ID 8325915
Impact factor: 2.476

II. **Lantos I**, Virok DP, Mosolygó T, Rázga Z, Burián K, Endrész V: Growth characteristics of *Chlamydia trachomatis* in human intestinal epithelial Caco-2 cells
Pathog Dis. 2018 April 1;76(3)
Impact factor: 2.337

Publications not related to the subject of the Thesis:

I. Bogdanov A, Janovák L, **Lantos I**, Endrész V, Sebők D, Szabó T, Dékány I, Deák J, Rázga Z, Burián K, Virok DP: Non-Activated Titanium-Dioxide Nanoparticles Promote the Growth of *Chlamydia trachomatis* and Decrease the Antimicrobial Activity of Silver Nanoparticles. J Appl Microbiol. 2017 November 123(5):1335-1345
Impact factor: 2.099

II. Eszik I, **Lantos I**, Önder K, Somogyvári F, Burián K, Endrész V, Virok DP: High dynamic range detection of *Chlamydia trachomatis* growth by direct quantitative PCR of the infected cells. J Microbiol Methods. 2016 January;120:15-22.
Impact factor: 1.790

III. Xia M, Chen D, Endresz V, **Lantos I**, Szabo A, Kakkar V, Lu X: Modulation of recombinant antigenic constructs containing multi-epitopes towards effective reduction of atherosclerotic lesion in B6;129S-Ldlr^{tm1Her}Apob^{tm2Sgy}/J mice. *PLOS ONE* 2015 April 1;10(4):e0123393.
Impact factor: 3.534

IV. Bogdanov A, Endrész V, Urbán S, **Lantos I**, Deák J, Burián K, Önder K, Ayaydin F, Balázs P, Virok DP: Application of DNA chip scanning technology for automatic detection of *Chlamydia trachomatis* and *Chlamydia pneumoniae* inclusions. Antimicrob Agents Chemother. 2014;58(1):405-13.
Impact factor: 4.48

Abstracts related to the Thesis

1. **Lantos I**, Mosolygó T, Virók DP, Burián K, Endrész V: *Chlamydophila pneumoniae* infection accelerates atherosclerosis development in "ApoB100only/LDLR$^{-/-}$" and ApoE$^{-/-}$ mouse strains in different manner. A Magyar Mikrobiológiai Társaság 2014. évi Nagygyűlése és EU FP7 PROMISE Regional Meeting: Absztrakt füzet. 82 p. Keszthely, Magyarország, 2014.10.15 -17. Magyar Mikrobiológiai Társaság, p. 37

2. **Lantos I**, Eszik I, Virok DP, Mosolygó T, Burián K, Endrész V: Intestinal Caco-2 cells support chlamydia replication and produce Human Beta-Defensin-2. 17th International Congress Of The Hungarian Society For Microbiology Eötvös Loránd University Convention Centre, Budapest, Hungary 8-10 July, 2015

3. Eszik I, **Lantos I**, Somogyvári F, Önder K, Burián K, Endrész V and Virók DP: Development of a QPCR based method for the quantitative measurement of *Chlamydia trachomatis* growth. 17th International Congress of the Hungarian Society for Microbiology Eötvös Loránd University Convention Centre, Budapest, Hungary 8-10 July, 2015

Abstracts not related to the Thesis:

1. **Lantos I**, Bogdanov A, Endrész V, Urbán Sz, Deák J, Burián K, Önder K, Balázs P, Virók DP: Application of DNA chip scanning technology for the automatic detection of *Chlamydia trachomatis* and *Chlamydia pneumoniae* inclusions. Acta Microbiologica et Immunologica Hungarica 60:(Suppl. 1.) pp. 173-174. (2013) 4th Central European Forum for Microbiology. Keszthely, Magyarország: 2013.10.16-18.

2. Burián K, Eszik I, **Lantos I**, Bogdanov A, Endrész V and Virók DP: Impact of interferon-gamma on the gene expression of human epithelial cells. 17th International Congress of the Hungarian Society for Microbiology Eötvös Loránd University Convention Centre, Budapest, Hungary 8-10 July, 2015

3. Burián K, Mosolygó T, Boros É, Bogdanov A, Nagymihály M, Horváth B, Endrész V, **Lantos I**, Kondorosi É, Virók DP and István Nagy: Impact of *Chlamydia trachomatis* infection and interferon-gamma treatment on the human polymorphonuclear leukocyte transcriptome 17TH International Congress of the Hungarian Society for Microbiology Eötvös Loránd University Convention Centre, Budapest, Hungary 8-10 July, 2015

4. Varga-Bogdanov A, Ildikó **Lantos I**, Eszik I, Balázs P, Deák J, Burián K, Endrész V and Virók DP: Detection of *Chlamydia trachomatis* attachment to epithelial cells by the chlamycount software using images produced by a DNA-chip scanner. 17th International Congress of the Hungarian Society for Microbiology Eötvös Loránd University Convention Centre, Budapest, Hungary 8-10 July, 2015

5. Kovács N, **Lantos I**, Endrész V, Berkecz R: Lipidomic approach to identify patterns in phospholipid profiles in atherosclerosis in ApoE deficient mice infected with *Chlamydia*

pneumoniae. 21st International Symposium On Analytical And Environmental Problems, University of Szeged, Department of Inorganic and Analytical Chemistry Szeged, Hungary September 28, 2015

6. Xia M, Endresz V, **Lantos I**, Szabo A, Mundkur L, Kakkar V and Lu X: Adoptive transfer of antigen-induced specific regulatory T cells (TREG) protects against atherosclerotic lesion formation in B6;129S-Ldlr$^{(tm1her)}$Apob$^{(tm2sgy)}$/J mice. XXV. Congress of the International Society on Thrombosis and Haemostasis, Toronto, Canada June 20–25, 2015

7. Xia M, Endresz V, Chen D, **Lantos I**, Szabo A, Mundkur L, Kakkar V and Lu X: Modulation of recombinant antigenic constructs containing multi-epitopes towards effective reduction of atherosclerotic lesion in B6;129S-LDLR$^{(tm1Her)}$Apob$^{(tm2Sgy)}$/J mice. XXV. Congress of the International Society on Thrombosis and Haemostasis, Toronto, Canada June 20–25, 2015

8. Xia M, Endresz V, **Lantos I**, Szabo A, Mundkur L, Kakkar V and Lu X: Swapping over two peptide epitopes derived from APOB and C5AR located at terminuses of recombinant proteins maintains the similar effective reduction on atherosclerotic lesion in B6;129S-LDLR$^{(tm1Her)}$Apob$^{(tm2Sgy)}$/J mice. XXV. Congress of the International Society on Thrombosis and Haemostasis, Toronto, Canada June 20–25, 2015

9. Xia M, Chen D, Endresz V, **Lantos I**, Szabo A, Mundkur L, Kakkar V and Lu X: Two peptide epitopes derived from human and mycobacterium, respectively, reduce atherosclerotic lesion in B6;129S-LDLR$^{(tm1Her)}$ Apob$^{(tm2Sgy)}$/J mice. XXV. Congress of the International Society on Thrombosis and Haemostasis, Toronto, Canada June 20–25, 2015

10. Burián K, Mosolygó T, **Lantos I**, Rafai T, Bogdanov A, Klivényi P, Endrész V, Virók DP: A *Chlamydia muridarum* fertőzés, ellentétben a korábbi in vitro kísérletek eredményeivel, indukálja az indolamin2,3-dioxigenáz termelését balb/c egerek tüdejében. A Magyar Mikrobiológiai Társaság Nagygyűlése és a XII. Fermentációs Kollokvium 2016. október 19-21. Helikon Hotel, Keszthely

Table of contents

Abbreviations

ApoE	apolipoprotein E
ApoB	apolipoprotein B
ATCC	American Type Culture Collection
bp	base pair
BSA	bovine serum albumin
cDNA	complementary DNA
Cpn	*Chlamydia pneumoniae*
C. trachomatis	*Chlamydia trachomatis*
cHsp60	chlamydial heat-shock protein 60
DNA	deoxyribonucleic acid
EB	elementary body
ELISA	enzyme linked immunosorbent assay
FITC	fluorescein isothiocyanate
GI	gastrointestinal tract
hBD-2	human beta defensin-2
HDL	high density lipoprotein
HNPs	human neutrophil peptides
IBD	irritable bowel disease
IFU	inclusion forming unit
IFN-γ	interferon-gamma
IL-1,	interleukin-1,
iNOS	inducible nitric oxide synthase
HDL	high density lipoprotein
LDL	low density lipoprotein

LOX-1	lectin-like ox-LDL receptor
LPS	lipopolysaccharide
MMP	matrix metalloproteinase
MOI	multiplicity of infection
MOMP	major outer membrane protein
PBS	phosphate buffered saline
PBMC	peripheral blood mononuclear cell
PCR	polymerase chain reaction
PID	pelvic inflammatory disease
RB	reticulate body
RT-PCR	real-time reverse transcription PCR
SPG	sucrose phosphate glutamic acid buffer
TLR	toll-like receptor
TNF-α	tumour necrosis factor-α

1. Introduction

1.1. *Chlamydiaceae*

Chlamydiaceae family comprises *Chlamydia* genus with eleven species [1] of which two are primarily human pathogens: *C. trachomatis* and *C. pneumoniae* [2]. The other species infect animals: *C. psittaci*, *C. abortus*, *C. felis*, *C. pecorum*, *C. suis*, *C. muridarum*, *C. caviae*, *C. avium* and *C. gallinacea*. *C. psittaci*, *C. abortus* and *C. felis* are occasionally transmitted to man [3]. Chlamydiae are Gram-negative obligate intracellular bacteria [4]. The developmental cycle of these pathogens is specific, unique and different from that of other bacteria in which the organism is present in two main forms. The elementary body (EB) is the extracellular infectious form of the bacterium, responsible for attaching to the target host cell and promoting its entry. The reticulate body (RB) is the larger, intracellular, metabolically active form of the organism that divides by binary fission. There is a third form which is larger than the size of an RB and is called atypical or aberrant body [5]. This altered developmental form is also named as a persistent body which is viable but non-culturable and is produced in response to stressful conditions.

The EB is the small, metabolically inactive, infectious and dense form. It has a rigid cell wall conferred by extensive disulphide cross-linking of the major outer membrane protein (MOMP) and cysteine-rich proteins, including OmcB, and OmcA [6]. They can survive outside the host cell for a limited time and then attach to and enter a new host cell. Inside the host cell, *Chlamydia* EB differentiates into RB. RBs are larger, metabolically active non-infectious less-rigid, extracellularly labile forms that do not survive outside the host cell [5]. The RB divide by binary fission within the expanding endosome that becomes visible as a microcolony referred to as the chlamydial inclusion. After a period of 36 or 72 hours, the RB reorganizes and condenses to form the infectious EB. The life cycle is complete when host cell lysis by chlamydiae or extrusion without lysis occurs, allowing the EBs to initiate a new infectious cycle [7].

The chlamydial developmental cycle is regulated at the transcriptional level [8]. There are three main stages of chlamydial gene expression, including early, mid and late gene expression [9]. Transcription begins within the differentiating EB almost immediately following internalization. Early genes are transcribed within 3 h of EB entry. One of the first early genes is the “early upstream open reading frame” (*euo)* [6] which regulates the late gene

expression and delays RB-to-EB conversion until after there has been sufficient RB replication [10]. Midcycle genes are involved in RB growth and replication. At this stage several groups of genes are expressed: genes whose products represent a variety of functions, for example cell envelope biogenesis components, energy metabolism, type III secretion system, protein folding including chaperonin *groEL,* one of the three heat-shock proteins of chlamydiae and genes responsible for DNA replication, repair and recombination [8]. Late genes are first transcribed and upregulated towards the end of the developmental cycle. Many late genes are involved in RB-to-EB conversion and EB function [8]. In the persistent phase of the chlamydial developmental cycle altered gene expression patterns were observed [11]. Tryptophan utilization, DNA repair and recombination, phospholipid utilization, protein translation, and general stress genes were up-regulated during persistence [12]. The persistent form of *Chlamydia* was induced by interferon-gamma (IFN-γ) [13], β-lactam antibiotics [14, 15], iron depletion [16] and in different cell types e. g. *C. trachomatis* becomes persistent in monocytes [17]. Persistent *Chlamydia* infection is serovar specific and manifests cell specific features [18].

1.1.1. *Chlamydia pneumoniae*

Chlamydia pneumoniae (*Cpn*) is a common respiratory pathogen for humans; it infects the respiratory tract, causes pharyngitis, sinusitis, acute or chronic bronchitis, exacerbations of chronic bronchitis and is a significant cause of community-acquired pneumonia [19]. *Cpn* infection is ubiquitous, with 50% of individuals seropositive by 20 years of age and approximately 80% in the elderly [20]. Chronic-persistent infections and reinfections are frequent [5]. In the past 30 years, a wide spectrum of extrapulmonary diseases has been linked to *Cpn*. Several studies documented the association of *Cpn* infection with asthma [21]. Evidence on the role of *Cpn* in the pathogenesis of asthma has been achieved by polymerase chain reaction (PCR), serological tests and by preliminary treatment trials [22]. Further diseases linked to *Cpn* are multiple sclerosis [23], age-related macular degeneration [24], Alzheimer's disease [25], chronic fatigue syndrome [26], and chronic skin ulcers [27]. However, the causative role of *Cpn* infection in these diseases has not been confirmed.

Numerous studies have demonstrated an association between *Cpn* infection and atherosclerosis [28–32].

1.2. Atherosclerosis

Atherosclerosis is one of the most frequent causes of death and morbidity in the world; it is the underlying cause of cardiovascular diseases as myocardial infarction, cerebrovascular accidents or peripheral vascular disease [33]. Atherosclerosis is a chronic disease with chronic inflammation, endothelial dysfunction and lipid accumulation in the vasculature [34]. There are several well-known atherosclerosis risk factors, such as diabetes mellitus [35], smoking [36], hypertension [37], hyperlipidaemia [38], hypercholesterolemia [39], abdominal obesity [40]. The knowledge about the contributory mechanisms of atherosclerosis development is incomplete [41]. Atherosclerosis begins in the early childhood with the appearance of aortic fatty streaks and development of fibrous plaques begins in the 20s [42, 43]. The central pathogenic event that promotes atherosclerotic lesion formation is a subendothelial retention and modification of low density lipoprotein (LDL) particles and subsequent accumulation of LDL-derived lipids in the intima [44]. LDL can be modified by oxidation and aggregation and this modified LDL and oxidized lipid moieties deriving from them, in turn act as chronic stimulators of the innate (monocyte/macrophage) and adaptive immune (dendritic cell, T-lymphocyte) response [41]. The damage to the endothelium of the arteries is the primary cause of initiation of the development of atherosclerosis and also stimulates monocytes to secrete pro-inflammatory cytokines [45]. High plasma LDL cholesterol concentrations, especially oxidized LDL contributes to the formation of the atherosclerotic lesion [46]. The endothelial injury leads to platelet aggregation and release of platelet factors which trigger the proliferation of smooth muscle cells in the arterial intima [47]. Several epidemiological studies have provided evidence that high high density lipoprotein (HDL)-cholesterol levels reduce the risk of atherosclerosis regardless of LDL levels. HDL remove cholesterol from the vasculature and deliver it to the liver for disposal in a process commonly referred to as reverse cholesterol transport [44].

The classical risk factors of atherosclerosis are responsible for up to 90% of cases of atherosclerosis-related morbidity. Other risk factors like infection may contribute to the disease development [28].

Several infectious agents (viruses [48], bacteria [49], and parasites [50]) have been associated with the risk of atherosclerosis. The first experimental evidence for contribution of infectious agents to atherosclerosis was that the Marek's disease virus (MDV), a chicken herpes virus, could induce atherosclerosis in chicken and vaccination prior to challenge prevented this

induction [51]. A wide range of pathogens have been identified by nucleic acid or antigen detection methods in human atherosclerotic plaques [52]. Bacterial pathogens found in atherosclerotic lesions are *Cpn* [53], *Mycoplasma pneumoniae* [54], *Helicobacter pylori* [55], *Enterobacter hormaechei* [56], and multiple periodontal organisms (e.g., *Porphyromonas gingivalis*) [57, 58]. Viral pathogens implicated in atherosclerosis development are cytomegalovirus [59], hepatitis C virus [60], human immunodeficiency virus [61], herpes simplex viruses [62], Epstein-Barr virus [63], enteroviruses [64], and parvovirus [65]. Only *Cpn* and *E. hormaechei* were cultured from human atheromas [56, 66]. The mechanism of the proatherogenic effect can be that bacterial and viral infections and the accompanying inflammatory response damage the endothelial cells and also stimulate monocytes to secrete pro-inflammatory cytokines [52].

Cpn has been shown to contribute to chronic inflammatory processes by direct mechanisms or indirect mechanisms [52]. A direct effect is indicated by the ability of the organisms to infect vascular cells and detection of the bacteria in atherosclerotic lesions and indirect effect of *Cpn* results from infection at a non-vascular site that increases the level of inflammatory cytokines and other acute phase proteins. [34] Seroepidemiological [67], histological studies [68], direct detection of bacterial components in atherosclerotic lesions by PCR [69] or electron microscopic studies, occasional isolation of viable organisms from atherosclerotic plaques and *in vitro* experiments and *in vivo* animal studies provided evidence for the role of *Cpn* in the pathogenesis of atherosclerosis. The first seroepidemiological studies showed that *Cpn* antibodies were significantly higher in patients with myocardial infarction and coronary heart disease than in control patients [67]. The meta-analysis of seroepidemiological studies suggested that a positive *Cpn* titre was related to increased risk of atherosclerosis compared with a negative titre, especially in cross-sectional studies [70]. The prevalence of antibodies ranges from 60 to 80% among patients with cardiovascular diseases [55].

Cpn could be detected in coronary artery fatty streaks and atheromas by immunocytochemistry, but couldn’t be detected in atheroma-free coronary arteries of controls [71]. In one study *Cpn* was detected in early, mature and advanced lesions of 50 different patients by electron microscopy [72] immunocytochemistry [73] and PCR technique [74]. In clinical studies *Cpn* DNA could be detected by nested PCR in peripheral blood mononuclear cells (PBMCs) of cardiovascular disease patients and in middle-aged blood donors with similar frequency [75]. *Cpn* was detected within atherosclerotic plaques and in some early fatty streak

lesions in autopsy cases with immunoperoxidase staining [73]. *Cpn* could be isolated from 11 of 70 specimens of coronary arteries and from coronary endarterectomy and restenotic bypass samples and *Cpn* DNA was amplified from 21 of 70 samples [76]. Jackson *et* al [77] also cultivated *Cpn* from one endarterectomy specimen and identified the bacterium. Ramirez [66] examined coronary arteries of 12 heart transplant patients and cultured *Cpn* from one sample but found 50% of samples positive for *Cpn* with at least one of the detection methods from PCR, immunocytochemistry, electron microscopy, or *in situ* hybridization. This pathogen was not present or very rarely in healthy arteries and this also may suggest that the organism is involved in the disease process [76].

In *in vitro* experiments *Cpn* infection of the cells that are constituents of the atherosclerotic plaques was successful, e.g. *Cpn* infected smooth muscle cells [78] and vascular endothelial cells, and stimulated the secretion of pro-inflammatory cytokines and the expression of leukocyte adhesion molecules by these cells [79]. *Cpn* infection induced macrophages to take up increased amounts of native LDL and become foam cells, possibly due to up-regulation of LDL receptors (LDLR) or by dysregulation of the lipid metabolism of the cells [80]. Chlamydial lipopolysaccharide (LPS) was shown to be responsible for this effect. cHsp60 (chlamydial heat-shock protein 60) can induce oxidation of LDL by monocytes [81]. Lectin-like ox-LDL receptor (LOX-1) on endothelial cells, smooth muscle cells and macrophages is responsible for binding and uptake of oxLDL and through this activity for the induction of many atherogenic factors. *Cpn* was shown to use LOX-1 as receptor and to induce LOX-1 protein expression in both endothelial cells (HUVEC) and RAW macrophages which resulted in production of adhesion molecules and matrix metalloproteases appearing as a proatherogenic mechanism of the infection [82, 83]. A study investigating the mechanism of stimulation of proinflammatory cytokine production by *Cpn* showed that it was mediated through toll-like receptor 2 (TLR2), as macrophages isolated from $TLR2^{-/-}$ mice produced 60–75% less tumour necrosis factor-α (TNF-α) and interleukin-1 (IL-1) compared with cells isolated from wild type mice [84].

In vivo studies showed an atherosclerotic lesion exacerbation following *Cpn* inoculation of hyperlipidaemic model animals of atherosclerosis [85].

1.3. Mouse models of atherosclerosis

There are several animal models for investigation of the pathogenesis of atherosclerosis [86]. Animal models help to clarify causalities in atherosclerosis and play an important role in experiments aiming to clarify the mechanisms involved in atherosclerosis development and in the current search for new therapeutics beyond the lipid-lowering drugs. Normal mice do not develop atherosclerosis and it requires long-term feeding of a high-fat diet to induce atherogenesis. However, there are well-established genetically modified inbred mouse lines that allow the investigation of atherosclerosis development in mouse models. The most frequently used mouse strains were ApoE-deficient ($ApoE^{-/-}$), LDL receptor-deficient ($LDLR^{-/-}$), human apoB100 transgenic and $LDLR^{-/-}ApoE^{-/-}$ [87] mice or ApoE-Leiden transgenic [88] mice which display marked atherogenesis throughout their arterial tree especially when fed with atherogenic diet [89, 90]. In $ApoE^{-/-}$ mice, atherosclerosis develops spontaneously. However, the lipid profile in these mice is distinct from that seen in most humans with atherosclerosis, i.e. apolipoprotein (apo) B48-containing LDL plasma level is high instead of apoB100 containing LDL level as in the case of humans with hypercholesterolemia [91, 92]. The mouse strain ApoB100only/$LDLR^{-/-}$ carries an *apoB* gene with a mutation preventing the expression of apoB48, the truncated form of apoB, similarly to humans where no apoB editing takes place in the liver [91, 93]. LDLR deficiency prevents the uptake of apoB100 containing LDL in tissues resulting in high plasma levels of apoB100-containing, cholesterol-rich LDL. The creating authors of this mouse strain described these mice as an authentic model of human familial hypercholesterolemia. In familial hypercholesterolemia the mutation in the LDLR gene causes the disease [91].

1.4. Effect of *Cpn* infection in animal models of atherosclerosis

In the first animal studies, in New Zealand white rabbits *Cpn* infection accelerated atherosclerosis lesion development on a normal diet [94]. Most frequently mice with genetic modification resulting in alterations in lipid metabolism were used to investigate the association of *Cpn* infection with atherogenesis [95].

In mice, intranasal *Cpn* infection causes lower respiratory tract disease similar to that seen in humans with *Cpn* infection. The infection is followed by dissemination of bacteria [80] and the chlamydial DNA can be detected in the circulation of mice [96]. It was shown that in animals infected via the respiratory tract the *Cpn* infected macrophages behave as vectors,

transmitting the pathogen to the vascular wall [80]. *Cpn* inoculation of wild type C57BL/6 mice, fed a standard rodent chow, resulted in inflammatory changes in the aorta [97, 98]. Most frequently, acceleration of atherosclerosis was studied after repeated *Cpn* infections which simulated chronic *Cpn* infection of humans in association with diet-induced hyperlipidaemia in C57BL/6J [99], $LDLR^{-/-}$ [100], in $ApoE^{-/-}$ [101], in $LDLR^{-/-}ApoE^{-/-}$ [87] mice or ApoE-Leiden transgenic [88] mice and mostly found exacerbation of atherosclerotic lesions. After multiple chlamydial infections in C57BL/6J mice kept on slightly cholesterol enriched diet, lesions with intimal lipid accumulation in the aortic sinus were detected and were larger than those from the uninfected control group [102]. Although in $ApoE^{-/-}/LDLR^{-/-}$ mice *Cpn* infection did not induce the formation of larger lesions but the elevated level of matrix metalloproteinase-2 (MMP)-2 and MMP-9 in the atherosclerotic lesions compared to that in mock infected mice resulted in thinning of the fibrous cap of lesion which ultimately leads to aggravation of the atherosclerotic process [87]. *Cpn* infected ApoE3-Leiden mice on atherogenic diet were infected with *Cpn* and the effect was an increase in lesion development and in T cell influx into atherosclerotic lesions in comparison to that in uninfected animals [88]. ApoB100only/$LDLR^{-/-}$ mice have not been used as a model for the investigation of the effect of *Cpn* infection on the atherosclerosis progression.

Although, repeated infections have been used to simulate human chronic infection, a recent study demonstrated in $ApoE^{-/-}$ mice on high-fat diet that a single intranasal inoculation with *Cpn* also exacerbated atherosclerosis [29]. An increased level of circulating pro-inflammatory cytokines and more numerous dendritic cells, T cells among them Treg cells in the aorta were observed. These phenomena indicate the activation of innate and adaptive immune responses contributing to systemic inflammation [29]. To investigate the immune mechanism of the effect of *Cpn* infection on atherosclerosis, different knockout mouse lines: TNF-α p55 receptor [103], IL-17A [99], TLR2, TLR4, MyD88 [104] and inducible nitric oxide synthase (iNOS) [105] knockout mice were used. Campbell et al. found that *Cpn* infection did not accelerate foam cell lesion development in the aortic sinus in hyperlipidemic TNF-α p55 receptor knockout mice and it was suggested that signalling through the p55 receptor may play a role in the atherogenic effects of *Cpn* in these mice [103]. A report by Naiki et *al*. demonstrated that *Cpn* infection-accelerated atherosclerosis was significantly inhibited in hypercholesterolemic $ApoE^{-/-}$ mice lacking TLR2, TLR4, or MyD88; thus proving that *Cpn*

infection together with hyperlipidaemia promotes atherosclerotic plaque development via activation of innate immunity through TLR/MyD88-dependent signalling pathways [104]. Role of IL-17A in the interplay between *Cpn* infection-and atherosclerosis was investigated in IL-17A$^{-/-}$ mice as IL-17A is known to be involved in the pathogenesis of autoimmune and inflammatory and infectious diseases. IL-17A$^{-/-}$ mice developed significantly less acceleration of lesion size following *Cpn* infection compared to wild-type controls which was coupled with increased circulating inflammatory cytokine level and macrophage content in plaques. iNOS have a proatherogenic effect in late stages of atherosclerosis but not in early phase. In iNOS$^{-/-}$ mice *Cpn* infection results in increased lesion area in comparison to that in uninfected mice. This suggest a protective effect of iNOS activity the mechanism of which is associated with the reported anti-chlamydial effect of iNOS activity [105].

1.5. *Chlamydia trachomatis*

Chlamydia trachomatis (*C. trachomatis*) is the most common sexually transmitted bacterial pathogen and the causative agent of blinding trachoma [106]. There are two different biovars of *C. trachomatis*: oculogenital biovar which cause a gamut of diseases, including blinding trachoma (serovars A–C), urogenital tract infections and adult inclusion conjunctivitis in women and in man (serovars D–K) and the LGV biovar (serovars L1–L3) causing a sexually transmitted systemic disease lymphogranuloma venereum (LGV) [106]. Over 100 million genital chlamydial infections are detected according to the World Health Organization (WHO) annually worldwide [107]; 13.5% of women under the age of 25 were infected with *C. trachomatis* and 4.4% of over 25 years old have lower genital tract infection [107]. Primary infection occurs in the cervix or urethra. In men the *Chlamydia* infection is identified as the causative agent in 50% of non-gonorrhoeal urethritis cases [108]. In women the infection results in inflammation of the cervix which frequently becomes ascending spreading to the uterus and the fallopian tubes. When the urethra is affected urinary syndrome can develop. *C. trachomatis* genital infections are very frequently asymptomatic in men and women too [109], asymptomatic infection produces a large reservoir of unrecognized, infected individuals who are capable of transmitting the infection to their sexual partners [110]. The acute infections and infections without symptoms and unrecognized and untreated infections lead to chronic infections which are associated with severe sequelae. Complications in man include

epididymitis, prostatitis that can negatively affect fertility, and reactive arthritis and Reiter's syndrome. Severe complication in women is the pelvic inflammatory disease (PID) during which the uterus, the ovaries and the fallopian tubes can be inflamed. Tubal factor infertility, ectopic pregnancy and chronic pelvic pain can be the most severe consequences of PID [111]. During *C. trachomatis* infection natural immunity develops by stimulating both humoral and cell mediated immune responses [112]. However after primary infection the immune response does not provide complete protection against reinfection nor prevents the development of damaging immunopathology [113]. According to the "cellular paradigm" of chlamydial immunopathology, in case of chronic or recurrent infections, the infected epithelial cells continue to produce numerous pro-inflammatory chemokines, cytokines and growth factors thus perpetuate the inflammation. Antigen non-specific innate immune cells are attracted to the site of infection then an additional level of specific immune responses is incited. These conditions promote cellular proliferation, tissue remodelling and eventual scarring [112, 114]. The "immunological paradigm" of chlamydial pathogenesis states that *Chlamydia*-induced antigen-specific adaptive cellular responses drive pathologies. The molecular mimicry model involves chlamydial Hsp60 and other antigens for which there is high homology between chlamydial protein and a human protein. In this model, the persistence of chlamydia or reinfection provides continuing antigen exposure, thus stimulating specific anti-chlamydial adaptive cellular responses promoting tissue damage and scarring [113].

1.6. Chlamydiae in the gastrointestinal tract

Animal pathogenic *Chlamydia* species were isolated from various animals, for example, ruminants, porcine, and avian species, and they were detected in different organs as well as in faeces. In most animals, chlamydiae persist in the gastrointestinal (GI) tract and are transmitted via the faecal-oral route [115]. Rank and Jeruva found that faeces samples from 10 of 15 calves were positive for chlamydiae, so the GI tract could be the natural habitat of chlamydiae in cattle and they demonstrated horizontal transfer of the infection, with faeces samples from the naive animals becoming *Chlamydia* positive [115]. Oral infection with *C. muridarum* has resulted in a long term, persistent infection of the mouse GI tract [116] which persisted for as long as 260 days after infection in the absence of pathology [117]. During *C. suis* infection of pig which was often subclinical and without obvious inflammatory response in the GI tract,

histopathologic and electron microscopic images of the GI tract showed both normal and aberrant chlamydial forms [118]. The GI tract seems to be an ideal site, in which *Chlamydia* can persist because of a down regulated host immune response.

Several studies investigated the possibility of *Chlamydia* reinfection from persistent infection in the GI tract in humans [119].

The nature of persistent or recurrent *C. trachomatis* infection of the female genital tract has not been identified. It has been suggested that genital tract infection can be accompanied by infection of the GI tract either via oral infection, or by autoinoculation from genital secretions or during sexual activity [120]. Anorectal samples taken from both men and women have been tested and found positive for *C. trachomatis* [121]. Studies by Yeruva et al. have suggested that especially in women, reinfection of the genital tract may occur via contamination of the genital tract from the infected GI tract [119]. Furthermore, *C. trachomatis* might have a role in irritable bowel disease (IBD) suggested by the detection of *C. trachomatis* antigen in the intestine of IBD patients [122].

1.7. Growth of *C. trachomatis* in different cell lines

Earlier with the purpose of diagnosis of chlamydial infections and in *in vitro* experiments to characterize the replication of chlamydiae mostly epithelial cells as the prime targets of chlamydial infection are being used [123]. It appears that the culture conditions and nature of the host cells used to grow chlamydiae *in vitro* are important parameters that influence growth of the organisms [124]. For optimal chlamydial growth an epithelial cell environment appears to be important but the anatomical origin of the cell lines used seems to be critical as well. For culture of *C. trachomatis* D-L serovars most commonly non-polarized cervix-derived HeLa cells, representative of low, squamo-columnar epithelia were used, but HEC-1B and Ishikawa endometrial carcinoma cell lines, representatives of tall columnar epithelia and the breast cancer lines MCF-7 and HCC-1806 were also applied [125]. The McCoy fibroblast cell line another commonly used host cell for *Chlamydia* growth originally was obtained from knee joint from a patient with arthritis but presumably became cross-contaminated with the McCoy B subline of mouse origin [126]. Human epithelial cell line Hep-2 can be regarded as conventional propagating host for *Chlamydia* [13] but human retinal pigment epithelium was proved to be highly susceptible to *C. trachomatis* infection too [127]. In human monocytes and

dendritic cells *C. trachomatis* urogenital serovars are metabolically active and viable, but most studies were not successful to recover the bacteria in HeLa cells. In monocytes persistent chlamydial forms were identified and in dendritic cells an abortive cycle was detected. In these cells different inflammation related genes were up-regulated in response to chlamydiae [17, 128].

Cell lines other than the conventional epithelial cells have been used to investigate the pathomechanism of *Chlamydia* species caused infections at extra genital sites. *C. trachomatis* D-K serovars have been implicated as organisms that can trigger reactive arthritis. Infection of human fibroblast-like synovial cells showed that these cells do not support the active replication of this bacterium, but aberrant persistent replication cycle occurred, accompanied with inflammatory cytokine production by the infected cells. These observations point to the arthritogenic role of *C. trachomatis.*

In earlier studies, the growth of animal *Chlamydia* species was investigated in cell lines of a variety of origin. In intestinal mucosal epithelial Caco-2 cells, inclusions have indicated a substantial growth of porcine *C. pecorum* and *C. suis*; therefore, Caco-2 cells can be regarded as suitable hosts for animal *Chlamydia* [129]. If *C. trachomatis* can persist in the human GI tract it is of relevance to look into the growth characteristics of *C. trachomatis* in Caco-2 cells. Caco-2 cell line could be a suitable model for investigation of *Chlamydia* infection in the human GI tract.

1.8. Defensins

Defensins are an important family of natural antimicrobial peptides acting against bacteria, fungi and enveloped viruses [130]. Human defensins are divided into two subfamilies, alfa and beta (β)-defensins (hBD). α-Defensins are found in neutrophil granulocytes (human neutrophil peptides (HNPs) and in small intestinal Paneth cells. hBD-1 is constituvely produced by various epithelial cells e.g. in the urogenital and respiratory tract. hBD-2 is mainly present in the skin and the respiratory and gastrointestinal tracts and is expressed mainly by epithelial cells in response to inflammatory stimuli and infection, but monocytes, macrophages and dendritic cells are also capable of hBD-2 production [131]. In the colonic mucosa, defensins, and among them hBD-2 represent the important effectors of the innate host defences not only

by their microbicidal activity but by providing a link to the adaptive immune system as they attract immature dendritic cells and memory T cells [132]. The intestinal mucosal epithelial cells have important role as physiological barrier for pathogens and function as a part of the innate immune system [133]. Several *in vitro* experiments showed the anti-chlamydial effect of antimicrobial peptides, e.g. the protegrin more efficiently than human defensin HNP1 and 2 inhibited infection of McCoy cells by *C. trachomatis* [134, 135]. *C. trachomatis* infection activates the production of hBD-2 which were detected quantitatively by RT-PCR in cervico-vaginal lavage of women with chlamydiasis [136]. Secretion of hBD-2 by these epithelial cells in response to *Chlamydia* infection would suggest the stimulation of the innate immune response in the GI.

2. Aims

The present study was designed to address the following aims:

Aim 1: to investigate the potentially atherogenic effect of multiple *Cpn* infections in ApoB100only/LDLR$^{-/-}$ mice.

Our aim was to examine how repeated *Cpn* infection influences the atherosclerotic lesion development in this - based on lipid profile - most suitable mouse model of human atherosclerosis. We compared the extent of atherosclerosis in this model with that seen in the most frequently utilized ApoE$^{-/-}$ mouse strain.

Aim 2: to investigate the growth characteristics of *C. trachomatis* in intestinal epithelial cells as potential target cell during human infection and the infection induced defensin production.

Our other aim was in this study, by applying several morphological and molecular approaches to investigate the growth characteristics of *C. trachomatis* in the human intestinal epithelial cell line Caco-2, and to examine whether *Chlamydia* infection induces hBD-2 production in these cells.

3. Materials and methods

3.1. Cell lines

Caco-2, HeLa 229, HEp-2 and McCoy cells were maintained in minimal essential medium (MEM) with Earle's salts completed with 10% FBS, 2 mmol/liter L-glutamine, 1x nonessential amino acids, 25 μg/mL gentamicin, and 0.5 μg/mL fungizone. The cell lines were purchased from American Types Culture Collection (ATCC).

3.2. Bacterial strains

Chlamydia pneumoniae, CWL029 strain and *Chlamydia trachomatis* serovar D, UW-3/CX strain from (ATCC) was used. *Cpn* was propagated in HEp-2 cells and concentrated as described earlier [137]. *C. trachomatis* was propagated in McCoy cell line, as described earlier [138]. The EBs from infected cells were purified by density gradient centrifugation. The concentrated and purified elementary bodies (EBs) were aliquoted in sucrose phosphate-glutamic acid buffer (SPG) and stored at -80°C until use. Infective chlamydiae were quantitated by inoculating 10-fold serial dilutions of the EB-containing preparations onto HEp-2 or McCoy cells. Infective *Chlamydia* was quantitated by indirect immunofluorescent method applying anti-*Chlamydia* lipopolysaccharide monoclonal antibody (AbD Serotec, Oxford, United Kingdom) and fluorescein isothiocyanate (FITC)-labelled anti-mouse IgG (Sigma-Aldrich, St. Louis, MO) as described earlier [139]. The number of infectious bacteria in the *Chlamydia* stock used for inoculation of mice or cell lines was expressed as inclusion forming units (IFU)/ml.

3.3. Mouse strains

Female ApoB100only/LDL$^{-/-}$ (B6;129S-*Ldlr*^{tm1Her}*Apob*^{tm2Sgy}/J) mice at 8-9 or 14-15 weeks of age and ApoE deficient (ApoE$^{-/-}$, B6.129P2-*Apoe*^{tm1Unc}/J) mice at 14-15 weeks of age were involved in our studies. B6;129S-*Ldlr*^{tm1Her}*Apob*^{tm2Sgy}/J breeding pairs purchased from The Jackson Laboratory (Bar Harbor, ME, USA) and B6.129P2-*Apoe*^{tm1Unc}/J breeding pairs purchased from Charles River Laboratories (Sulzfeld, Germany) were housed and bred under standard conditions. Considering that numerous atherosclerosis-related studies used female mice [140–143], furthermore it was shown that female mice of both mouse strains develop atherosclerosis, with no gender-related difference in ApoE$^{-/-}$ mice and with less extensive lesions in female than in male ApoB100only/LDLR$^{-/-}$ mice [91, 93], we chose to

work with female mice which were available in sufficient quantity in our breeding colony. The mice were kept on normal rodent regular chow (VRF1, Altromin GmbH & Co. KG, Lage, Germany) or high-fat/high-cholesterol diet containing 21% milkfat and 1.25% cholesterol manufactured by Altromin GmbH & Co. KG according to Teklad custom diet formula TD.19121, for 12 weeks after the first infection. All experiments were approved by the Animal Welfare Committee of the University of Szeged and conform to the Directive 2010/63/EU of the European Parliament (Permit Number: III./2187/2015.).

3.4. Infection of mice with *Cpn*

Mice were intranasally infected with *Cpn*; $2x10^5$ inclusion-forming units (IFU) of *Cpn* in 20 μl PBS were administered intranasally three times with 2-week intervals under mild anaesthesia by intraperitoneal injection of 100 mg/kg sodium pentobarbital. One week after each infection and at the end of the experiment at week 12 plasma samples with heparinised capillaries (Natelson blood collecting tubes, Fisher Scientific, Pittsburg, PA, USA) were harvested from the retroorbital plexus under anaesthesia as described above. For RNA detection in the aorta tissue additional groups of mice were infected once and sacrificed 1 and 4 weeks after single infection and 5 weeks after the third infection. The control animals were left uninfected.

3.5. Mouse tissue preparation and quantification of atherosclerosis

Twelve weeks after the first infection with *Cpn* the mice were sacrificed. In deep pentobarbital sodium anaesthesia (i.p. injection of 400 mg/kg pentobarbital sodium) hearts and aortas were perfusion–fixed using 10% buffered formalin administered through the left ventricle. The adequacy of anaesthesia was assessed by pedal withdrawal reflex in hind limbs, mice displaying no locomotor activity were processed. After formalin-perfusion, the upper part of the heart and the descending aorta were dissected. Aortic sinus samples were also collected for RNA extraction from mice anaesthetized as described above. The basis of the heart was separated from the aorta which was dissected until the iliac bifurcation. The upper part of the hearts was embedded in paraffin and sectioned for morphometric analyses according to the method described by Paigen [144]. From the end of the aortic sinus 10-μm sections were prepared until the point where the valve cusps disappeared and stained with hematoxylin eosin. Images of aortic root sections (8 sections/mouse, every third sections)

were acquired with a light microscope (Leitz Optical microscope) and Olympus C-7070 digital compact camera. Percentage length of the plaque-covered perimeter of aorta lumen and percentage of aorta lumen area occupied by plaque were analysed with JMicroVision software. The aortic arch and the adjoining descending aorta were cleared from adjacent tissue and were opened longitudinally. The aortas were laid flat on black plastic surface and pictures of the longitudinally opened vessels were taken applying the same illumination, magnification and focal distance using a CMOS camera (DCM 510; pixel size: 2.2 μm x 2.2 μm, 2592 x 1944 pixels; 5 Mpixel; Hangzhou Scopetek Opto-Electric Co., Ltd, Hangzhou, Zheijang, China) and the ScopePhoto software (Hangzhou Scopetek Opto-Electric Co., Ltd) attached to a stereomicroscope (Alpha STO 44, Elektro-Optika Kft., Érd, Hungary). The digital image of the luminal surface was evaluated for the extent of atherosclerosis by tracing and measuring the plaque area and the total luminal surface using JMicroVision software. The percentage of the luminal area covered by plaque was calculated for each aorta sample.

3.6. RNA extraction from mouse aorta and quantitative real time-PCR for *Chlamydia* 16SrRNA expression

Aorta sinus with aortic arch for RNA extraction was collected from mice (in deep pentobarbital sodium anaesthesia as described in the previous paragraph) at the indicated time points after *Cpn* inoculation for one time or three times and pools of 3 samples at each time points were snap-frozen in liquid nitrogen. Aorta samples from non-infected mice were also dissected parallel with the samples collected one week after one infection. Total RNA was isolated from the pooled aorta samples with RNA-extraction kit (Nucleospin RNA XS kit, Macherey-Nagel GmbH, Düren, Germany). Concentration and purity (OD260/280) of RNA was determined by spectrophotometry. The extracted RNA was treated with DNaseI (Sigma, St. Louis, MO, USA). Complementary DNA (cDNA) was synthetized from 1 μg DNase-treated RNA with qScript cDNA Supermix synthesis kit (Quanta Biosciences, Gaithersburg, MD, USA). RNA and cDNA were stored at -80 °C until use. By using cDNA as template qRT-PCR was performed with PerfeCTa SYBR Green Supermix (Quanta) in CFX96 Real Time C1000 Thermal Cycler (BioRad, Hercules, CA, USA). All experiments involved control reactions containing distilled water as template. Chlamydia 16SrRNA and mouse β-actin sequences were amplified. The sequences of primers used for RT-PCR were the following: *Cpn* 16S rRNA: 5'-GGCGAAGGCGCTTTTCTAA-3', 5'-CCAGGGTATCTAATCCTGTTTGCT-3' [145];

mouse β-actin: 5'TGGAATCCTGTGGCATCCATGAAA-3', 5'-TAAAACGCAGCTCAGTAACAGTCCG-3' [146]. A BLAST search was performed to check the specificity of the product target sequence of the primer sets. The primers were synthesized by Integrated DNA Technologies Inc. (Montreal, Quebec, Canada). The PCR cycles consisted of a 3 min denaturation at 95°C followed by 55 cycles each of 10 s of denaturation at 94°C, 10 s of annealing at 60°C and 10 s of extension at 72°C. The specificity of amplification was confirmed by carrying out a melting curve analysis. The sensitivity of amplification was controlled using standard as described earlier [38]. Amplicon standard was generated by amplifying *Cpn* cDNA with 16S rRNA primers, amplicons were purified with the PCR Clean-Up Kit (GeneElute PCR Clean Up Kit, Sigma-Aldrich); the DNA concentration was measured with NanoDrop 1000 Spectrophotometer. The copy number was calculated using the following formula: Copy number/µl = [6.022 × 1023 (molecules/mole) × DNA concentration (g/µl)] / (Number of bases pairs x 660 daltons) and standard curve were generated from 10-fold serial dilutions of the amplicon (from 1000 000 to 1 copies). qPCR analysis of the dilution series showed that the sensitivity threshold of our method was ten 16SrRNA copies.

3.7. ELISA for detection of *Cpn*-specific antibodies

Plasma samples of mice collected one week after each infection and at the end of the experiment were tested in duplicates for *Cpn*-specific IgG, IgM and IgA by an in-house developed ELISA test as described earlier [96], where NP-40 treated partially purified *Cpn* and similarly treated Hep-2 mock preparation were used as antigens. Briefly, NUNC Maxisorp ELISA plates were coated with *Cpn* and mock antigen (0.625 µg protein in 50 µl PBS/well), respectively overnight at 4°C. Blocking was done with 1% skim milk in PBS with 0.05% TWEEN 20 for 1 h. The serum samples were diluted in 0.4% skim milk in PBS with 0.05% TWEEN 20. Mouse IgG, IgM and IgA were detected with HRP-anti-mouse IgG (Jackson ImmunoResearch Laboratories West Grove, PA, USA), α-mouse IgA-HRP (Sigma) and anti-mouse IgM µ–chain (ab97260, Abcam, Cambridge, UK) secondary antibodies, respectively. Optical densities (OD-s) detected on *Cpn* antigen were corrected with OD values measured on the control antigen. *Cpn*-specific IgG antibody titres were determined by testing serial 2-fold dilutions of the serum samples on *Cpn* and control ELISA antigen, and reciprocal of the dilution producing OD ≥0.1 after correction with OD values measured on control antigen was regarded as titre. Geometric mean of titres of individual serum samples was calculated. For determination

of *Cpn*-specific IgM and IgA levels serum samples were tested at 1:50 dilution and determined as the measured and corrected OD values.

3.8 Serum lipoprotein analysis

Levels of total cholesterol, triglycerides, high-density lipoprotein (HDL) and LDL cholesterol were determined in plasma samples of mice through a service from the Department of Laboratory Medicine, University of Szeged, Hungary.

3.9. Infection of different cell lines with *C. trachomatis*

The cells were grown in 6-well ($1x10^6$ cells/well), 96 well ($4x10^4$ cells/well), or 24-well culture plates ($2.5x10^5$ cells/well) with 13 mm glass coverslips. The plates were kept for 1 h at room temperature (RT), and then incubated overnight in 5% CO^2 atmosphere at 37°C to reach 90% confluency. The cells were then infected with *Chlamydia* at a multiplicity of infection (MOI) of 1 or 5 in complete MEM with 0.5% glucose and centrifuged at 800 x g for 1 h RT. The medium was replaced in the wells with a cycloheximide-containing one (1 μg/mL). Cycloheximide was not added to the medium of cells in 6-well plates infected for testing defensin secretion or RNA expression analyses. For DNA quantitation, the infected cells in 96-well plates were incubated in cycloheximide containing medium or cycloheximide-free medium. The culture plates were incubated for different time periods in CO^2 incubator at 37°C.

Assessment of the infectivity of *C. trachomatis* D replicating in Caco-2 or HeLa cells was done by inoculation of the infected cell lysates onto McCoy cells in 24-well plates with glass coverslips. Cell lysates were prepared by scraping the infected cells into the culture medium at each examination time point. After two freeze-thaw cycles and sonication in water bath, the lysates were centrifuged at 800 x g for 1 h onto McCoy cells grown in 24-well plates with 13 mm glass coverslips. After 48 h, the cells were fixed with acetone at -20°C for 10 min.

3.10. Immunofluorescent staining of infected cells for visualization of inclusions and quantitation of recoverable *C. trachomatis*

The staining of *Chlamydia*-infected cells on coverslips was performed via using anti-cLPS and FITC-labelled anti-mouse IgG as secondary antibody. The coverslips were treated with Evan's Blue at room temperature for 1 min. The chlamydial inclusions were photographed and counted under a fluorescent microscope.

3.11. Transmission electron microscopy (TEM)

The cells were cultured in 6-well plates and infected with Chlamydia at an MOI of 1. After 24 and 48 h, the infected cells were washed in plates with 3 mL PBS and collected after trypsin treatment. After sedimentation with 400 x g for 5 min, the cells were fixed with 2% glutaraldehyde and 1% osmium tetroxide overnight at 4°C. Samples were embedded in Embed 812 (EMS, USA) using a routine TEM embedding protocol. Ultrathin sections (70 nm) were cut with an Ultracut S ultra-microtome (Leica, Austria). After staining with uranyl acetate and lead citrate, the sections were examined with a Philips CM10 electron microscope. Images were acquired by using Olympus Soft Imagine Viewer program.

3.12. *C. trachomatis* DNA quantitation

For the quantitative assessment of chlamydial replication, we followed a direct DNA quantitation method described previously [147]. The cells cultured in 96 or 24-well plates were infected with Chlamydia. After 0, 24, 48 and 72 h, the infected cells in 3 parallel wells were washed in the plates twice with 200 µL/well phosphate buffered saline (PBS). Then, either 100 or 625 µL Milli-Q water was added to the wells, and the plates were stored at -80°C. Two freeze-thaw cycles were applied to free the DNA from the cells. Thoroughly mixed lysates were used as templates directly for quantitative PCR (qPCR) using SsoFast™ EvaGreen ®Supermix (BioRad). *Pyk* primers were used for the detection of *C. trachomatis* D genomes (Table 1).

3.13. RNA extraction from infected cell lines

For the analysis of gene expression, total RNA was extracted from the infected cells in 6-well plates at 2, 24, 48 or 72 h after infection (3 parallel cultures at each time point) with GenElute Mammalian Total RNA Miniprep Kit (Sigma) according to the manufacturer's protocol. Concentration of RNA was determined by spectrophotometry. The extracted RNA was treated with DNase I (Sigma). cDNA was synthetized from DNase-treated RNA with qScript cDNA Supermix synthesis kit (Quanta Biosciences). RNA and cDNA were stored at -80°C until use.

3.14. *C. trachomatis* gene expression analysis by quantitative RT-PCR

By using cDNA as template, qRT-PCR was performed with PerfeCTa SYBR Green Supermix (Quanta) in CFX96 Real Time C1000 Thermal Cycler (BioRad). 16SrRNA was used as the internal standard for counting the relative expression of *Chlamydia* genes as this gene

was previously shown to be an accurate normalizing gene for gene expression analysis in *C. trachomatis* [148]. The relative expression of *euo*, *groEL*, *ftsK*, *omcB*, *ompA* and *pyk* transcripts of *C. trachomatis* was evaluated. The sequences of all primers used for RT-PCR are shown in Table 1. All primers were synthetized by Integrated DNA Technologies Inc. (Montreal, Quebec, Canada). The PCR cycles consisted of a 3-min denaturation at 95°C followed by 55 cycles of 10 s of denaturation at 94°C; 10 s of annealing at 61.5°C for *16S rRNA*, *groEL*, *omcB*, *ompA*, *pyk*, 54°C for *ftsK*, and 10 s of extension at 72°C. The samples were tested in triplicates, and no-template controls with distilled water were run in each case. The melt curve analysis was performed to prove the specificity of the amplification.

The relative gene expression levels (RQ) were given by calculating the delta-deltaCt (ΔΔCt) value. The lowest cycle number, at which the various transcripts were detectable, referred to as Ct, was compared with that of the 16S rRNA, and the difference was referred to as ΔCt (Borges et al. 2010). The relative expression level was given as $2^{-(\Delta\Delta Ct)}$, where ΔΔCt = ΔCt for the experimental sample minus ΔCt for the control sample at 2 h.

Table 1. Primer sequences used for qRT-PCR detection of expression of *C. trachomatis* genes.

Target gene	Sequence	PCR product size (bp)
16S rRNA F	5’-CACAAGCAGTGGAGCATGTGGTTT-3’	191
16S rRNA R	5’-ACTAACGATAAGGGTTGCGCTCGT-3’	
euo F	5’-TCCCCGACGCTCTCCTTTCA-3’	263
euo R	5’-CTCGTCAGGCTATCTATGTTGCT-3’	
ftsK F	5’ CGGAAGAAAGCAAGCGTTTC 3’	70
ftsK R	5’ GGGCTAGATACACGCATGTTTTAAC 3’	
groEL F	5’-TCACTCTAGGGCCTAAAGGACG-3’	115
groEL R	5’-TCATGTTTGTCGGCAAGCTC-3’	
omcB F	5’ TGAAGCAGAGTTCGTACGCAGTG 3’	179
omcB R	5’ AACGGATCTCTGGACAAGCGCAT 3’	
ompA F	5’-TCGACGGAATTC TGTGGGAAGGTT-3’	171
ompA R	5’-TATCAGTTGTAGGCTTGGCACCCA-3’	
pyk F	5’-GTTGCCAACGCCATTTACGATGGA-3’	81
pyk R	5’-TGCATGTACAGGATGGGCTCCTAA-3’	

3.15. ELISA for detection of hBD-2

The supernatant of the infected cells from 3 parallel wells’ 24-well plates were harvested at different time points post infection. For the detection of hBD-2 production, the supernatants of the cells were tested by using hBD-2 ELISA kit (Alpha Diagnostic, San Antonio, TX, USA). The level of the hBD-2 (12.5–200 pg/mL detection range) was determined according to the manufacturer’s instructions. The supernatant of Caco-2 cells treated with heated (1 h, 56°C) overnight culture of *Escherichia coli* Nissle 1917 strain (MOI of 100), a potent inducer of HBD-2, was used as positive control.

3.16. Statistical analysis

Data are expressed as mean ± SD. Independent-samples t-test was used with SigmaPlot for Windows Version 11.0 software. A *P* value of less than 0.05 was considered to indicate statistically significant difference.

4. Results

4.1. Infection of ApoB100only/LDLR$^{-/-}$ mice with *Cpn*

Mice infected 3 times with *Cpn* showed mild symptoms of a disease as ruffled fur and moderate food consumption, especially during the first week after the first infection. At the time of the first infection half of the mice were given a high-fat/high-cholesterol diet the other half was kept on normal rodent chow. Non-infected mice were kept under similar conditions. All infected mice produced *Cpn*-specific antibodies which were not seen in the non-infected mice. Normal and high-fat/high-cholesterol diet-fed mice produced similar level of *Cpn*-specific IgG antibodies (OD 0.36-0.4 at dilution 1:100).

4.2. Repeated *Cpn* infection aggravates atherosclerosis development in the aorta sinus and in the descending aorta of ApoB100only/LDLR$^{-/-}$ mice kept on normal diet

The mice received the first *Cpn* infection at the age of 8-9 weeks; uninfected mice with same age served as controls. Fed with an atherogenic diet very similar pathology was observed in the aorta sinus of the mice that received three chlamydia infections and in those remained uninfected. The quantitative evaluation did not disclose significant difference in the length of the plaque-covered perimeter of the lumen (Figure 1A), neither in the size of the plaque-occupied area in the aorta lumen (Figure 1B). The aorta sections of the normal diet-fed non-infected animals demonstrated very early-stage and small extent of atherosclerosis with a single layer of foam cells. However, in the aorta sections of repeatedly *Cpn*-infected mice we observed a significant increase in the length of the plaque-covered perimeter of the lumen ($P < 0.05$) (Figure 1A) and in the size of the plaque-occupied area in the aorta lumen ($P < 0.05$) (Figure 1B) compared with that in the non-infected counterpart in normal diet-fed group.

On the luminal surface of the longitudinally opened descending aorta well discernible plaques could be observed. Small areas corresponding to atherosclerotic alteration were seen in the case of the aorta of the non-infected animals fed with normal diet. The atherosclerosis-affected areas were measured significantly larger in the descending aorta of the infected animals. In the high-fat/high-cholesterol diet-fed animals, significantly increased plaque-covered spots were visible compared to that in the normal diet fed mice however the infection did not enhance the lesion formation in this part of the aorta (Figure 1C).

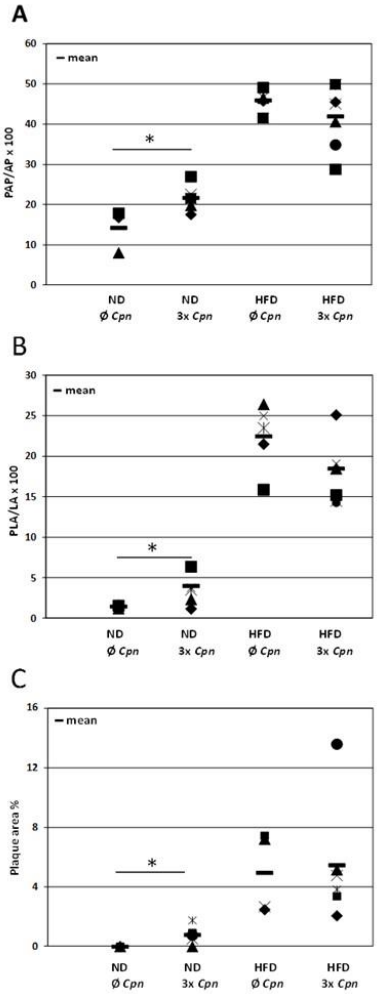

Figure 1. Morphometric analyses of atherosclerotic plaques in ApoB100only/LDLR$^{-/-}$ mice. **(**A) Measurements for the length of the aortic luminal surface (perimeter) covered by plaque (PAP/APx100); (B) percentage of aortic lumen area occupied by plaques (PLA/LAx100) in 8 cross-sections of aortic root from each ApoB100only/LDLR$^{-/-}$ mouse in groups kept on normal diet without *Cpn* infection (number of mice (N)=6) or infected with *Cpn* 3 times (N=8) or on high-fat/high-cholesterol diet for 12 weeks without *Cpn* infection (N=6) or infected with *Cpn* 3 times (N=8). Average percentage values from individual mice and mean percentages in groups are shown. PAP – plaque-covered aorta perimeter, AP - aorta perimeter, PLA - Plaque-occupied lumen area, LA - aorta lumen area; (C) Plaque size was measured in the longitudinally opened descending aorta of each ApoB100only/LDLR$^{-/-}$ mouse in groups kept on normal or high-fat/high-cholesterol diet for 12 weeks without *Cpn* infection or infected with *Cpn* 3 times. The percentage of total aorta area covered by plaques was calculated. Data show the results of one of two independent experiments. For comparison of groups independent-samples t-test was used, * P<0.05. ND - normal diet, HFD – high-fat/high-cholesterol diet, 3x – three intranasal *Cpn* infections.

4.3 Viable *Cpn* was detectable in the aorta of ApoB100only/LDLR$^{-/-}$ mice

As Figure 2A shows the persistence of the bacterium was tested early i.e. one week after the first infection, again four weeks after single infection and at 9 and 12-week time points after three chlamydial infections by RT-PCR. An equal amount of RNA purified from pooled ascending aorta samples of mice was DNase-treated then reverse-transcribed and mouse *β-actin* as housekeeping gene was amplified from all samples. One and four weeks after single inoculation the expression of chlamydial 16SrRNA was detectable (Figure 2B) with a ~1000-fold lower relative expression level at four weeks than at 1 week time point (Figure 2C). Five weeks after the third infection one aorta sample of 2 showed metabolically active *Cpn* in the aorta and the relative expression level was similar to that after single infection at 4 weeks (Figure 2C). At later time point, our test was not able to detect chlamydial gene expression.

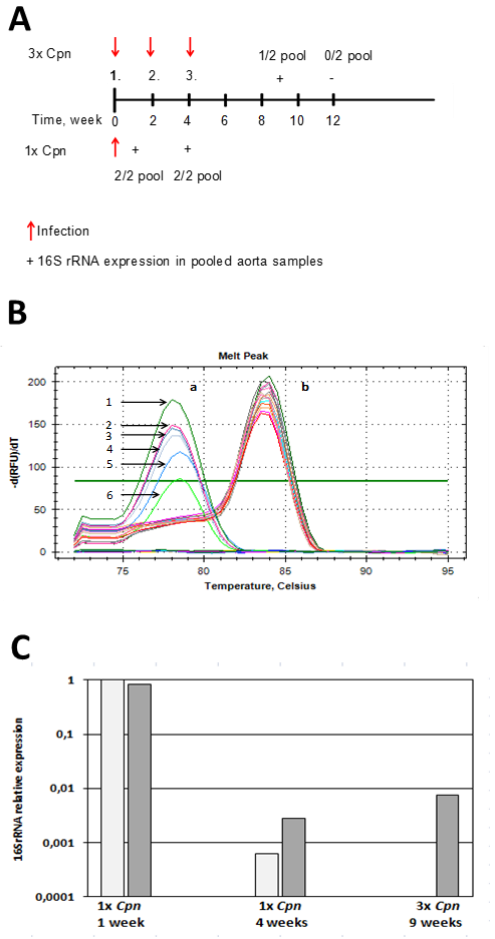

Figure 2. *Chlamydia* RNA in the aorta tissues. (A) Experimental design for *Cpn* infection of ApoB100only/LDLR$^{-/-}$ mice, and 16SrRNA transcript detection in pooled aorta samples (two pools of 3 aortas from 6 mice) of once (1x *Cpn*), 3 times (3x *Cpn*) *Cpn* infected and non-infected

mice ("+" – aorta samples tested positive, "-" - aorta samples tested negative for expression of 16SrRNA by qRT-PCR). (Ba) Identification of the RT-PCR-amplified *Cpn* 16SrRNA cDNA in the aorta of *Cpn*-infected ApoB100only/LDLR$^{-/-}$ mice. Melt curves show *Cpn* 16SrRNA amplicons in **1.** *Cpn*-infected McCoy cells (positive control), aorta samples tested **2., 3.** 1 week after single *Cpn* infection, **4.** 5 weeks after third *Cpn* infections, **5., 6.** 4 weeks after a single *Cpn* infection; (Bb) β-actin amplicons in all tested aorta samples and *Cpn*-infected McCoy cells. (C) Expression of *Cpn* 16SrRNA normalized to the expression level of mouse β-actin at 1 week after single *Cpn* infection was set as 1 and relative mouse β-actin-normalized *Cpn* 16SrRNA expression level in all pooled aorta samples giving positive 16SrRNA signal was calculated. The measurements were repeated two times with same results.

4.4 Infection of ApoB100only/LDLR$^{-/-}$ and ApoE$^{-/-}$ mice with *Cpn* induces similar kinetics of antibody production

Based on the above results we aimed at performing a comparative experiment by applying our infection protocol both in ApoB100only/LDLR$^{-/-}$ and in ApoE$^{-/-}$ mice (14-15 weeks of age) while keeping them on a non-atherogenic diet. The humoral immune response induced by the infections was compared by measuring the titre of *Cpn*-specific IgG antibodies (Figure 3A) and the level of IgM (Figure 3B) and IgA (Figure 3C) antibodies one week after all three infections and at the end of the experiment. The level of antibody response did not differ significantly in the two mouse strains. The IgA level tended to be lower in ApoE$^{-/-}$ mice (Figure 3C) however, the difference was not significant. Two independent experiments gave similar results.

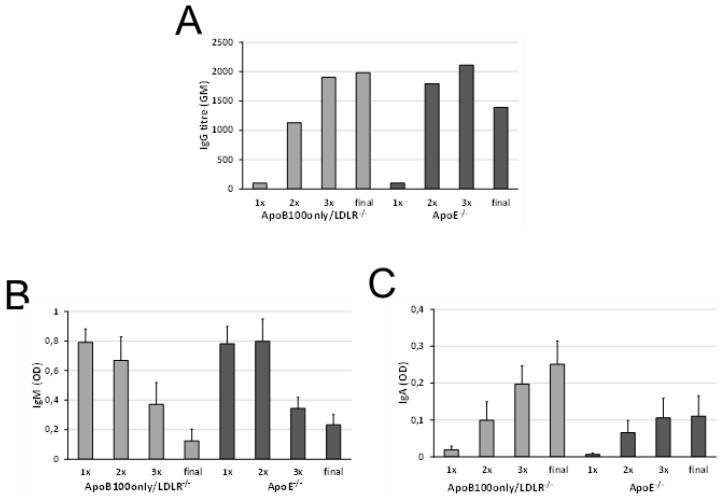

Figure 3. *Cpn* specific antibodies in the mice. The serum antibody levels were measured in ApoB100only/LDLR$^{-/-}$ and ApoE$^{-/-}$ mice 1 week after first (1x), second (2x), third (3x) *Cpn* infection and at the end of the experiment (week 12) by an in-house ELISA test with *Cpn* antigen. (A) Geometric mean (GM) of IgG titres – reciprocal of dilutions producing OD ≥0.1 is shown. (B) For detection of *Cpn* specific IgM and (C) IgA level in the sera 1:50 dilutions of serum samples (ApoB100only/LDLR$^{-/-}$: N=7, ApoE$^{-/-}$ mice: N=8) were tested with the ELISA test. OD values and standard deviations (SD) are shown. Data represent the results of one of two independent experiments.

4.5 The extent of atherosclerosis is similarly increased in the aorta of *Cpn*-infected and normal diet-fed ApoB100only/LDLR$^{-/-}$ and ApoE$^{-/-}$ mice

In normal chow-fed ApoB100only/LDLR$^{-/-}$ mice at the age of 24-25 weeks the lesions consisted of mainly single or multiple layers of macrophage foam cells but some more advanced plaques with cholesterol crystals and necrotic core were also seen. In ApoE$^{-/-}$ mice at same age more numerous advanced lesions with necrotic core and cholesterol cleft were found. In *Cpn*-infected ApoB100only/LDLR$^{-/-}$ mice larger advanced plaques and in infected ApoE$^{-/-}$mice more plaques with necrotic core and accumulated cholesterol crystals appeared. Representative sections from the experimental groups are shown in Figure 4A.

The measurements proved that in ApoE$^{-/-}$ mice the atherosclerosis was more pronounced than in ApoB100only/LDLR$^{-/-}$ mice. The difference was seen in respect of the size of plaque-occupied lumen area in the aortic sinus (Figure 4B) and the length of the plaque-covered aorta surface in the lumen (Figure 4C). Lesions in the descending aorta also were larger in ApoE$^{-/-}$ mice than in ApoB100only/LDLR$^{-/-}$ mice (Figures 4D, E). When the effect of *Cpn* infection was analysed, significant enhancement in the measured values was found. The plaque-covered perimeter of the lumen in the aorta sinus sections (Figure 4B), the plaque-occupied lumen area (Figure 4C), and the plaque size in the descending aorta (Figure 4E) increased 2.08 fold (P = 0.035), 1.7 fold (P = 0.004), 2.5 fold (P = 0.001), respectively in ApoB100only/LDLR$^{-/-}$, and 2.04 fold (P = 0.019), 1.32 fold (P = 0.026), 2.56 fold (P = 0.002), respectively in ApoE$^{-/-}$mice.

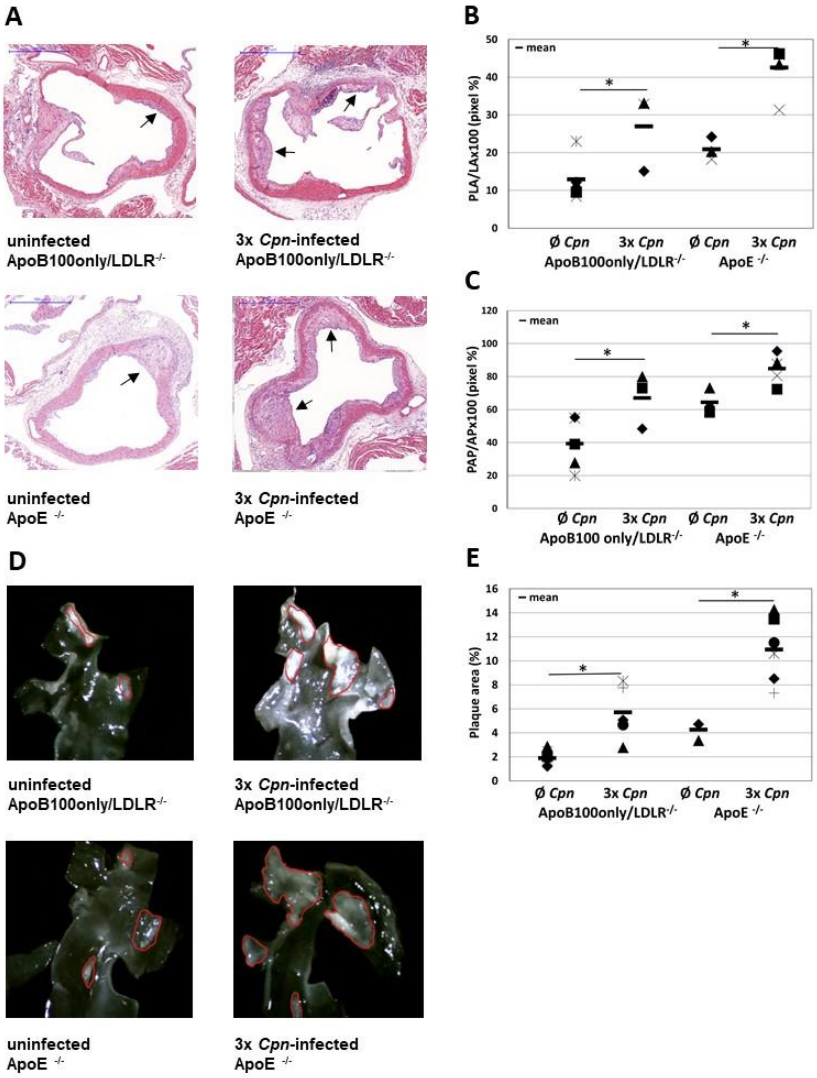

Figure 4. Comparative quantitative assessment of atherosclerosis in ApoB100only/LDLR$^{-/-}$ and ApoE$^{-/-}$ mice. Atherosclerosis development was assessed by histological and morphometric analyses in the aorta sinus and descending aorta of ApoB100only/LDLR$^{-/-}$ and ApoE$^{-/-}$ mice without and with 3 *Cpn* infections, 12 weeks after the first infection kept on normal diet. (A) Photo of representative hematoxylin and eosin-stained cross-sections of the non-infected and *Cpn*-infected ApoB100only/LDLR$^{-/-}$ mice and non-infected and *Cpn*-infected ApoE$^{-/-}$ mice (scale bar: 500 μm). Arrows point to atherosclerotic lesions. (B) The percentage length of the aortic luminal surface (perimeter) covered by atherosclerotic plaque (PAP/APx100); (C) percentage of aortic lumen area occupied by atherosclerotic plaques (PLA/LAx100) in 8 sections of aortic root from non-infected (N=6), *Cpn* infected (N=7) ApoB100only/LDLR$^{-/-}$, and non-infected (N=6) and *Cpn* infected (N=8) ApoE$^{-/-}$ mice. Average percentage values from individual mice and mean percentages in groups are shown. (D) *In situ* microscopic pictures of en face proximal aorta of non-infected and *Cpn*-infected ApoB100only/LDLR$^{-/-}$ and ApoE$^{-/-}$ mice, respectively. (E) Plaque size was measured on the length of the luminal surface of the descending aorta of 6-8 mice, and the percentage of total aorta area covered by plaques was calculated. Percentage values in individual mice and mean percentages in groups are shown.

Data demonstrate the results of one of two independent experiments. For comparison of groups independent-samples t-test was used, * $P<0.05$. PAP – plaque-covered aorta perimeter, AP - aorta perimeter, PLA - Plaque-occupied lumen area, LA - aorta lumen area, 3x – three intranasal *Cpn* infections.

4.6. Plasma lipid levels in ApoB100only/LDLR$^{-/-}$ and ApoE$^{-/-}$ mice

Plasma samples of mice were tested for lipid levels. At each tested time point irrespective of the infection status ApoE$^{-/-}$ mice carried a higher level of total cholesterol than the ApoB100only/LDLR$^{-/-}$ mice (Figure 5A). In the plasma of uninfected ApoB100only/LDLR$^{-/-}$ mice the triglyceride concentration was elevated compared to that in ApoE$^{-/-}$ mice (Figure 5B). Infection one or two times did not cause increase in triglyceride level, but the third *Cpn* inoculation resulted in a significant elevation (P = 0.001) in ApoE$^{-/-}$ mice. In ApoB100only/LDLR$^{-/-}$ mice no infection-related change in triglyceride level was obvious (Figure 5B). Plasma concentration of LDL was higher in ApoE$^{-/-}$ mice than in ApoB100only/LDLR$^{-/-}$ mice (Figure 5C). Infection-related significant increase in LDL level was associated with the first infection in ApoB100only/LDLR$^{-/-}$ mice only (P = 0.04). HDL plasma concentration was generally higher in ApoB100only/LDLR$^{-/-}$ mice than in ApoE$^{-/-}$ mice and in these mice the concentration decreased by the end of the observation period but remained high in ApoB100only/LDLR$^{-/-}$ mice (Figure 5D). No infection-associated change in HDL level was detected.

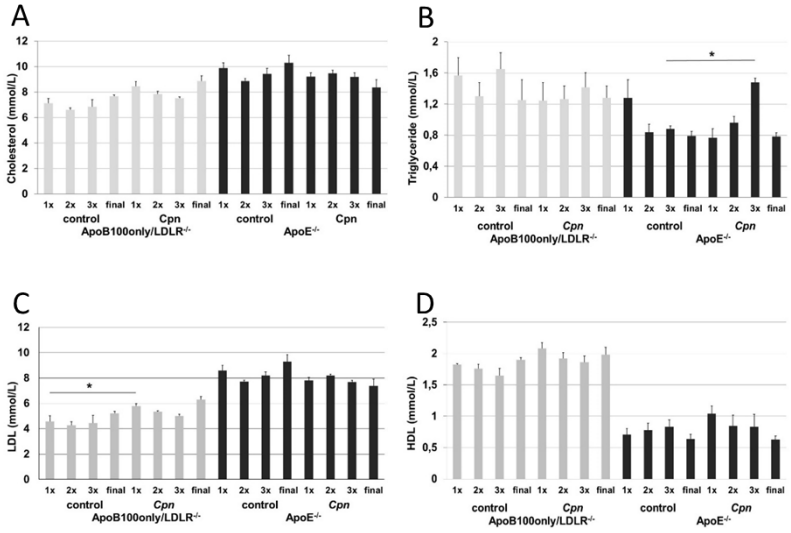

Figure 5. Plasma lipid levels in the mice. Plasma samples of ApoB100only/LDLR$^{-/-}$ and ApoE$^{-/-}$ mice taken at 1 week after the first (1x), second (2x), third (3x) *Cpn* infection and at the end

of the experiment (week 12) and from the non-infected control mice at the same time points were tested for concentration of (A) total cholesterol, (B) triglyceride, (C) LDL and (D) HDL content. Lipid concentrations are expressed as mmol/L, mean of values measured in individual mouse sera (ApoB100only/LDLR$^{-/-}$non-infected (N=6), *Cpn* infected (N=7), and ApoE$^{-/-}$ mice non-infected (N=6), *Cpn* infected (N=8)) and standard deviations (SD) are shown; independent-samples t-test was used, * P=0.01. The figure demonstrates the results of one of two independent experiments.

4.7. Detection of *Chlamydia* growth by immunofluorescence staining in Caco-2 and conventional host cells

After indirect immunofluorescence staining with anti-cLPS antibody, inclusions of *C. trachomatis* were seen in Caco-2 and HeLa cells. The detection of the inclusions suggested ongoing replication in both cell types; however, the morphology of the inclusions demonstrated different growth kinetics in the different cell types. *C. trachomatis* D formed compact inclusions in Caco-2 cells with cLPS appearing in the cell membrane (Figure 6A), and Hela cells showed inclusions with dense core and expanding cLPS signal at 24 h post-infection (Figure 6B); at 48 h in Caco-2 cells (Figure 6C) the inclusions grew larger but in the permissive HeLa cells expanding fluorescing areas had shown the final stage of replication cycle by this time (Figure 6D).

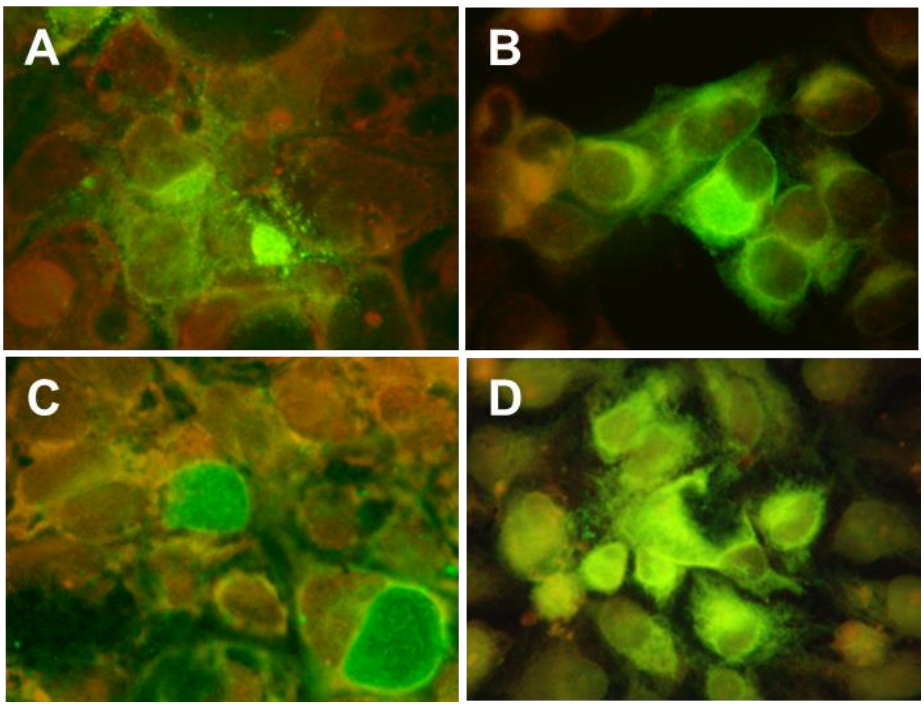

Figure 6. Immunofluorescence-stained inclusions of *C. trachomatis* D in Caco-2 and HeLa cells. The cells were grown on 13 mm coverslips, and the monolayers were infected at an MOI of 1. *C. trachomatis* D-infected Caco-2 cells were incubated for 24 h (A) or for 48 h (C), and *C. trachomatis* infected HeLa cells were incubated for 24 h (B) and for 48 h (D). After the indicated times, the cells were stained by indirect immunofluorescence using anti-cLPS antibody and FITC-labelled anti-mouse IgG secondary antibody. Pictures were acquired by a digital camera attached to a fluorescence microscope using 625-fold magnification.

4.8. Transmission electron microscopy of *Chlamydia* infected Caco-2 and conventional host cells

With TEM, *C. trachomatis* D inclusions were observed both in Caco-2 (Figure 7A, B) and HeLa (Figure 7C, D) cells. The developmental stage of the bacteria in the inclusions at 48 h post-infection was rather heterogeneous in Caco-2 cells; however, in HeLa cells fully developed inclusions with numerous EBs were seen.

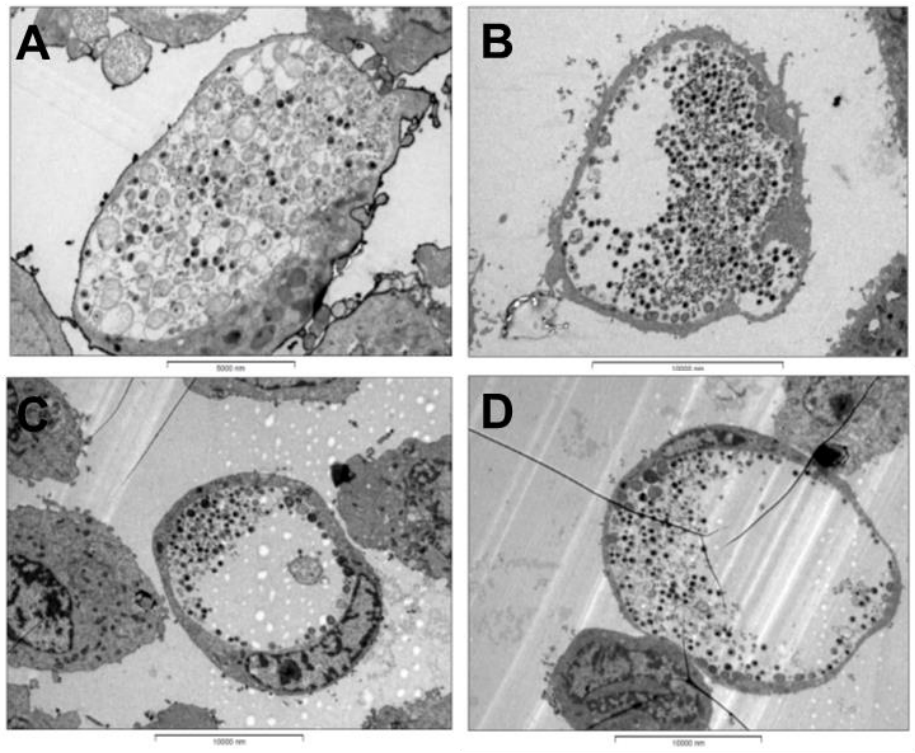

Figure 7. TEM images of *C. trachomatis* D inclusions in infected cells. Cells grown in 6-well plates were infected with chlamydiae at an MOI of 1. At the indicated time points after infection, the cells were fixed and processed for electron microscopy. Chlamydial inclusions in (A, B) *C. trachomatis* serovar D infected Caco-2 cells 48 h post-infection; (C, D) *C. trachomatis* D infected HeLa cells 48 h post-infection. Magnification is shown by the scale bars.

4.9. *Chlamydia* genome accumulation in Caco-2 and conventional host cells

The quantitative features of *Chlamydia* replication in the intestinal epithelial cells in comparison with that in conventional host cells were investigated with a novel DNA quantitation method [147]. We followed the accumulation of *Chlamydia* genomes during a 3-day culture period in Caco-2 and in HeLa cells. The lysates of infected cells were used as templates, and the quantity of chlamydial genomes was estimated with qPCR at different time points after infection. Fold increase in the amount of *pyk* gene of *C. trachomatis* was calculated in comparison with the amount detected at 0 h of infection. *C. trachomatis* growth seemed unrestricted in Caco-2 cells, chlamydia genomes propagated to similar amount by 72 h as in HeLa cells (Figure 8A). As suggested by the microscopic findings, the kinetics of replication followed a slower course in Caco-2 cells. In cycloheximide-free conditions, the yield was lower in Caco-2 cells and in HeLa cells, too (Figure 8B). In HeLa cells the replication peaked at 48 h and declined thereafter; the latter was not seen in Caco-2 cells. In Caco-2 cells, the effect of cycloheximide did not cause any major change in the course of the replication opposite to that in HeLa cells.

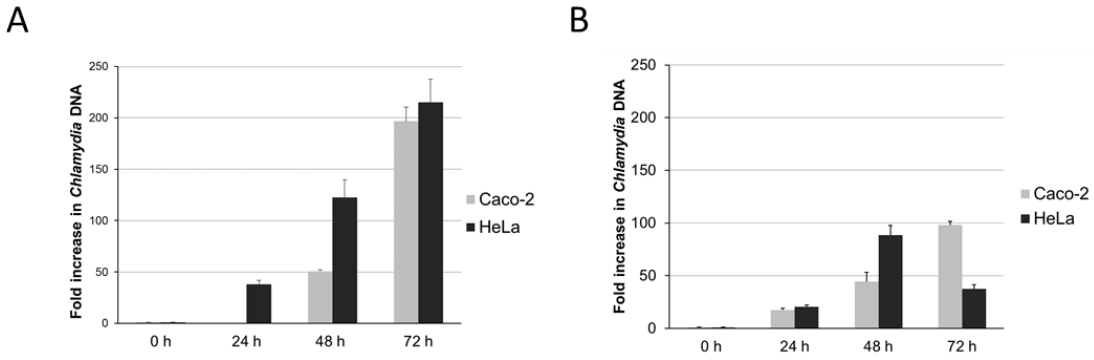

Figure 8. Analysis of *C. trachomatis* D growth based on the quantitation of chlamydial DNA by qPCR in *Chlamydia* infected cells. Caco-2 and HeLa cells were infected in 96-well plates at an MOI of 5 in a medium with cycloheximide or without cycloheximide; direct detection of *Chlamydia* genes in the lysate of infected cells was done at 0, 24, 48 and 72 h post-infection. Increase in the quantity of chlamydial DNA was compared to the quantities detected at 0 h of infection. (A) Increase in the amount of *C. trachomatis* D *pyk* gene in the presence of cycloheximide, and (B) in the absence of cycloheximide. The mean of fold change in 3 parallel cultures and SD is shown. The data represent the results of one of three independent experiments.

4.10. Production of infective *Chlamydia* progeny in Caco-2 and conventional host cells

In order to see whether the production of infective chlamydiae paralleled DNA accumulation, the infected cells were collected together with their supernatant, and the recoverable viable *C. trachomatis* bacteria were quantitated by inoculation of the sonicated cell in their media onto McCoy cells. Infective chlamydiae were recoverable showing that a full replication cycle takes place in Caco-2 cell line. The growth of *C. trachomatis* was somewhat delayed in Caco-2 cells, but at 72 h post-infection, similar amount of *C. trachomatis* was cultured from Caco-2 cells to that from HeLa cells (Figure 9).

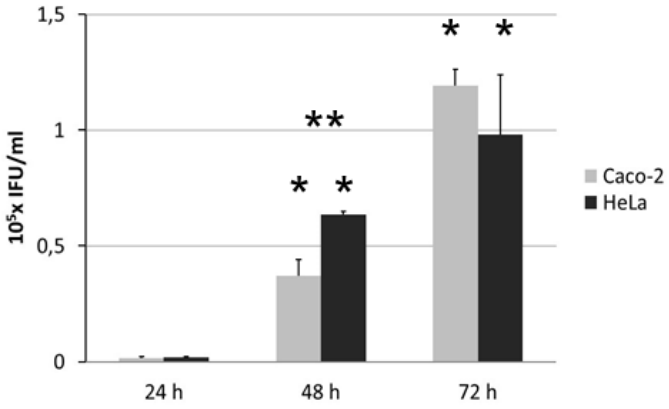

Figure 9. Kinetics of replication of *C. trachomatis* D in Caco-2 cells and in the conventional host cells as assayed by quantitation of recoverable infective bacteria. Lysates of *C. trachomatis* infected (MOI 5) Caco-2 and HeLa cells in their supernatants were collected at different time points after infection, and they were inoculated onto McCoy cells grown on cover slips. After 48 h incubation, the inclusions were visualized by immunofluorescence staining. The mean of titres expressed as IFU/mL in 3 parallel cultures and SDs are shown. The single asterisk (*) shows statistically significant differences between IFU values in the same cell type at different time points; the double asterisk (**) indicates statistically significant difference between values measured in supernatants of different cell types: $P<0.05$. The data represent the results of one of three independent experiments.

4.11. Transcript patterns for selected *Chlamydia* genes during infection of Caco-2 and conventional host cells

As the kinetics of *C. trachomatis* replication exhibited difference in Caco-2 cells compared to that in HeLa cells, we investigated the expression of selected *Chlamydia* genes

during a 3-day period. Intrinsic characteristics of the intestinal epithelial cells as growth environment could be reflected in a change of gene expression pattern of chlamydiae. The relative gene expression levels normalized to 16S rRNA expression are shown in Figure 10. At 24 h post-infection, the earliest time point evaluated, the relative expression of the early cluster gene *euo* (Figure 10A) was at much lower level in HeLa cells than in Caco-2 cells, and it increased at later time points, when the replication was already at lower rate. After 24 h, *euo* expression level moved to the opposite direction in Caco-2 cells in parallel with the continued replication.

The relative expression of *pyk, ompA, ftsK* and *omcB* (Figure 10) genes of *C. trachomatis* D followed similar trends in both examined cell lines, but the relative expression persisted at higher levels in Caco-2 cells than in HeLa cells. After 24 h, the level of *pyk* gene expression decreased gradually over time at similar rates (Figure 10B) in both examined cell lines. The highest level of *ompA* gene expression was observed at 24 h and persisted at high level for a longer time in Caco-2 than in HeLa cells (Figure 10E). The highest level of *ftsK* gene expression was observed at 24 h after infection, at the time of frequent cytokinesis, and it remained at high level in Caco-2 cells at later time points, too (Figure 10D). The expression of the late gene *omcB* peaked at 48 h post-infection with again a higher level in Caco-2 cells than in HeLa cells (Figure 10F).

Constantly high relative amount of *groEL* transcripts was observed in Caco-2 cells, including the earliest time point tested at 24 h (Figure 10C). An increased relative high rate of expression of *groEL* gene occurred only from 48 h post-infection in HeLa cells. Further analysis and summary of the above data are shown in Figure 10G on the ratios of gene expression values seen in Caco-2 cells versus that in HeLa cells. These data demonstrate the delayed and prolonged replication cycle in Caco-2 cells with higher *euo* expression at early time point (24 h) and decreased euo expression at late time point (72 h), with higher cytokinesis related (*ftsK*) and membrane protein gene (*ompA, omcB*) expressions at later time points in Caco-2 cells. An outstanding *groEL* gene transcription, especially at 24 h post-infection in Caco-2 cells, is detectable.

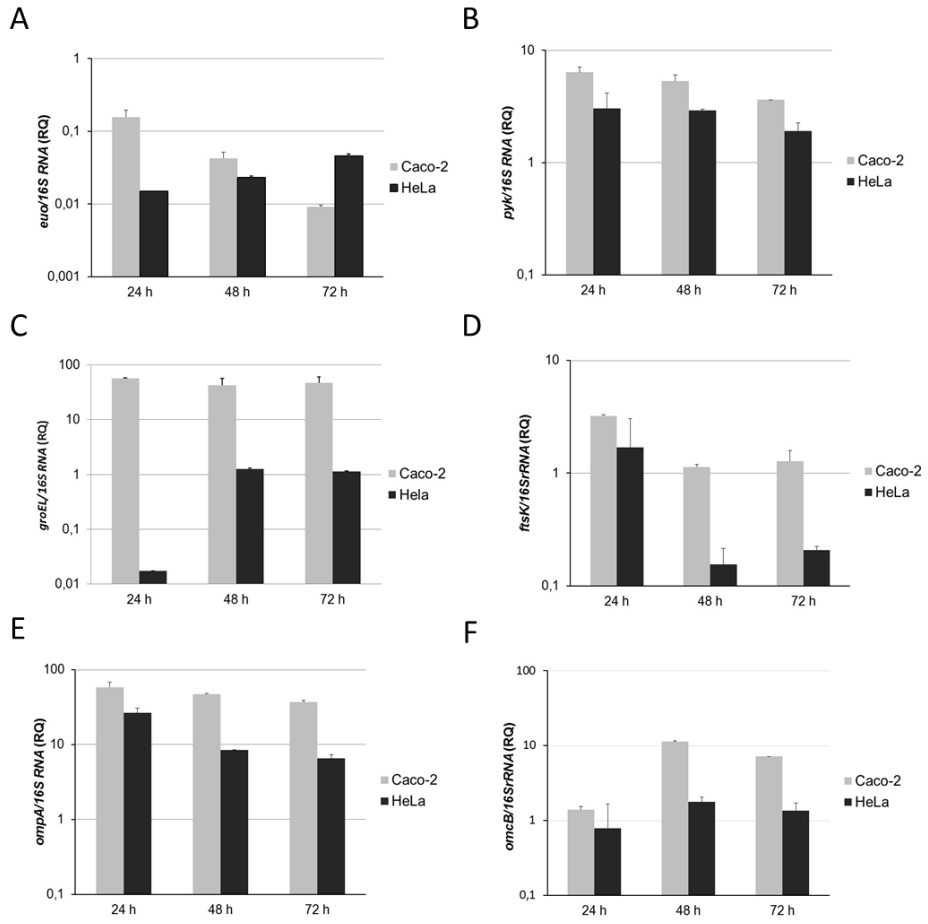

G

Gene	Caco-2/HeLa		
	24 h	48 h	72 h
euo	10,46	1,85	0,20
ftsK	1,90	7,32	6,16
groEL	3285,74	33,97	42,02
pyk	2,09	1,83	1,90
ompA	2,20	5,59	5,67
omcB	1,77	6,37	5,33

4000	10	2	0,1

Figure 10. The time course of relative expression of different *C. trachomatis* D genes in Caco-2 cells and in conventional permissive HeLa cells. cDNA was prepared from Caco-2 and HeLa cells at different time points (24, 48, 72 h) after infection with *C. trachomatis* D at an MOI of 5 in 6-well plates in a medium without cycloheximide. Real time qRT-PCR for quantitation of relative expression of (A) *euo*, (B) *pyk*, (C) *groEL*, (D) *ftsK*, (E) *ompA*, and (F) *omcB* genes was performed; the expression levels were normalized to *16S rRNA* gene expression. The fold change in relative expression levels is shown (RQ). The data represent the mean values and SD measured in three parallel samples of one of two independent experiments. (G) Calculated ratios of relative gene expression values detected in Caco-2 cells versus in HeLa cells are shown. A bar indicating the color scale for calculated differences is given: boxes with different shades of

red through white color denote increased expression; green colored boxes denote decreased expression.

4.12. HBD-2 inducing capability of *C. trachomatis* in Caco-2 cells

Since Caco-2 cells are intestinal mucosal epithelial cells, and this cell type has an important role as a physiological barrier for pathogens in the colon, and hBD-2 is induced by microbial molecules, it was investigated whether *C. trachomatis* was able to induce production of this antimicrobial peptide by Caco-2 cells. By hBD-2 ELISA, hBD-2 protein was detectable in high levels in the supernatant of Nissle-stimulated control Caco-2 cultures with a peak at 48 h post-treatment (Figure 11). *C. trachomatis* D-infected cells showed similar time course of hBD-2 release, however at a significantly lower level than in the case of stimulation with *E. coli* Nissle.

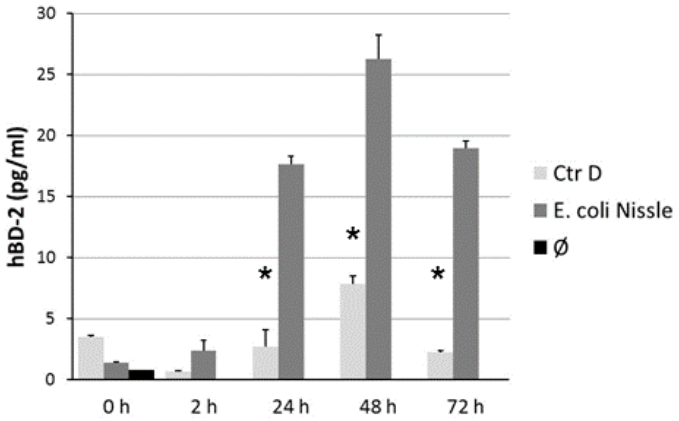

Figure 11. hBD-2 production by Caco-2 cells in response to *Chlamydia* infection. The supernatants of non-infected cells (ø) and the cells infected with *C. trachomatis* D (Ctr D) at an MOI of 5 or treated with heat-treated *E. coli* Nissle strain in 24-well plates were harvested at different time points post-infection. For the detection of hBD-2 production, the supernatants of the cells were tested by hBD-2 specific ELISA. The mean concentration values in 3 parallel cultures and SDs are shown. The asterisk (*) shows statistically significant differences between values measured in the supernatant of *Chlamydia* infected cells and values measured in supernatants of *E. coli* Nissle treated cells; $P<0.05$.

5. Discussion

5.1. Aim 1:

ApoE$^{-/-}$mice are widely used as animal models of atherosclerosis; however, the lipoprotein metabolism of this mouse strain is different from that in humans with hypercholesterolemia. ApoE$^{-/-}$ mice accumulate in their plasma large quantities of ApoB48 containing lipoprotein of the very low-density lipoprotein (VLDL) class while humans with atherosclerosis almost always have high level of cholesterol-rich LDL containing ApoB100 [93, 140]. Many publications investigating the relation of *Cpn* with atherosclerosis have used this model to disclose the nature of the association between infection with this pathogen and initiation and/or acceleration of atherosclerosis [29, 101, 149–151]. It has been suggested that *Cpn* infection exacerbate atherosclerosis in conjunction with hyperlipidaemia however ApoE deficiency might influence the immune response to this pathogen and provides increased resistance to vascular infection [150]. We aimed at examining the influence of repeated *Cpn* infection on the formation of atherosclerotic plaques in ApoB100only/LDLR$^{-/-}$ mouse strain another model for lipoprotein abnormalities which can be regarded as the most faithful model of human familial hypercholesterolemia [91].

ApoB100only/LDLR$^{-/-}$ mouse strain was created by genetic modification, so that majority of their plasma cholesterol is in the LDL class with ApoB100 and develops atherosclerosis on low-fat, chow diet. First, we wanted to establish that ApoB100only/LDLR$^{-/-}$ mice can serve as a model for investigating the role of *Cpn* in atherosclerosis. Therefore groups of mice were fed with a normal or high-fat/high-cholesterol diet and were repeatedly infected with *Cpn* or left uninfected, and development of atherosclerosis was followed. As our experiments showed, in ApoB100only/LDLR$^{-/-}$ mice which were fed with normal diet repeated three *Cpn* infections resulted in an enhanced atherosclerosis development in the aortic sinus and the descending aorta. High-fat/high-cholesterol diet-induced enhanced atherosclerosis was not exacerbated by *Cpn* infections. Thus all further experiments were done with mice kept on normal diet. As it is said that *Cpn* acts in cooperation with hyperlipidaemia it seems that the effect of hyperlipidaemia in ApoB100only/LDLR$^{-/-}$ mice can be aggravated by *Cpn* infection but *Cpn* does not exacerbate atherosclerosis further in the presence of high-fat/high-cholesterol diet [152–154]. Nevertheless, the bacterium influenced the course of atherosclerosis development indicating that ApoB100only/LDLR$^{-/-}$ mice are suitable for further research. Our

results are consistent with findings of Moazed et al. who described atherosclerosis-accelerating effect of *Cpn* infection in ApoE$^{-/-}$ mice eating regular chow diet [153]. However, atherosclerosis was also exacerbated in ApoE$^{-/-}$ mice kept on high fat diet by single or 3 repeated *Cpn* infections [29, 104].

We hypothesized that based on the genetic difference between ApoB100only/LDLR$^{-/-}$ and ApoE$^{-/-}$ mice, features that characterize *Cpn* infection or atherosclerosis may also differ, and therefore we compared the effects of the bacterium in these mouse strains. In our infection model the successful infection was demonstrated by detecting *Cpn*-specific IgG, IgA and IgM antibodies in the mice throughout the course of the experiment and at the time of sacrifice. When IgG antibody level was compared in ApoB100only/LDLR$^{-/-}$ and ApoE$^{-/-}$ mice, no significant difference was observed. Nazzal et al. [150] reported that ApoE$^{-/-}$ mice produced more *Cpn*-specific antibodies than wild-type mice which was attributed to ApoE deficiency. Our results do not support this suggestion considering that in ApoB100only/LDLR$^{-/-}$ mice repeated *Cpn* infection led to high level of antibody production without the contribution of ApoE deficiency.

Not only antibody response was the sign of infection, but we were able to detect metabolically active *Cpn* in the aorta samples for nine weeks after the first infection. Previous studies demonstrated the presence of *Cpn* in the aorta of repeatedly infected ApoE$^{-/-}$ mice by isolating the bacterium early two weeks after infection. Furthermore, bacterial DNA was amplified by PCR at later time points [155]. As reviewed by Campbell and Rosenfeld [156] several lines of evidence point to the ability of *Cpn* to establish persistent infection *in vivo*. Our results provide additional information about persisting chlamydiae as 16SrRNA gene transcripts suggest metabolically active bacteria not only persisting DNA or antigen late after repeated infections. Long-term presence of viable chlamydia in the aorta tissues of some infected mice might contribute to the atherogenic effect of the infection.

In female ApoE$^{-/-}$ mice we have disclosed more advanced atherosclerosis than in ApoB100only/LDLR$^{-/-}$ mice at the same age at the end of the 12-week observation period. Less pronounced difference was disclosed by Powell-Braxton et al. [91]. Nevertheless, in ApoE$^{-/-}$ mice, similarly to ApoB100only/LDLR$^{-/-}$ mice, the infection resulted in an enhanced lesion formation without the need of feeding the mice with high-fat diet confirming the results with ApoE$^{-/-}$ mice of Moazed et al. [153].

It has been described that *Cpn* can cause hepatic fatty acid imbalance [157] dysregulation of lipid metabolic genes in the liver [158], altered macrophage cholesterol homeostasis [159] however, most of the studies in mice did not detect major changes in plasma lipid profile after *Cpn* infection [29, 160]. Increase in triglyceride concentration after repeated infection of ApoE$^{-/-}$ mice similarly to our results has been noted by Rothstein et al. [142]. The reason of increase in triglyceride level in chronic infection induced by multiple inoculations in ApoE$^{-/-}$ mice may be the absence of ApoE. ApoE is known to provide protection against the inflammation induced by bacterial lipopolysaccharide [161] and the inflammation related change in lipid metabolism [162]. Early increase of LDL level in ApoB100only/LDLR$^{-/-}$ mice after primary infection may also be due to the primary infection caused inflammation [163]. Our findings are concordant with results of a study by Kontula et al [164] suggesting a significant association between chronic infection with *Cpn* and increased risk of coronary heart disease in patients with familial hypercholesterolemia.

5.2. Aim 2:

In this study, we investigated the morphological and molecular features of *Chlamydia trachomatis* infection in Caco-2 human intestinal cells. We selected this cell line for our investigation because it shows the characteristics of enterocytes, and in recent publications, the hypothesis of chlamydial persistence in the GI tract and the infected GI tract behaving a source of genital tract reinfection has been proposed [165]. Furthermore, *C. trachomatis* has been implicated in GI tract pathologies. As hBD-2 is produced by epithelial cells in the GI tract in response to infection as part of the innate defense [166], we tested the defensin inducing capability of *Chlamydia* in Caco-2 cells.

C. trachomatis D inclusions in Caco-2 cells visualized by immunofluorescence staining and TEM suggested similar but prolonged replication cycle of this *Chlamydia* strain compared to that in HeLa cells. The slower accumulation of chlamydiae was also detectable by finding lower amount of genomes and infective chlamydiae at 48 h post-infection in Caco-2 cells. However, by 72 h post–infection, the values had reflected similar level of chlamydial reproduction in the two cell lines. These results allow us to conclude that for this human genital *Chlamydia* strain, Caco-2 cells provide a growth-conducive environment. In case the growth medium of the host cells is supplemented with cycloheximide, *Chlamydia* replication cycle occurs in optimal conditions, where the host cell protein synthesis has less influence on the

bacterial growth. When cycloheximide was omitted from the medium, chlamydial genome accumulation reached a lower level and suffered early decline in HeLa cells, but this phenomenon was not as pronounced in Caco-2 cells. Gene expression analyses were done in the absence of cycloheximide, when the natural cellular environment would prevail.

It has been described that chlamydial developmental cycle is regulated at transcriptional level [8]. The change in the transcription profile has been demonstrated in *in vitro* models, where different stimuli (IFN-γ, penicillin) induced a persistent phase of chlamydiae. Certain cell types proved to be non-permissive for normal *Chlamydia* growth, and the transcription pattern suggested a persistent form of infection in these cells [167]. Since the growth kinetics in Caco-2 cells was found different from that in the optimal *in vitro* host cell line, we aimed to examine the expression of *C. trachomatis* genes in Caco-2 cells and compared it to that in HeLa cells. The expression level of selected chlamydial genes representing early (*euo*), mid-cycle (*ompA, groEL, pyk*) and late stage (*omcB*) replication cycles, and cell divisions related *ftsK* gene were analyzed and was normalized to the expression level of *16S rRNA* gene. As the *euo* gene products were described as suppressors of the late genes [168, 169], decreased expression of this gene could explain the higher expression level of *omcB* gene encoding the membrane protein of EBs [166] in Caco-2 cells, even at later time points during the infection. As EUO protein binding to *ftsK* promoter has been detected earlier [168], the persisting high level of the cytokinesis related *ftsK* gene might be associated with this decreased *euo* expression in Caco-2 cells. Transcripts from the *ftsK* gene required for cytokinesis were detectable at a relatively high level during the first day of *C. trachomatis* growth, when bacterial division occurs at the highest rate. It seems that cytokinesis dropped earlier in HeLa cells than in Caco-2 cells. The expression of the ATP synthesis related *pyk* gene of *C. trachomatis* declined in HeLa cells after 48 h. It occurred synchronously with the decrease in the amount of the chlamydial chromosome detected in this cell line. In concordance, longer high level of *pyk* expression paralleled a more extended genome accumulation in Caco-2 cells. The tendency of the change in *ompA* gene expression level was similar in both cell lines. *pyk* and *ompA* genes are regarded as genes of the mid-cycle [8], when reticulate bodies accumulate and EBs start to be formed. The *groEL* gene of *C. trachomatis*, a heat shock protein 60 (GroEL-1) encoding gene was highly upregulated throughout the observation period in Caco-2 cells. A stress response related increase in the

production of GroEL-1 has been described for *C. trachomatis* [170]. Our results suggest that replication of *C. trachomati*s in Caco-2 cells evoked a certain stress response by the bacteria.

It has been suggested that in the male and female reproductive tracts, small antibacterial molecules may contribute to a sustained inflammatory response [171], or they may control inflammatory and adaptive immune response [172]. According to Niyonsaba et al. [173], hBD-2 can be regarded as a potent chemoattractant of neutrophils. Increased hBD-2 expression could contribute to host defence by recruiting neutrophils. The role of hBDs in the attraction of immature dendritic cells and memory T cells to the site of microbial invasion [174] has been described. Expression of hBD has been reported in women with *C. trachomatis* positive cervicovaginal samples, albeit at a significantly lower level than in non-infected controls [175]. In our experiments with Caco-2 cell line, *C. trachomatis* infection induced the production of hBD-2 at a moderate level compared to the effect of a strong inducer, the *E.coli* Nissle strain. In a murine model of *C. muridarum* infection, oral application of the bacterium resulted in long carriage and a lack of inflammatory response in the large intestine; however, the infection of the genital tract was cleared after a short period and following inflammation at the infection site [176]. The low level of hBD-2 production by the *Chlamydia* infected Caco-2 cell line might be a sign of suppressed innate immune response, and potentially, a subsequently suppressed adaptive response as well.

In conclusion, Caco-2 cell line representing the epithelial cell lining in the large intestine seems to be a sufficiently permissive host cell for *C. trachomatis*, which primarily infects the genital tract, thus allowing these bacteria to survive at this body site. Together with the low hBD-2 inducing capacity, *C. trachomatis* might be able to replicate there without provoking an inflammatory response. These results seem to support the theory that the gastrointestinal tract could serve as a site of extra genital survival of chlamydiae, and it could potentially serve as a source of reinfection in the genital tract, especially in women. Our data have relevance to the published data on high co-occurrence of urogenital *Chlamydia* infection with anorectal infection in women [177]. Our data are also in concordance with the previously published data that more infected men are detected among homosexuals when rectal samples were taken [121].

6. Summary

Chlamydiae are ubiquitous obligate intracellular bacteria causing infection in the human eyes, urogenital and respiratory tract.

Chlamydia pneumoniae (*Cpn*) a common respiratory pathogen has been implicated in the pathomechanism of several chronic non-infectious diseases. Association between atherosclerosis and *Cpn* infection has been investigated most thoroughly. Hyperlipidaemia model animals have been used to elucidate the role of *Cpn* infection in atherosclerosis. The aims of this study were to investigate the proatherogenic effect of multiple *Cpn* infections in ApoB100only/LDLR$^{-/-}$ mice which based on the lipid profile can be regarded as the most suitable mouse model of human hypercholesterolemia, and to compare the lesion development to that in a major atherosclerosis model ApoE$^{-/-}$ mice. Aorta samples of ApoB100only/LDLR$^{-/-}$ mice infected three times with *Cpn* were subjected to morphometric analyses. RT-PCR was used for searching for viable *Cpn* was detected in the ascending aorta. Morphometric evaluation disclosed that *Cpn* infections exacerbated atherosclerosis development in the aortic root and descending aorta of the mice fed with normal diet but further increase in response to *Cpn* infection was not observed in the mice kept on high fat-high cholesterol diet. Chlamydial 16SrRNA expression showed the presence of viable *Cpn* in the aorta of infected animals. A similar rate of acceleration of atherosclerosis was observed when the infection protocol was applied in ApoB100only/LDLR$^{-/-}$ and in ApoE$^{-/-}$ mice. In conclusion, similarly to ApoE$^{-/-}$ mice, ApoB100only/LDLR$^{-/-}$ mice with more human relevant serum lipoprotein composition, develop increased atherosclerosis after *Cpn* infections thus this mouse strain can be used as a model of infection-related atherosclerosis enhancement and provide further evidence for the proatherogenic influence of *Cpn* in mice.

C. trachomatis causes infections of the eyes, urogenital and respiratory tracts. It is the most frequently identified sexually transmitted pathogen. Asymptomatic, repeat and chronic infections with *C. trachomatis* are common in the urogenital tract potentially causing severe reproductive pathology. Animal models of infection and epidemiological studies suggested the gastrointestinal tract as a reservoir of chlamydiae and as a source of repeat urogenital infections. Thus, we investigated the growth characteristics of *C. trachomatis* urogenital serovar D in human intestinal epithelial Caco-2 cells and the infection induced defensin production. Immunofluorescence staining and transmission electron microscopy showed the presence of chlamydial inclusions in the cells. Chlamydial DNA and viable *C. trachomatis* were recovered

from Caco-2 cells in similar quantity compared to that detected in the usual in vitro host cell of this bacterium. The kinetics of expression of selected *C. trachomatis* genes in Caco-2 cells indicated prolonged replication with persisting high expression level of late genes and of heat shock protein gene *groEL*. Replication of *C. trachomatis* induced moderate level of β-defensin-2 production by Caco-2 cells, which might contribute to avoidance of immune recognition in the intestine. According to our results, Caco-2 cells support *C. trachomatis* replication, suggesting that the gastrointestinal tract is a site of residence for these bacteria.

The following of our results are considered novel

- In ApoB100only/LDLR$^{-/-}$ mouse strain as another mouse model for lipoprotein abnormalities, repeated *Cpn* infection has exacerbating effect on the formation of atherosclerotic plaques.
- The enhanced atherosclerosis development in *Cpn* infected ApoB100only/LDLR$^{-/-}$ mice was observed in normal diet-fed animals but not on high fat/high cholesterol diet.
- Metabolically active *Cpn* was detected in the aorta samples with RT-PCR method.
- Caco-2 cells provide a growth-conducive environment for the human genital *C. trachomatis* strain.
- Growth characteristics of *C. trachomatis* D in Caco-2 cells suggested prolonged replication cycle of this *Chlamydia* strain compared to that in HeLa conventional host cells.
- The *groEL* gene of *C. trachomatis*, a heat shock protein 60 (GroEL-1) encoding gene was highly upregulated throughout the observation period in Caco-2 cells which might be a sign of stressful growth environment.
- In Caco-2 cell line *C. trachomatis* infection induced the production of hBD-2 at a moderate level which might be an immune evasion mechanism for the bacteria.

7. Összefoglalás

A chlamydiák széles körben elterjedt obligát intracelluláris baktériumok, melyek az emberi szem, az urogenitális és légutak fertőzését okozzák.

A *Chlamydia pneumoniae* (*Cpn*) egy gyakori légúti patogén, szerepe számos krónikus nem fertőző betegség patomechanizmusában felmerült. A legintenzívebben az ateroszklerosis és a *Cpn* közötti kapcsolatot vizsgálták. A *Cpn* fertőzés ateroszklerózisban betöltött szerepének vizsgálatára hiperlipidémiás állat modelleket alkalmaznak. A kísérleteink célja az volt, hogy megvizsgáljuk a többszöri *Cpn* fertőzés ateroszklerózis kialakulására gyakorolt hatását ApoB100only/LDLR$^{-/-}$ egerekben, melyek a szérum lipid profiljukat illetően az emberi familiáris hiperkoleszterinémia legmegfelelőbb modelljének tekinthetők, és hogy összehasonlítsuk az ateroszklerotikus léziók fejlődését az ApoB100only/LDLR$^{-/-}$ törzsben és a leggyakrabban használt ateroszklerózis modellnek számító ApoE$^{-/-}$ egerekben. *Cpn*-val háromszor fertőzött ApoB100only/LDLR$^{-/-}$ egerek aorta mintáit morfometriai analízisnek vetettük alá. Életképes *Cpn* kimutatása céljából a leszálló aortákat RT-PCR módszerrel vizsgáltuk. A morfomertiai kiértékelés feltárta, hogy a *Cpn* fertőzés fokozta az ateroszklerózis fejlődését az aortagyökben és a leszálló aortában normál diétán tartott egerekben, de nem okozott fokozást magas zsír/magas koleszterol tartalmú diétán tartott egerekben. A Chlamydia 16SrRNS gén expressziójának kimutatásával életképes *Cpn* jelenlétét igazoltuk a fertőzött egerek aortájában. Az ateroszklerózis fokozódásának hasonló mértékét figyeltük meg, amikor összehasonlítottuk az alkalmazott fertőzési protokoll hatását ApoB100only/LDLR$^{-/-}$ és ApoE$^{-/-}$ egerekben. Következtetésképpen elmondhatjuk, hogy az ApoE$^{-/-}$ egerekben megfigyeltekhez hasonlóan az ApoB100only/LDLR$^{-/-}$ egerekben - melyek szérum lipoprotein összetételük tekintetében jobban hasonlítanak hiperkoleszterinémiás emberekhez - fokozódott az ateroszklerózis fejlődése a *Cpn* fertőzés hatására, ezért ez az egér törzs alkalmas modellje lehet a fertőzéssel összefüggő ateroszklerósis fokozódás vizsgálatának és további bizonyítékot szolgáltat a *Cpn* fertőzés proatherogén hatására egerekben.

C. trachomatis a szem, az urogenitális traktus és a légutak fertőzését okozza. Ez a baktérium a leggyakrabban azonosított szexuális úton terjedő kórokozó. A tünetmentes, ismétlődő és krónikus *C. trachomatis* fertőzés gyakori az urogenitális traktusban, és súlyos reproduktív betegséget okozhat. A fertőzés állat modelljei és az epidemiológiai vizsgálatok azt

sugallják, hogy a GI traktusban tartózkodó *Chlamydia* lehet az ismételt urogenitális fertőzések forrása.

Ezért tanulmányoztuk a *C. trachomatis* urogenitális traktusban betegséget okozó szerovariánsának szaporodási tulajdonságait a human bél epitheliális Caco-2 sejtben, és vizsgáltuk a sejtek fertőzés által indukált defenzin termelését. Az immunfluoreszcens festés és a transzmissziós elektronmikroszkópia *Chlamydia* zárványok jelenlétét mutatta a sejtekben. Hasonló mennyiségben mutattunk ki Chlamydia DNS-t és életképes *C. trachomatis*-t Caco-2 sejtekben, mint a baktérium *in vitro* szaporítására általánosan használt gazdasejtben. A kiválasztott *C. trachomatis* gének kifejeződésének kinetikája elnyújtott szaporodási ciklusra utal Caco-2 sejtekben, amit a késői gének és a hősokk protein groEL-1 gén tartósan magas szinten való kifejeződése jelez. A *C. trachomatis* szaporodása alacsony szintű β-defensin-2 termelést váltott ki Caco-2 sejtekben, ami hozzájárulhat ahhoz, hogy a baktérium elkerülje a bélcsatornában működő immunrendszer általi felismerést. Eredményeink szerint a Caco-2 alkalmas gazdasejt a *C. trachomatis* szaporodásához, tehát a GI traktus a *C. trachomatis* baktérium tartózkodási helye lehet.

8. Acknowledgements

I would like to thank all of the people who have helped and inspired me during my Ph.D studies.

I would especially like to mention the following people:

Valéria Endrész Ph.D., my supervisor for sharing here knowledge. This thesis would not have been possible without her help and support.

Professor Yvette Mándi, head of Doctoral School of Interdisciplinary Medicine, former head of the Department of Medical Microbiology and Immunobiology for accepting me as Ph.D. student, and **Katalin Burián** the present head, for providing support and working facilities.

I wish to thank to **my fellow Ph.D. students** for creating great atmosphere at work.

Colleagues and **staff members** at the Department of Medical Microbiology are gratefully thanked for creating a supportive and pleasant environment.

I thank **Istvánné Lévai, Kitti Ürmös and Szilvia Urbán** for excellent technical assistance, **Krisztián Daru** for histotechnological and **Zsolt Rázga** for electron microscopy work.

All my **Friends**, for always being there and for having no idea what I do at work.

My **Family** and **Love** who have always supported, encouraged and believed in me.

This dissertation is dedicated to my **Mother** and **Father**.

This work was supported by Thrombosis Research Institute, London, UK; Human Resources Development Operational Programme EFOP-3.6.1-16-2016-00008.

9. References

1. Sachse, K., Laroucau, K., Riege, K., Wehner, S., Dilcher, M., Creasy, H.H., Weidmann, M., Myers, G., Vorimore, F., Vicari, N., Magnino, S., Liebler-Tenorio, E., Ruettger, A., Bavoil, P.M., Hufert, F.T., Rosselló-Móra, R., Marz, M.: Evidence for the existence of two new members of the family Chlamydiaceae and proposal of Chlamydia avium sp. nov. and Chlamydia gallinacea sp. nov. Syst. Appl. Microbiol. 37, 79–88 (2014). doi:10.1016/j.syapm.2013.12.004
2. Kalman, S., Mitchell, W., Marathe, R., Lammel, C., Fan, J., Hyman, R.W., Olinger, L., Grimwood, J., Davis, R.W., Stephens, R.S.: Comparative genomes of Chlamydia pneumoniae and C. trachomatis. Nat. Genet. 21, 385–389 (1999). doi:10.1038/7716
3. Beeckman, D.S.A., Vanrompay, D.C.G.: Zoonotic Chlamydophila psittaci infections from a clinical perspective. Clin. Microbiol. Infect. Off. Publ. Eur. Soc. Clin. Microbiol. Infect. Dis. 15, 11–17 (2009). doi:10.1111/j.1469-0691.2008.02669.x
4. Vivoda, M., Cirković, I., Aleksić, D., Ranin, L., Dukić, S.: [Biology and intracellular life of chlamydia]. Med. Pregl. 64, 561–564 (2011)
5. Beatty, W.L., Morrison, R.P., Byrne, G.I.: Persistent chlamydiae: from cell culture to a paradigm for chlamydial pathogenesis. Microbiol. Rev. 58, 686–699 (1994)
6. Abdelrahman, Y.M., Belland, R.J.: The chlamydial developmental cycle. FEMS Microbiol. Rev. 29, 949–959 (2005). doi:10.1016/j.femsre.2005.03.002
7. E, B.A. and B.: Chlamydophila pneumoniae. - PubMed - NCBI, https://www.ncbi.nlm.nih.gov/pubmed/20171546
8. Nicholson, T.L., Olinger, L., Chong, K., Schoolnik, G., Stephens, R.S.: Global stage-specific gene regulation during the developmental cycle of Chlamydia trachomatis. J. Bacteriol. 185, 3179–3189 (2003)
9. Roulis, E., Polkinghorne, A., Timms, P.: Chlamydia pneumoniae: modern insights into an ancient pathogen. Trends Microbiol. 21, 120–128 (2013). doi:10.1016/j.tim.2012.10.009
10. Rosario, C.J., Hanson, B.R., Tan, M.: The transcriptional repressor EUO regulates both subsets of Chlamydia late genes. Mol. Microbiol. 94, 888–897 (2014). doi:10.1111/mmi.12804
11. Mathews, S., George, C., Flegg, C., Stenzel, D., Timms, P.: Differential expression of ompA, ompB, pyk, nlpD and Cpn0585 genes between normal and interferon-gamma treated cultures of Chlamydia pneumoniae. Microb. Pathog. 30, 337–345 (2001). doi:10.1006/mpat.2000.0435
12. Belland, R.J., Nelson, D.E., Virok, D., Crane, D.D., Hogan, D., Sturdevant, D., Beatty, W.L., Caldwell, H.D.: Transcriptome analysis of chlamydial growth during IFN-gamma-mediated persistence and reactivation. Proc. Natl. Acad. Sci. U. S. A. 100, 15971–15976 (2003). doi:10.1073/pnas.2535394100
13. Kokab, A., Jennings, R., Eley, A., Pacey, A.A., Cross, N.A.: Analysis of modulated gene expression in a model of Interferon-γ-induced persistence of Chlamydia trachomatis in HEp-2 cells. Microb. Pathog. 49, 217–225 (2010). doi:10.1016/j.micpath.2010.06.002
14. Kintner, J., Lajoie, D., Hall, J., Whittimore, J., Schoborg, R.V.: Commonly prescribed β-lactam antibiotics induce C. trachomatis persistence/stress in culture at

physiologically relevant concentrations. Front. Cell. Infect. Microbiol. 4, 44 (2014). doi:10.3389/fcimb.2014.00044
15. Phillips-Campbell, R., Kintner, J., Schoborg, R.V.: Induction of the Chlamydia muridarum stress/persistence response increases azithromycin treatment failure in a murine model of infection. Antimicrob. Agents Chemother. 58, 1782–1784 (2014). doi:10.1128/AAC.02097-13
16. Mäurer, A.P., Mehlitz, A., Mollenkopf, H.J., Meyer, T.F.: Gene expression profiles of Chlamydophila pneumoniae during the developmental cycle and iron depletion-mediated persistence. PLoS Pathog. 3, e83 (2007). doi:10.1371/journal.ppat.0030083
17. Datta, B., Njau, F., Thalmann, J., Haller, H., Wagner, A.D.: Differential infection outcome of Chlamydia trachomatis in human blood monocytes and monocyte-derived dendritic cells. BMC Microbiol. 14, 209 (2014). doi:10.1186/s12866-014-0209-3
18. Datta, B., Njau, F., Thalmann, J., Haller, H., Wagner, A.D.: Differential infection outcome of Chlamydia trachomatis in human blood monocytes and monocyte-derived dendritic cells. BMC Microbiol. 14, 209 (2014). doi:10.1186/s12866-014-0209-3
19. Gieffers, J., van Zandbergen, G., Rupp, J., Sayk, F., Krüger, S., Ehlers, S., Solbach, W., Maass, M.: Phagocytes transmit Chlamydia pneumoniae from the lungs to the vasculature. Eur. Respir. J. 23, 506–510 (2004)
20. Blasi, F., Tarsia, P., Aliberti, S.: Chlamydophila pneumoniae. Clin. Microbiol. Infect. Off. Publ. Eur. Soc. Clin. Microbiol. Infect. Dis. 15, 29–35 (2009). doi:10.1111/j.1469-0691.2008.02130.x
21. Hahn, D.L., Anttila, T., Saikku, P.: Association of Chlamydia pneumoniae IgA antibodies with recently symptomatic asthma. Epidemiol. Infect. 117, 513–517 (1996)
22. Johnston, S.L., Martin, R.J.: Chlamydophila pneumoniae and Mycoplasma pneumoniae: a role in asthma pathogenesis? Am. J. Respir. Crit. Care Med. 172, 1078–1089 (2005). doi:10.1164/rccm.200412-1743PP
23. Pawate, S., Sriram, S.: The role of infections in the pathogenesis and course of multiple sclerosis. Ann. Indian Acad. Neurol. 13, 80–86 (2010). doi:10.4103/0972-2327.64622
24. Turgut, B., Uyar, F., Ilhan, F., Demir, T., Celiker, U.: Mycoplasma pneumoniae and Chlamydia pneumoniae seropositivity in patients with age-related macular degeneration. J. Clin. Med. Res. 2, 85–89 (2010). doi:10.4021/jocmr2010.03.282w
25. Hammond, C.J., Hallock, L.R., Howanski, R.J., Appelt, D.M., Little, C.S., Balin, B.J.: Immunohistological detection of Chlamydia pneumoniae in the Alzheimer's disease brain. BMC Neurosci. 11, 121 (2010). doi:10.1186/1471-2202-11-121
26. Chia, J.K., Chia, L.Y.: Chronic Chlamydia pneumoniae infection: a treatable cause of chronic fatigue syndrome. Clin. Infect. Dis. Off. Publ. Infect. Dis. Soc. Am. 29, 452–453 (1999). doi:10.1086/520239
27. King, L.E., Stratton, C.W., Mitchell, W.M.: Chlamydia pneumoniae and chronic skin wounds: a focused review. J. Investig. Dermatol. Symp. Proc. 6, 233–237 (2001). doi:10.1046/j.0022-202x.2001.00050.x
28. Watson, C., Alp, N.J.: Role of Chlamydia pneumoniae in atherosclerosis. Clin. Sci. Lond. Engl. 1979. 114, 509–531 (2008). doi:10.1042/CS20070298
29. Sorrentino, R., Yilmaz, A., Schubert, K., Crother, T.R., Pinto, A., Shimada, K., Arditi, M., Chen, S.: A single infection with Chlamydia pneumoniae is sufficient to exacerbate atherosclerosis in ApoE deficient mice. Cell. Immunol. 294, 25–32 (2015). doi:10.1016/j.cellimm.2015.01.007

30. Honarmand, H.: Atherosclerosis Induced by Chlamydophila pneumoniae: A Controversial Theory. Interdiscip. Perspect. Infect. Dis. 2013, 941392 (2013). doi:10.1155/2013/941392
31. Fazio, G., Giovino, M., Gullotti, A., Bacarella, D., Novo, G., Novo, S.: Atherosclerosis, inflammation and Chlamydia pneumoniae. World J. Cardiol. 1, 31–40 (2009). doi:10.4330/wjc.v1.i1.31
32. Belland, R.J., Ouellette, S.P., Gieffers, J., Byrne, G.I.: Chlamydia pneumoniae and atherosclerosis. Cell. Microbiol. 6, 117–127 (2004)
33. Weber, C., Noels, H.: Atherosclerosis: current pathogenesis and therapeutic options. Nat. Med. 17, 1410–1422 (2011). doi:10.1038/nm.2538
34. Campbell, L.A., Rosenfeld, M.E.: Infection and Atherosclerosis Development. Arch. Med. Res. 46, 339–350 (2015). doi:10.1016/j.arcmed.2015.05.006
35. Saeed, A., Ballantyne, C.M.: Assessing Cardiovascular Risk and Testing in Type 2 Diabetes. Curr. Cardiol. Rep. 19, 19 (2017). doi:10.1007/s11886-017-0831-4
36. Gordon, P., Flanagan, P.: Smoking: A risk factor for vascular disease. J. Vasc. Nurs. Off. Publ. Soc. Peripher. Vasc. Nurs. 34, 79–86 (2016). doi:10.1016/j.jvn.2016.04.001
37. Leong, X.-F., Ng, C.-Y., Jaarin, K.: Animal Models in Cardiovascular Research: Hypertension and Atherosclerosis. BioMed Res. Int. 2015, 528757 (2015). doi:10.1155/2015/528757
38. Baumer, Y., McCurdy, S., Weatherby, T.M., Mehta, N.N., Halbherr, S., Halbherr, P., Yamazaki, N., Boisvert, W.A.: Hyperlipidemia-induced cholesterol crystal production by endothelial cells promotes atherogenesis. Nat. Commun. 8, 1129 (2017). doi:10.1038/s41467-017-01186-z
39. van Rooy, M.-J., Pretorius, E.: Obesity, hypertension and hypercholesterolemia as risk factors for atherosclerosis leading to ischemic events. Curr. Med. Chem. 21, 2121–2129 (2014)
40. Lloyd-Jones, D., Adams, R., Carnethon, M., De Simone, G., Ferguson, T.B., Flegal, K., Ford, E., Furie, K., Go, A., Greenlund, K., Haase, N., Hailpern, S., Ho, M., Howard, V., Kissela, B., Kittner, S., Lackland, D., Lisabeth, L., Marelli, A., McDermott, M., Meigs, J., Mozaffarian, D., Nichol, G., O'Donnell, C., Roger, V., Rosamond, W., Sacco, R., Sorlie, P., Stafford, R., Steinberger, J., Thom, T., Wasserthiel-Smoller, S., Wong, N., Wylie-Rosett, J., Hong, Y., American Heart Association Statistics Committee and Stroke Statistics Subcommittee: Heart disease and stroke statistics--2009 update: a report from the American Heart Association Statistics Committee and Stroke Statistics Subcommittee. Circulation. 119, 480–486 (2009). doi:10.1161/CIRCULATIONAHA.108.191259
41. Bentzon, J.F., Otsuka, F., Virmani, R., Falk, E.: Mechanisms of plaque formation and rupture. Circ. Res. 114, 1852–1866 (2014). doi:10.1161/CIRCRESAHA.114.302721
42. Strong, J.P., Malcom, G.T., Newman, W.P., Oalmann, M.C.: Early lesions of atherosclerosis in childhood and youth: natural history and risk factors. J. Am. Coll. Nutr. 11 Suppl, 51S-54S (1992)
43. Natural history of aortic and coronary atherosclerotic lesions in youth. Findings from the PDAY Study. Pathobiological Determinants of Atherosclerosis in Youth (PDAY) Research Group. Arterioscler. Thromb. J. Vasc. Biol. Am. Heart Assoc. 13, 1291–1298 (1993)

44. Badimon, L., Storey, R.F., Vilahur, G.: Update on lipids, inflammation and atherothrombosis. Thromb. Haemost. 105 Suppl 1, S34-42 (2011). doi:10.1160/THS10-11-0717
45. Lusis, A.J.: Atherosclerosis. Nature. 407, 233–241 (2000). doi:10.1038/35025203
46. Aikawa, M., Rabkin, E., Voglic, S.J., Shing, H., Nagai, R., Schoen, F.J., Libby, P.: Lipid lowering promotes accumulation of mature smooth muscle cells expressing smooth muscle myosin heavy chain isoforms in rabbit atheroma. Circ. Res. 83, 1015–1026 (1998)
47. Libby, P., Ridker, P.M., Hansson, G.K., Leducq Transatlantic Network on Atherothrombosis: Inflammation in atherosclerosis: from pathophysiology to practice. J. Am. Coll. Cardiol. 54, 2129–2138 (2009). doi:10.1016/j.jacc.2009.09.009
48. Muhlestein, J.B., Horne, B.D., Carlquist, J.F., Madsen, T.E., Bair, T.L., Pearson, R.R., Anderson, J.L.: Cytomegalovirus seropositivity and C-reactive protein have independent and combined predictive value for mortality in patients with angiographically demonstrated coronary artery disease. Circulation. 102, 1917–1923 (2000)
49. Kurita-Ochiai, T., Jia, R., Cai, Y., Yamaguchi, Y., Yamamoto, M.: Periodontal Disease-Induced Atherosclerosis and Oxidative Stress. Antioxid. Basel Switz. 4, 577–590 (2015). doi:10.3390/antiox4030577
50. Fernandes, L.R., Ribeiro, A.C.C., Segatto, M., Santos, L.F.F.F., Amaral, J., Portugal, L.R., Leite, J.I.A.: Leishmania major Self-Limited Infection Increases Blood Cholesterol and Promotes Atherosclerosis Development. Cholesterol. 2013, 754580 (2013). doi:10.1155/2013/754580
51. Fabricant, C.G., Fabricant, J.: Atherosclerosis induced by infection with Marek's disease herpesvirus in chickens. Am. Heart J. 138, S465-468 (1999)
52. Rosenfeld, M.E., Campbell, L.A.: Pathogens and atherosclerosis: update on the potential contribution of multiple infectious organisms to the pathogenesis of atherosclerosis. Thromb. Haemost. 106, 858–867 (2011). doi:10.1160/TH11-06-0392
53. Assar, O., Nejatizadeh, A., Dehghan, F., Kargar, M., Zolghadri, N.: Association of Chlamydia pneumoniae Infection With Atherosclerotic Plaque Formation. Glob. J. Health Sci. 8, 48916 (2016). doi:10.5539/gjhs.v8n4p260
54. Bayram, A., Erdoğan, M.B., Ekşi, F., Yamak, B.: Demonstration of Chlamydophila pneumoniae, Mycoplasma pneumoniae, Cytomegalovirus, and Epstein-Barr virus in atherosclerotic coronary arteries, nonrheumatic calcific aortic and rheumatic stenotic mitral valves by polymerase chain reaction. Anadolu Kardiyol. Derg. AKD Anatol. J. Cardiol. 11, 237–243 (2011). doi:10.5152/akd.2011.057
55. Tewari, R., Nijhawan, V., Mishra, M., Dudeja, P., Salopal, T.: Prevalence of Helicobacter pylori, cytomegalovirus, and Chlamydia pneumoniae immunoglobulin seropositivity in coronary artery disease patients and normal individuals in North Indian population. Med. J. Armed Forces India. 68, 53–57 (2012). doi:10.1016/S0377-1237(11)60121-4
56. Rafferty, B., Dolgilevich, S., Kalachikov, S., Morozova, I., Ju, J., Whittier, S., Nowygrod, R., Kozarov, E.: Cultivation of Enterobacter hormaechei from human atherosclerotic tissue. J. Atheroscler. Thromb. 18, 72–81 (2011)
57. Padilla, C., Lobos, O., Hubert, E., González, C., Matus, S., Pereira, M., Hasbun, S., Descouvieres, C.: Periodontal pathogens in atheromatous plaques isolated from patients

with chronic periodontitis. J. Periodontal Res. 41, 350–353 (2006). doi:10.1111/j.1600-0765.2006.00882.x
58. Rath, S.K., Mukherjee, M., Kaushik, R., Sen, S., Kumar, M.: Periodontal pathogens in atheromatous plaque. Indian J. Pathol. Microbiol. 57, 259–264 (2014). doi:10.4103/0377-4929.134704
59. Priyanka, S., Kaarthikeyan, G., Nadathur, J.D., Mohanraj, A., Kavarthapu, A.: Detection of cytomegalovirus, Epstein-Barr virus, and Torque Teno virus in subgingival and atheromatous plaques of cardiac patients with chronic periodontitis. J. Indian Soc. Periodontol. 21, 456–460 (2017). doi:10.4103/jisp.jisp_205_17
60. Babiker, A., Jeudy, J., Kligerman, S., Khambaty, M., Shah, A., Bagchi, S.: Risk of Cardiovascular Disease Due to Chronic Hepatitis C Infection: A Review. J. Clin. Transl. Hepatol. 5, 343–362 (2017). doi:10.14218/JCTH.2017.00021
61. Zizza, A., Guido, M., Tumolo, M.R., De Donno, A., Bagordo, F., Grima, P.: Atherosclerosis is associated with a higher risk of hepatic steatosis in HIV-infected patients. J. Prev. Med. Hyg. 58, E219–E224 (2017)
62. Wu, Y.P., Sun, D.D., Wang, Y., Liu, W., Yang, J.: Herpes Simplex Virus Type 1 and Type 2 Infection Increases Atherosclerosis Risk: Evidence Based on a Meta-Analysis. BioMed Res. Int. 2016, 2630865 (2016). doi:10.1155/2016/2630865
63. Binkley, P.F., Cooke, G.E., Lesinski, A., Taylor, M., Chen, M., Laskowski, B., Waldman, W.J., Ariza, M.E., Williams, M.V., Knight, D.A., Glaser, R.: Evidence for the role of Epstein Barr Virus infections in the pathogenesis of acute coronary events. PloS One. 8, e54008 (2013). doi:10.1371/journal.pone.0054008
64. Kwon, T.W., Kim, D.K., Ye, J.S., Lee, W.J., Moon, M.S., Joo, C.H., Lee, H., Kim, Y.K.: Detection of enterovirus, cytomegalovirus, and Chlamydia pneumoniae in atheromas. J. Microbiol. Seoul Korea. 42, 299–304 (2004)
65. Liu, S.-C., Tsai, C.-T., Wu, C.-K., Yu, M.-F., Wu, M.-Z., Lin, L.-I., Wang, S.-S., Hwang, J.-J., Tseng, Y.-Z., Chiang, F.-T., Tseng, C.-D.: Human parvovirus b19 infection in patients with coronary atherosclerosis. Arch. Med. Res. 40, 612–617 (2009). doi:10.1016/j.arcmed.2009.09.002
66. Ramirez, J.A.: Isolation of Chlamydia pneumoniae from the coronary artery of a patient with coronary atherosclerosis. The Chlamydia pneumoniae/Atherosclerosis Study Group. Ann. Intern. Med. 125, 979–982 (1996)
67. Saikku, P., Leinonen, M., Mattila, K., Ekman, M.R., Nieminen, M.S., Mäkelä, P.H., Huttunen, J.K., Valtonen, V.: Serological evidence of an association of a novel Chlamydia, TWAR, with chronic coronary heart disease and acute myocardial infarction. Lancet Lond. Engl. 2, 983–986 (1988)
68. Pigarevskii, P.V., Mal'tseva, S.V., Snegova, V.A., Davydova, N.G., Guseva, V.A.: Chlamydia Pneumoniae and Immunoinflammatory Reactions in an Unstable Atherosclerotic Plaque in Humans. Bull. Exp. Biol. Med. 159, 278–281 (2015). doi:10.1007/s10517-015-2941-6
69. Dabiri, H., Rezadehbashi, M., Badami, N., Aghanouri, R., Ahmadi, H., Khoramizadeh, M.R., Emaneini, M., Izadi, M., Zali, M.R.: Detection of Chlamydia pneumoniae in atherosclerotic plaques of patients in Tehran, Iran. Jpn. J. Infect. Dis. 62, 195–197 (2009)
70. Bloemenkamp, D.G.M., Mali, W.P.T.M., Visseren, F.L.J., van der Graaf, Y.: Meta-analysis of sero-epidemiologic studies of the relation between Chlamydia pneumoniae

and atherosclerosis: does study design influence results? Am. Heart J. 145, 409–417 (2003). doi:10.1067/mhj.2003.20

71. Puolakkainen, M., Kuo, C.C., Shor, A., Wang, S.P., Grayston, J.T., Campbell, L.A.: Serological response to Chlamydia pneumoniae in adults with coronary arterial fatty streaks and fibrolipid plaques. J. Clin. Microbiol. 31, 2212–2214 (1993)
72. Shor, A., Phillips, J.I.: Histological and ultrastructural findings suggesting an initiating role for Chlamydia pneumoniae in the pathogenesis of atherosclerosis. Cardiovasc. J. South Afr. Off. J. South. Afr. Card. Soc. South Afr. Soc. Card. Pract. 11, 16–23 (2000)
73. Shor, A., Kuo, C.C., Patton, D.L.: Detection of Chlamydia pneumoniae in coronary arterial fatty streaks and atheromatous plaques. South Afr. Med. J. Suid-Afr. Tydskr. Vir Geneeskd. 82, 158–161 (1992)
74. Kuo, C.C., Shor, A., Campbell, L.A., Fukushi, H., Patton, D.L., Grayston, J.T.: Demonstration of Chlamydia pneumoniae in atherosclerotic lesions of coronary arteries. J. Infect. Dis. 167, 841–849 (1993)
75. Boman, J., Söderberg, S., Forsberg, J., Birgander, L.S., Allard, A., Persson, K., Jidell, E., Kumlin, U., Juto, P., Waldenström, A., Wadell, G.: High prevalence of Chlamydia pneumoniae DNA in peripheral blood mononuclear cells in patients with cardiovascular disease and in middle-aged blood donors. J. Infect. Dis. 178, 274–277 (1998)
76. Maass, M., Bartels, C., Engel, P.M., Mamat, U., Sievers, H.H.: Endovascular presence of viable Chlamydia pneumoniae is a common phenomenon in coronary artery disease. J. Am. Coll. Cardiol. 31, 827–832 (1998)
77. Jackson, L.A., Campbell, L.A., Kuo, C.C., Rodriguez, D.I., Lee, A., Grayston, J.T.: Isolation of Chlamydia pneumoniae from a carotid endarterectomy specimen. J. Infect. Dis. 176, 292–295 (1997)
78. Rödel, J., Woytas, M., Groh, A., Schmidt, K.H., Hartmann, M., Lehmann, M., Straube, E.: Production of basic fibroblast growth factor and interleukin 6 by human smooth muscle cells following infection with Chlamydia pneumoniae. Infect. Immun. 68, 3635–3641 (2000)
79. Molestina, R.E., Miller, R.D., Ramirez, J.A., Summersgill, J.T.: Infection of human endothelial cells with Chlamydia pneumoniae stimulates transendothelial migration of neutrophils and monocytes. Infect. Immun. 67, 1323–1330 (1999)
80. Yang, Z.P., Kuo, C.C., Grayston, J.T.: Systemic dissemination of Chlamydia pneumoniae following intranasal inoculation in mice. J. Infect. Dis. 171, 736–738 (1995)
81. Kalayoglu, M.V., Hoerneman, B., LaVerda, D., Morrison, S.G., Morrison, R.P., Byrne, G.I.: Cellular Oxidation of Low- Density Lipoprotein by *Chlamydia pneumoniae*. J. Infect. Dis. 180, 780–790 (1999). doi:10.1086/314931
82. Campbell, L.A., Puolakkainen, M., Lee, A., Rosenfeld, M.E., Garrigues, H.J., Kuo, C.-C.: Chlamydia pneumoniae binds to the lectin-like oxidized LDL receptor for infection of endothelial cells. Microbes Infect. 14, 43–49 (2012). doi:10.1016/j.micinf.2011.08.003
83. Campbell, L.A., Lee, A.W., Rosenfeld, M.E., Kuo, C.: Chlamydia pneumoniae induces expression of proatherogenic factors through activation of the lectin-like oxidized LDL receptor-1. Pathog. Dis. 69, 1–6 (2013). doi:10.1111/2049-632X.12058
84. Netea, M.G., Kullberg, B.J., Jacobs, L.E.H., Verver-Jansen, T.J.G., van der Ven-Jongekrijg, J., Galama, J.M.D., Stalenhoef, A.F.H., Dinarello, C.A., Van der Meer,

J.W.M.: Chlamydia pneumoniae stimulates IFN-gamma synthesis through MyD88-dependent, TLR2- and TLR4-independent induction of IL-18 release. J. Immunol. Baltim. Md 1950. 173, 1477–1482 (2004)
85. Campbell, L.A., Blessing, E., Rosenfeld, M., Lin, T. m, Kuo, C.: Mouse models of C. pneumoniae infection and atherosclerosis. J. Infect. Dis. 181 Suppl 3, S508-513 (2000). doi:10.1086/315629
86. Xiangdong, L., Yuanwu, L., Hua, Z., Liming, R., Qiuyan, L., Ning, L.: Animal models for the atherosclerosis research: a review. Protein Cell. 2, 189–201 (2011). doi:10.1007/s13238-011-1016-3
87. Ezzahiri, R., Stassen, F.R.M., Kurvers, H. a. J.M., van Pul, M.M.L., Kitslaar, P.J.E.H.M., Bruggeman, C.A.: Chlamydia pneumoniae infection induces an unstable atherosclerotic plaque phenotype in LDL-receptor, ApoE double knockout mice. Eur. J. Vasc. Endovasc. Surg. Off. J. Eur. Soc. Vasc. Surg. 26, 88–95 (2003)
88. Ezzahiri, R., Nelissen-Vrancken, H.J.M.G., Kurvers, H. a. J.M., Stassen, F.R.M., Vliegen, I., Grauls, G.E.L.M., van Pul, M.M.L., Kitslaar, P.J.E.H.M., Bruggeman, C.A.: Chlamydophila pneumoniae (Chlamydia pneumoniae) accelerates the formation of complex atherosclerotic lesions in Apo E3-Leiden mice. Cardiovasc. Res. 56, 269–276 (2002)
89. Jawień, J., Nastałek, P., Korbut, R.: Mouse models of experimental atherosclerosis. J. Physiol. Pharmacol. Off. J. Pol. Physiol. Soc. 55, 503–517 (2004)
90. Kapourchali, F.R., Surendiran, G., Chen, L., Uitz, E., Bahadori, B., Moghadasian, M.H.: Animal models of atherosclerosis. World J. Clin. Cases. 2, 126–132 (2014). doi:10.12998/wjcc.v2.i5.126
91. Powell-Braxton, L., Véniant, M., Latvala, R.D., Hirano, K.I., Won, W.B., Ross, J., Dybdal, N., Zlot, C.H., Young, S.G., Davidson, N.O.: A mouse model of human familial hypercholesterolemia: markedly elevated low density lipoprotein cholesterol levels and severe atherosclerosis on a low-fat chow diet. Nat. Med. 4, 934–938 (1998)
92. Plump, A.S., Smith, J.D., Hayek, T., Aalto-Setälä, K., Walsh, A., Verstuyft, J.G., Rubin, E.M., Breslow, J.L.: Severe hypercholesterolemia and atherosclerosis in apolipoprotein E-deficient mice created by homologous recombination in ES cells. Cell. 71, 343–353 (1992)
93. Rader, D.J., FitzGerald, G.A.: State of the art: atherosclerosis in a limited edition. Nat. Med. 4, 899–900 (1998)
94. Muhlestein, J.B., Anderson, J.L., Hammond, E.H., Zhao, L., Trehan, S., Schwobe, E.P., Carlquist, J.F.: Infection with Chlamydia pneumoniae accelerates the development of atherosclerosis and treatment with azithromycin prevents it in a rabbit model. Circulation. 97, 633–636 (1998)
95. de Kruif, M.D., van Gorp, E.C.M., Keller, T.T., Ossewaarde, J.M., ten Cate, H.: Chlamydia pneumoniae infections in mouse models: relevance for atherosclerosis research. Cardiovasc. Res. 65, 317–327 (2005). doi:10.1016/j.cardiores.2004.09.031
96. Kis, Z., Burian, K., Treso, B., Acs, K., Prohaszka, Z., Fust, G., Gonczol, E., Endresz, V.: Inflammatory- and immune responses in relation to bacterial replication in mice following re-infections with Chlamydophila pneumoniae. Inflamm. Res. Off. J. Eur. Histamine Res. Soc. Al. 57, 287–295 (2008). doi:10.1007/s00011-007-7124-0
97. Burian, K., Berencsi, K., Endresz, V., Gyulai, Z., Valyi-Nagy, T., Valyi-Nagy, I., Bakay, M., Geng, Y., Virok, D., Kari, L., Hajnal-Papp, R., Trinchieri, G., Gonczol, E.: Chlamydia pneumoniae Exacerbates Aortic Inflammatory Foci Caused by Murine

Cytomegalovirus Infection in Normocholesterolemic Mice. Clin. Vaccine Immunol. 8, 1263–1266 (2001). doi:10.1128/CDLI.8.6.1263-1266.2001
98. Blessing, E., Lin, T.M., Campbell, L.A., Rosenfeld, M.E., Lloyd, D., Kuo, C.: Chlamydia pneumoniae induces inflammatory changes in the heart and aorta of normocholesterolemic C57BL/6J mice. Infect. Immun. 68, 4765–4768 (2000)
99. Chen, S., Shimada, K., Zhang, W., Huang, G., Crother, T.R., Arditi, M.: IL-17A is proatherogenic in high-fat diet-induced and Chlamydia pneumoniae infection-accelerated atherosclerosis in mice. J. Immunol. Baltim. Md 1950. 185, 5619–5627 (2010). doi:10.4049/jimmunol.1001879
100. Liu, L., Hu, H., Ji, H., Murdin, A.D., Pierce, G.N., Zhong, G.: Chlamydia pneumoniae infection significantly exacerbates aortic atherosclerosis in an LDLR-/- mouse model within six months. Mol. Cell. Biochem. 215, 123–128 (2000)
101. Blessing, E., Campbell, L.A., Rosenfeld, M.E., Chesebro, B., Kuo, C.-C.: A 6 week course of azithromycin treatment has no beneficial effect on atherosclerotic lesion development in apolipoprotein E-deficient mice chronically infected with Chlamydia pneumoniae. J. Antimicrob. Chemother. 55, 1037–1040 (2005). doi:10.1093/jac/dki128
102. Törmäkangas, L., Erkkilä, L., Korhonen, T., Tiirola, T., Bloigu, A., Saikku, P., Leinonen, M.: Effects of repeated Chlamydia pneumoniae inoculations on aortic lipid accumulation and inflammatory response in C57BL/6J mice. Infect. Immun. 73, 6458–6466 (2005). doi:10.1128/IAI.73.10.6458-6466.2005
103. Campbell, L.A., Nosaka, T., Rosenfeld, M.E., Yaraei, K., Kuo, C.-C.: Tumor necrosis factor alpha plays a role in the acceleration of atherosclerosis by Chlamydia pneumoniae in mice. Infect. Immun. 73, 3164–3165 (2005). doi:10.1128/IAI.73.5.3164-3165.2005
104. Naiki, Y., Sorrentino, R., Wong, M.H., Michelsen, K.S., Shimada, K., Chen, S., Yilmaz, A., Slepenkin, A., Schröder, N.W.J., Crother, T.R., Bulut, Y., Doherty, T.M., Bradley, M., Shaposhnik, Z., Peterson, E.M., Tontonoz, P., Shah, P.K., Arditi, M.: TLR/MyD88 and liver X receptor alpha signaling pathways reciprocally control Chlamydia pneumoniae-induced acceleration of atherosclerosis. J. Immunol. Baltim. Md 1950. 181, 7176–7185 (2008)
105. Chesebro, B.B., Blessing, E., Kuo, C.-C., Rosenfeld, M.E., Puolakkainen, M., Campbell, L.A.: Nitric oxide synthase plays a role in Chlamydia pneumoniae-induced atherosclerosis. Cardiovasc. Res. 60, 170–174 (2003)
106. Bastidas, R.J., Elwell, C.A., Engel, J.N., Valdivia, R.H.: Chlamydial intracellular survival strategies. Cold Spring Harb. Perspect. Med. 3, a010256 (2013). doi:10.1101/cshperspect.a010256
107. Malhotra, M., Sood, S., Mukherjee, A., Muralidhar, S., Bala, M.: Genital Chlamydia trachomatis: an update. Indian J. Med. Res. 138, 303–316 (2013)
108. Choroszy-Król, I.C.-K., Frej-Mądrzak, M., Jama-Kmiecik, A., Bober, T., Jolanta Sarowska, J.: Characteristics of the Chlamydia trachomatis species - immunopathology and infections. Adv. Clin. Exp. Med. Off. Organ Wroclaw Med. Univ. 21, 799–808 (2012)
109. Amirshahi, A., Wan, C., Beagley, K., Latter, J., Symonds, I., Timms, P.: Modulation of the Chlamydia trachomatis In vitro transcriptome response by the sex hormones estradiol and progesterone. BMC Microbiol. 11, 150 (2011). doi:10.1186/1471-2180-11-150

110. Moodley, D., Moodley, P., Sebitloane, M., Soowamber, D., McNaughton-Reyes, H.L., Groves, A.K., Maman, S.: High prevalence and incidence of asymptomatic sexually transmitted infections during pregnancy and postdelivery in KwaZulu Natal, South Africa. Sex. Transm. Dis. 42, 43–47 (2015). doi:10.1097/OLQ.0000000000000219
111. KW, C.K. and B.: Male genital tract chlamydial infection: implications for pathology and infertility. - PubMed - NCBI, https://www.ncbi.nlm.nih.gov/pubmed/18480466?dopt=Abstract
112. Zdrodowska-Stefanow, B., Ostaszewska-Puchalska, I., Puciło, K.: The immunology of Chlamydia trachomatis. Arch. Immunol. Ther. Exp. (Warsz.). 51, 289–294 (2003)
113. Darville, T., Hiltke, T.J.: Pathogenesis of genital tract disease due to Chlamydia trachomatis. J. Infect. Dis. 201 Suppl 2, S114-125 (2010)
114. Hafner, L.M.: Pathogenesis of fallopian tube damage caused by Chlamydia trachomatis infections. Contraception. 92, 108–115 (2015). doi:10.1016/j.contraception.2015.01.004
115. Rank, R.G., Yeruva, L.: Hidden in plain sight: chlamydial gastrointestinal infection and its relevance to persistence in human genital infection. Infect. Immun. 82, 1362–1371 (2014). doi:10.1128/IAI.01244-13
116. Igietseme, J.U., Portis, J.L., Perry, L.L.: Inflammation and clearance of Chlamydia trachomatis in enteric and nonenteric mucosae. Infect. Immun. 69, 1832–1840 (2001). doi:10.1128/IAI.69.3.1832-1840.2001
117. Perry, L.L., Su, H., Feilzer, K., Messer, R., Hughes, S., Whitmire, W., Caldwell, H.D.: Differential sensitivity of distinct Chlamydia trachomatis isolates to IFN-gamma-mediated inhibition. J. Immunol. Baltim. Md 1950. 162, 3541–3548 (1999)
118. Pospischil, A., Borel, N., Chowdhury, E.H., Guscetti, F.: Aberrant chlamydial developmental forms in the gastrointestinal tract of pigs spontaneously and experimentally infected with Chlamydia suis. Vet. Microbiol. 135, 147–156 (2009). doi:10.1016/j.vetmic.2008.09.035
119. Yeruva, L., Spencer, N., Bowlin, A.K., Wang, Y., Rank, R.G.: Chlamydial infection of the gastrointestinal tract: a reservoir for persistent infection. Pathog. Dis. 68, 88–95 (2013). doi:10.1111/2049-632X.12052
120. van Liere, G.A.F.S., Hoebe, C.J.P.A., Wolffs, P.F.G., Dukers-Muijrers, N.H.T.M.: High co-occurrence of anorectal chlamydia with urogenital chlamydia in women visiting an STI clinic revealed by routine universal testing in an observational study; a recommendation towards a better anorectal chlamydia control in women. BMC Infect. Dis. 14, 274 (2014). doi:10.1186/1471-2334-14-274
121. Bax, C.J., Quint, K.D., Peters, R.P.H., Ouburg, S., Oostvogel, P.M., Mutsaers, J. a. E.M., Dörr, P.J., Schmidt, S., Jansen, C., van Leeuwen, A.P., Quint, W.G.V., Trimbos, J.B., Meijer, C.J.L.M., Morré, S.A.: Analyses of multiple-site and concurrent Chlamydia trachomatis serovar infections, and serovar tissue tropism for urogenital versus rectal specimens in male and female patients. Sex. Transm. Infect. 87, 503–507 (2011). doi:10.1136/sti.2010.048173
122. Dlugosz, A., Törnblom, H., Mohammadian, G., Morgan, G., Veress, B., Edvinsson, B., Sandström, G., Lindberg, G.: Chlamydia trachomatis antigens in enteroendocrine cells and macrophages of the small bowel in patients with severe irritable bowel syndrome. BMC Gastroenterol. 10, 19 (2010). doi:10.1186/1471-230X-10-19
123. Dessus-Babus, S., Darville, T.L., Cuozzo, F.P., Ferguson, K., Wyrick, P.B.: Differences in innate immune responses (in vitro) to HeLa cells infected with

nondisseminating serovar E and disseminating serovar L2 of Chlamydia trachomatis. Infect. Immun. 70, 3234–3248 (2002)
124. Dessus-Babus, S., Moore, C.G., Whittimore, J.D., Wyrick, P.B.: Comparison of Chlamydia trachomatis serovar L2 growth in polarized genital epithelial cells grown in three-dimensional culture with non-polarized cells. Microbes Infect. 10, 563–570 (2008). doi:10.1016/j.micinf.2008.02.002
125. Guseva, N.V., Dessus-Babus, S.C., Whittimore, J.D., Moore, C.G., Wyrick, P.B.: Characterization of estrogen-responsive epithelial cell lines and their infectivity by genital Chlamydia trachomatis. Microbes Infect. 7, 1469–1481 (2005). doi:10.1016/j.micinf.2005.05.004
126. Guseva, N.V., Dessus-Babus, S., Moore, C.G., Whittimore, J.D., Wyrick, P.B.: Differences in Chlamydia trachomatis Serovar E Growth Rate in Polarized Endometrial and Endocervical Epithelial Cells Grown in Three-Dimensional Culture. Infect. Immun. 75, 553–564 (2007). doi:10.1128/IAI.01517-06
127. Boiko, E., Maltsev, D., Savicheva, A., Shalepo, K., Khusnutdinova, T., Pozniak, A., Kvetnoi, I., Polyakova, V., Suetov, A.: Infection of Human Retinal Pigment Epithelium with Chlamydia trachomatis. PloS One. 10, e0141754 (2015). doi:10.1371/journal.pone.0141754
128. Gérard, H.C., Köhler, L., Branigan, P.J., Zeidler, H., Schumacher, H.R., Hudson, A.P.: Viability and gene expression in Chlamydia trachomatis during persistent infection of cultured human monocytes. Med. Microbiol. Immunol. (Berl.). 187, 115–120 (1998)
129. Schiller, I., Schifferli, A., Gysling, P., Pospischil, A.: Growth characteristics of porcine chlamydial strains in different cell culture systems and comparison with ovine and avian chlamydial strains. Vet. J. Lond. Engl. 1997. 168, 74–80 (2004). doi:10.1016/S1090-0233(03)00039-X
130. Ganz, T.: Defensins: antimicrobial peptides of innate immunity. Nat. Rev. Immunol. 3, 710–720 (2003). doi:10.1038/nri1180
131. Porter, E., Yang, H., Yavagal, S., Preza, G.C., Murillo, O., Lima, H., Greene, S., Mahoozi, L., Klein-Patel, M., Diamond, G., Gulati, S., Ganz, T., Rice, P.A., Quayle, A.J.: Distinct defensin profiles in Neisseria gonorrhoeae and Chlamydia trachomatis urethritis reveal novel epithelial cell-neutrophil interactions. Infect. Immun. 73, 4823–4833 (2005). doi:10.1128/IAI.73.8.4823-4833.2005
132. Kim, J.M.: Antimicrobial proteins in intestine and inflammatory bowel diseases. Intest. Res. 12, 20–33 (2014). doi:10.5217/ir.2014.12.1.20
133. Gácser, A., Tiszlavicz, Z., Németh, T., Seprényi, G., Mándi, Y.: Induction of human defensins by intestinal Caco-2 cells after interactions with opportunistic Candida species. Microbes Infect. 16, 80–85 (2014). doi:10.1016/j.micinf.2013.09.003
134. Yasin, B., Harwig, S.S., Lehrer, R.I., Wagar, E.A.: Susceptibility of Chlamydia trachomatis to protegrins and defensins. Infect. Immun. 64, 709–713 (1996)
135. Chong-Cerrillo, C., Selsted, M.E., Peterson, E.M., de la Maza, L.M.: Susceptibility of human and murine Chlamydia trachomatis serovars to granulocyte- and epithelium-derived antimicrobial peptides. J. Pept. Res. Off. J. Am. Pept. Soc. 61, 237–242 (2003)
136. Wiechuła, B., Cholewa, K., Ekiel, A., Romanik, M., Dolezych, H., Martirosian, G.: [HBD-1 and hBD-2 are expressed in cervico-vaginal lavage in female genital tract due to microbial infections]. Ginekol. Pol. 81, 268–271 (2010)

137. Burián, K., Hegyesi, H., Buzás, E., Endrész, V., Kis, Z., Falus, A., Gönczöl, E.: Chlamydophila (Chlamydia) pneumoniae induces histidine decarboxylase production in the mouse lung. Immunol. Lett. 89, 229–236 (2003)
138. Burián, K., Hegyesi, H., Buzás, E., Endrész, V., Kis, Z., Falus, A., Gönczöl, E.: Chlamydophila (Chlamydia) pneumoniae induces histidine decarboxylase production in the mouse lung. Immunol. Lett. 89, 229–236 (2003)
139. Bogdanov, A., Endrész, V., Urbán, S., Lantos, I., Deák, J., Burián, K., Önder, K., Ayaydin, F., Balázs, P., Virok, D.P.: Application of DNA chip scanning technology for automatic detection of Chlamydia trachomatis and Chlamydia pneumoniae inclusions. Antimicrob. Agents Chemother. 58, 405–413 (2014). doi:10.1128/AAC.01400-13
140. Farese, R.V., Véniant, M.M., Cham, C.M., Flynn, L.M., Pierotti, V., Loring, J.F., Traber, M., Ruland, S., Stokowski, R.S., Huszar, D., Young, S.G.: Phenotypic analysis of mice expressing exclusively apolipoprotein B48 or apolipoprotein B100. Proc. Natl. Acad. Sci. U. S. A. 93, 6393–6398 (1996)
141. Wuttge, D.M., Sirsjö, A., Eriksson, P., Stemme, S.: Gene expression in atherosclerotic lesion of ApoE deficient mice. Mol. Med. Camb. Mass. 7, 383–392 (2001)
142. Rothstein, N.M., Quinn, T.C., Madico, G., Gaydos, C.A., Lowenstein, C.J.: Effect of azithromycin on murine arteriosclerosis exacerbated by Chlamydia pneumoniae. J. Infect. Dis. 183, 232–238 (2001). doi:10.1086/317941
143. Erkkilä, L., Laitinen, K., Haasio, K., Tiirola, T., Jauhiainen, M., Lehr, H.A., Aalto-Setälä, K., Saikku, P., Leinonen, M.: Heat shock protein 60 autoimmunity and early lipid lesions in cholesterol-fed C57BL/6JBom mice during Chlamydia pneumoniae infection. Atherosclerosis. 177, 321–328 (2004). doi:10.1016/j.atherosclerosis.2004.08.021
144. Paigen, B., Morrow, A., Holmes, P.A., Mitchell, D., Williams, R.A.: Quantitative assessment of atherosclerotic lesions in mice. Atherosclerosis. 68, 231–240 (1987)
145. Mannonen, L., Kamping, E., Penttilä, T., Puolakkainen, M.: IFN-gamma induced persistent Chlamydia pneumoniae infection in HL and Mono Mac 6 cells: characterization by real-time quantitative PCR and culture. Microb. Pathog. 36, 41–50 (2004)
146. Mosolygó, T., Korcsik, J., Balogh, E.P., Faludi, I., Virók, D.P., Endrész, V., Burián, K.: Chlamydophila pneumoniae re-infection triggers the production of IL-17A and IL-17E, important regulators of airway inflammation. Inflamm. Res. Off. J. Eur. Histamine Res. Soc. Al. 62, 451–460 (2013). doi:10.1007/s00011-013-0596-1
147. Eszik, I., Lantos, I., Önder, K., Somogyvári, F., Burián, K., Endrész, V., Virok, D.P.: High dynamic range detection of Chlamydia trachomatis growth by direct quantitative PCR of the infected cells. J. Microbiol. Methods. 120, 15–22 (2016). doi:10.1016/j.mimet.2015.11.010
148. Borges, V., Ferreira, R., Nunes, A., Nogueira, P., Borrego, M.J., Gomes, J.P.: Normalization strategies for real-time expression data in Chlamydia trachomatis. J. Microbiol. Methods. 82, 256–264 (2010). doi:10.1016/j.mimet.2010.06.013
149. Damy, S.B., Higuchi, M.L., Timenetsky, J., Reis, M.M., Palomino, S.P., Ikegami, R.N., Santos, F.P., Osaka, J.T., Figueiredo, L.P.: Mycoplasma pneumoniae and/or Chlamydophila pneumoniae inoculation causing different aggravations in cholesterol-induced atherosclerosis in apoE KO male mice. BMC Microbiol. 9, 194 (2009). doi:10.1186/1471-2180-9-194

150. Nazzal, D., Therville, N., Yacoub-Youssef, H., Garcia, V., Thomsen, M., Levade, T., Segui, B., Benoist, H.: Apolipoprotein E-deficient mice develop an anti-Chlamydophila pneumoniae T helper 2 response and resist vascular infection. J. Infect. Dis. 202, 782–790 (2010). doi:10.1086/655700
151. Moazed, T.C., Kuo, C., Grayston, J.T., Campbell, L.A.: Murine models of Chlamydia pneumoniae infection and atherosclerosis. J. Infect. Dis. 175, 883–890 (1997)
152. Hu, H., Pierce, G.N., Zhong, G.: The atherogenic effects of chlamydia are dependent on serum cholesterol and specific to Chlamydia pneumoniae. J. Clin. Invest. 103, 747–753 (1999). doi:10.1172/JCI4582
153. Moazed, T.C., Campbell, L.A., Rosenfeld, M.E., Grayston, J.T., Kuo, C.C.: Chlamydia pneumoniae infection accelerates the progression of atherosclerosis in apolipoprotein E-deficient mice. J. Infect. Dis. 180, 238–241 (1999). doi:10.1086/314855
154. Blessing, E., Campbell, L.A., Rosenfeld, M.E., Chough, N., Kuo, C.C.: Chlamydia pneumoniae infection accelerates hyperlipidemia induced atherosclerotic lesion development in C57BL/6J mice. Atherosclerosis. 158, 13–17 (2001)
155. Campbell, L.A., Moazed, T.C., Kuo, C.-C., Grayston, J.T.: Preclinical models for Chlamydia pneumoniae and cardiovascular disease: hypercholesterolemic mice. Clin. Microbiol. Infect. Off. Publ. Eur. Soc. Clin. Microbiol. Infect. Dis. 4 Suppl 4, S23–S32 (1998)
156. Campbell, L.A., Rosenfeld, M.E.: Persistent C. pneumoniae infection in atherosclerotic lesions: rethinking the clinical trials. Front. Cell. Infect. Microbiol. 4, 34 (2014). doi:10.3389/fcimb.2014.00034
157. Hyvärinen, K., Tuomainen, A.M., Laitinen, S., Alfthan, G., Salminen, I., Leinonen, M., Saikku, P., Kovanen, P.T., Jauhiainen, M., Pussinen, P.J.: The effect of proatherogenic pathogens on adipose tissue transcriptome and fatty acid distribution in apolipoprotein E-deficient mice. BMC Genomics. 14, 709 (2013). doi:10.1186/1471-2164-14-709
158. Marangoni, A., Fiorino, E., Gilardi, F., Aldini, R., Scotti, E., Nardini, P., Foschi, C., Donati, M., Montagnani, M., Cevenini, M., Franco, P., Roda, A., Crestani, M., Cevenini, R.: Chlamydia pneumoniae acute liver infection affects hepatic cholesterol and triglyceride metabolism in mice. Atherosclerosis. 241, 471–479 (2015). doi:10.1016/j.atherosclerosis.2015.05.023
159. Tuomainen, A.M., Hyvärinen, K., Ehlers, P.I., Mervaala, E., Leinonen, M., Saikku, P., Kovanen, P.T., Jauhiainen, M., Pussinen, P.J.: The effect of proatherogenic microbes on macrophage cholesterol homeostasis in apoE-deficient mice. Microb. Pathog. 51, 217–224 (2011). doi:10.1016/j.micpath.2011.03.003
160. Erkkilä, L., Laitinen, K., Haasio, K., Tiirola, T., Jauhiainen, M., Lehr, H.A., Aalto-Setälä, K., Saikku, P., Leinonen, M.: Heat shock protein 60 autoimmunity and early lipid lesions in cholesterol-fed C57BL/6JBom mice during Chlamydia pneumoniae infection. Atherosclerosis. 177, 321–328 (2004). doi:10.1016/j.atherosclerosis.2004.08.021
161. Van Oosten, M., Rensen, P.C., Van Amersfoort, E.S., Van Eck, M., Van Dam, A.M., Breve, J.J., Vogel, T., Panet, A., Van Berkel, T.J., Kuiper, J.: Apolipoprotein E protects against bacterial lipopolysaccharide-induced lethality. A new therapeutic approach to treat gram-negative sepsis. J. Biol. Chem. 276, 8820–8824 (2001). doi:10.1074/jbc.M009915200
162. Khovidhunkit, W., Kim, M.-S., Memon, R.A., Shigenaga, J.K., Moser, A.H., Feingold, K.R., Grunfeld, C.: Effects of infection and inflammation on lipid and lipoprotein

metabolism: mechanisms and consequences to the host. J. Lipid Res. 45, 1169–1196 (2004). doi:10.1194/jlr.R300019-JLR200
163. Feingold, K.R., Hardardottir, I., Memon, R., Krul, E.J., Moser, A.H., Taylor, J.M., Grunfeld, C.: Effect of endotoxin on cholesterol biosynthesis and distribution in serum lipoproteins in Syrian hamsters. J. Lipid Res. 34, 2147–2158 (1993)
164. Kontula, K., Vuorio, A., Turtola, H., Saikku, P.: Association of seropositivity for Chlamydia pneumoniae and coronary artery disease in heterozygous familial hypercholesterolaemia. Lancet Lond. Engl. 354, 46–47 (1999). doi:10.1016/S0140-6736(99)01691-8
165. Bavoil, P.M., Marques, P.X., Brotman, R., Ravel, J.: Does Active Oral Sex Contribute to Female Infertility? J. Infect. Dis. (2017). doi:10.1093/infdis/jix419
166. Eduardo R. Cobo, Kris Chadee: Antimicrobial Human β-Defensins in the Colon and Their Role in Infectious and Non-Infectious Diseases. Pathogens. 2, 177–192 (2013)
167. Gérard, H.C., Köhler, L., Branigan, P.J., Zeidler, H., Schumacher, H.R., Hudson, A.P.: Viability and gene expression in Chlamydia trachomatis during persistent infection of cultured human monocytes. Med. Microbiol. Immunol. (Berl.). 187, 115–120 (1998)
168. Rosario, C.J., Tan, M.: The early gene product EUO is a transcriptional repressor that selectively regulates promoters of Chlamydia late genes. Mol. Microbiol. 84, 1097–1107 (2012). doi:10.1111/j.1365-2958.2012.08077.x
169. Rosario, C.J., Hanson, B.R., Tan, M.: The transcriptional repressor EUO regulates both subsets of Chlamydia late genes. Mol. Microbiol. 94, 888–897 (2014). doi:10.1111/mmi.12804
170. Gérard, H.C., Whittum-Hudson, J.A., Schumacher, H.R., Hudson, A.P.: Differential expression of three Chlamydia trachomatis hsp60-encoding genes in active vs. persistent infections. Microb. Pathog. 36, 35–39 (2004)
171. Redgrove, K.A., McLaughlin, E.A.: The Role of the Immune Response in Chlamydia trachomatis Infection of the Male Genital Tract: A Double-Edged Sword. Front. Immunol. 5, 534 (2014). doi:10.3389/fimmu.2014.00534
172. Hemshekhar, M., Anaparti, V., Mookherjee, N.: Functions of Cationic Host Defense Peptides in Immunity. Pharm. Basel Switz. 9, (2016). doi:10.3390/ph9030040
173. Niyonsaba, F., Ogawa, H., Nagaoka, I.: Human beta-defensin-2 functions as a chemotactic agent for tumour necrosis factor-alpha-treated human neutrophils. Immunology. 111, 273–281 (2004)
174. Yang, D., Chertov, O., Bykovskaia, S.N., Chen, Q., Buffo, M.J., Shogan, J., Anderson, M., Schröder, J.M., Wang, J.M., Howard, O.M., Oppenheim, J.J.: Beta-defensins: linking innate and adaptive immunity through dendritic and T cell CCR6. Science. 286, 525–528 (1999)
175. Noda-Nicolau, N.M., Bastos, L.B., Bolpetti, A.N., Pinto, G.V.S., Marcolino, L.D., Marconi, C., Ferreira, C.S.T., Polettini, J., Vieira, E.P., da Silva, M.G.: Cervicovaginal Levels of Human β-Defensin 1, 2, 3, and 4 of Reproductive-Aged Women With Chlamydia trachomatis Infection. J. Low. Genit. Tract Dis. 21, 189–192 (2017). doi:10.1097/LGT.0000000000000315
176. Igietseme, J.U., Portis, J.L., Perry, L.L.: Inflammation and clearance of Chlamydia trachomatis in enteric and nonenteric mucosae. Infect. Immun. 69, 1832–1840 (2001). doi:10.1128/IAI.69.3.1832-1840.2001
177. van Liere, G.A.F.S., Hoebe, C.J.P.A., Wolffs, P.F.G., Dukers-Muijrers, N.H.T.M.: High co-occurrence of anorectal chlamydia with urogenital chlamydia in women

visiting an STI clinic revealed by routine universal testing in an observational study; a recommendation towards a better anorectal chlamydia control in women. BMC Infect. Dis. 14, 274 (2014). doi:10.1186/1471-2334-14-274

10. Annexes

I.

Hindawi
BioMed Research International
Volume 2018, Article ID 8325915, 12 pages
https://doi.org/10.1155/2018/8325915

Research Article

Chlamydia pneumoniae Infection Exacerbates Atherosclerosis in ApoB100only/LDLR$^{-/-}$ Mouse Strain

Ildikó Lantos[1], **Valéria Endrész**[1], **Dezső Péter Virok**[1], **Andrea Szabó**[2], **Xinjie Lu**[3], **Tímea Mosolygó**[1] and **Katalin Burián**[1]

[1]*Department of Medical Microbiology and Immunobiology, University of Szeged, Dóm Tér 10, Szeged 6720, Hungary*
[2]*Institute of Surgical Research, University of Szeged, Szőkefalvi-Nagy Béla U. 6, Szeged 6720, Hungary*
[3]*The Mary and Garry Weston Molecular Immunology Laboratory, Thrombosis Research Institute, Emmanuel Kaye Building, Manresa Road, London SW3 6LR, UK*

Correspondence should be addressed to Valéria Endrész; endresz.valeria@med.u-szeged.hu

Received 14 November 2017; Revised 31 January 2018; Accepted 18 February 2018; Published 25 March 2018

Academic Editor: Daniele Corsaro

Aims. Hyperlipidaemia model animals have been used to elucidate the role of *Chlamydia pneumoniae (Cpn)* infection in atherosclerosis. The aims of this study were to investigate the proatherogenic effect of multiple *Cpn* infections in ApoB100only/LDLR$^{-/-}$ mice which based on lipid profile can be regarded as the most suitable mouse model of human hypercholesterolemia and to compare the lesion development to that in a major atherosclerosis model ApoE$^{-/-}$ mice. *Methods and Results*. Aorta samples of ApoB100only/LDLR$^{-/-}$ mice infected three times with *Cpn* were subjected to morphometric analyses. Morphometric evaluation disclosed that *Cpn* infections exacerbated atherosclerosis development in the aortic root and descending aorta of the mice fed with normal diet. Viable Cpn was detected in the ascending aorta by RT-PCR. Chlamydial 16SrRNA expression showed the presence of viable *Cpn* in the aorta of infected animals. A similar rate of acceleration of atherosclerosis was observed when the infection protocol was applied in ApoB100only/LDLR$^{-/-}$ and in ApoE$^{-/-}$ mice. *Conclusion*. Similar to ApoE$^{-/-}$ mice, ApoB100only/LDLR$^{-/-}$ mice with more human-relevant serum lipoprotein composition develop increased atherosclerosis after *Cpn* infections; thus this mouse strain can be used as a model of infection-related atherosclerosis enhancement and can provide further evidence for the proatherogenic influence of *Cpn* in mice.

1. Introduction

Atherosclerosis is one of the most frequent causes of death in the world [1]. There are several well-known atherosclerosis risk factors, such as diabetes mellitus, smoking, hypertension, hyperlipidaemia, hypercholesterolemia, and abdominal obesity [2, 3]. The knowledge about the contributory mechanisms is incomplete [4]. Atherosclerosis begins in the early childhood [5] and has been characterized as a chronic inflammatory disease in which both innate and adaptive immune responses play a role [6]. The damage to the endothelium of the arteries is the primary cause of initiation of the development of atherosclerosis. High plasma low-density lipoprotein (LDL) cholesterol concentrations, especially oxidized LDL, contribute to the formation of the atherosclerotic lesions [7, 8].

Several infectious agents have been associated with the risk of atherosclerosis [9–12]. The infections and the accompanying inflammatory response damage the endothelial cells and also stimulate monocytes to secrete proinflammatory cytokines. Numerous studies have demonstrated an association between *Chlamydia pneumoniae (Cpn)* infection and atherosclerosis [12–14]. *Cpn* infection is ubiquitous, with 50% of individuals being seropositive by 20 years of age and approximately 80% in the elderly [13, 15]. Chronic-persistent infections and reinfections are frequent which may contribute through the induced inflammation to atherosclerosis [16]. The prevalence of antibodies ranges from 60 to 80% among patients with cardiovascular diseases [17, 18]. Animal models that help to clarify the pathogenic steps and causalities in atherosclerosis play an important role in the current

search for new therapeutics beyond the lipid-lowering drugs. Normal mice do not develop atherosclerosis and it requires long-term feeding of a high-fat diet to induce atherogenesis. However, there are well-established genetically modified inbred mouse lines that allow the investigation of atherosclerosis development in mouse models. The most frequently used were ApoE-deficient ($ApoE^{-/-}$), LDL receptor-deficient ($LDLR^{-/-}$), and human apoB100 transgenic mice which display marked atherogenesis throughout their arterial tree especially when fed with atherogenic diet [19, 20]. In $ApoE^{-/-}$ mice, atherosclerosis develops spontaneously. However, the lipid profile in these mice is distinct from that seen in most humans with atherosclerosis; that is, apolipoprotein (apo) B48-containing LDL plasma level is high instead of apoB100 containing LDL level as in the case of humans with hypercholesterolemia [21, 22]. The mouse strain ApoB100only ($ApoB^{100/100}$)/$LDLR^{-/-}$ carries an *apoB* gene with a mutation preventing the expression of apoB48, the truncated form of apoB, similar to humans where no apoB editing takes place in the liver [21, 23]. LDLR deficiency prevents the uptake of apoB100 containing LDL in tissues resulting in high plasma levels of apoB100-containing cholesterol-rich LDL. The creating authors of this mouse strain described these mice as an authentic model of human familial hypercholesterolemia [21].

In mice, intranasal *Cpn* infection causes lower respiratory tract disease similar to that seen in humans with *Cpn* infection. The infection is followed by dissemination of bacteria [24] and the chlamydial DNA can be detected in the circulation of mice [25]. Most frequently, acceleration of atherosclerosis was studied after repeated *Cpn* infections which simulated chronic *Cpn* infection of humans in association with diet-induced hyperlipidaemia in C57Bl/6J [26], $LDLR^{-/-}$ [27], or $ApoE^{-/-}$ [28] mice and mostly found accelerated lesion development. ApoB100only/$LDLR^{-/-}$ mice have not been used as a model for the investigation of the effect of *Cpn* infection on the atherosclerosis progression.

Our aim was to examine how repeated *Cpn* infection influences the atherosclerotic lesion development in this, based on lipid profile, most suitable mouse model of human hypercholesterolemia and atherosclerosis. We compared the extent of atherosclerosis in this model with that seen in the most frequently utilized $ApoE^{-/-}$ mouse strain.

2. Methods

2.1. Chlamydia pneumoniae. *Chlamydia pneumoniae*, CWL029 strain from American Types Culture Collection (ATCC), was used. *Cpn* was propagated in HEp-2 cells (ATCC), as described earlier [29]. The partially purified and concentrated elementary bodies (EBs) were aliquoted in sucrose-phosphate-glutamic acid buffer (SPG) and stored at −80°C until use. Chlamydia was quantitated by indirect immunofluorescent method applying anti-chlamydia lipopolysaccharide monoclonal antibody (AbD Serotec, Oxford, United Kingdom) and fluorescein isothiocyanate- (FITC-) labelled anti-mouse IgG (Sigma-Aldrich, St. Louis, MO) as described earlier [30]. The number of infectious bacteria in the *Cpn* stock used for inoculation of mice was expressed as inclusion-forming units (IFU)/ml.

2.2. Mouse Strains. ApoB100only/$LDL^{-/-}$ (B6.129S-$Ldlr^{tm1Her}Apob^{tm2Sgy}$/J) mice at 8-9 or 14-15 weeks of age and ApoE-deficient ($ApoE^{-/-}$, B6.129P2-$Apoe^{tm1Unc}$/J) mice at 14-15 weeks of age were involved in our studies. B6.129S-$Ldlr^{tm1Her}Apob^{tm2Sgy}$/J breeding pairs purchased from the Jackson Laboratory (Bar Harbor, ME, USA) and B6.129P2-$Apoe^{tm1Unc/J}$ breeding pairs purchased from Charles River Laboratories (Sulzfeld, Germany) were housed and bred under standard conditions. Considering that numerous atherosclerosis-related studies used female mice [31–34], furthermore it was shown that female mice of both mouse strains develop atherosclerosis, with no gender-related difference in $ApoE^{-/-}$ mice and with less extensive lesions in female than in male ApoB100only/$LDLR^{-/-}$ mice [21, 23]; we chose to work with female mice which were available in sufficient quantity in our breeding colony.

The mice were kept on normal rodent regular chow (VRF1, Altromin GmbH & Co. KG, Lage, Germany) or high-fat/high-cholesterol diet containing 21% milkfat and 1.25% cholesterol manufactured by Altromin GmbH & Co. KG according to Teklad custom diet formula TD.19121, [composition, g/Kg: casein high protein 195.0, DL-methionine 3.0, sucrose 341.46, corn starch 150.0, anhydrous milkfat 210.0, cholesterol 12.5, cellulose (fiber) 39.0, mineral mix, AIN-76 (170915) 35.0, calcium carbonate CaCO3 4.0, vitamin mix, Teklad (40060) 10.0, ethoxyquin (antioxidant) 0.04] for 12 weeks after the first infection. All experiments were approved by the Animal Welfare Committee of the University of Szeged and conform to the Directive 2010/63/EU of the European Parliament (Permit Number: III./2187/2015.).

2.3. Infection with Cpn. Mice were intranasally infected with *Cpn*; 2×10^5 IFU of *Cpn* in 20 μl PBS were administered intranasally three times with 2-week intervals under mild anaesthesia by intraperitoneal injection of 100 mg/kg sodium pentobarbital. One week after each infection and at the end of the experiment at week 12, plasma samples with heparinised capillaries (Natelson blood collecting tubes, Fisher Scientific, Pittsburg, PA, USA) were harvested from the retroorbital plexus under anaesthesia as described above. For RNA detection in the aorta tissue additional groups of mice were infected once and sacrificed 1 and 4 weeks after single infection and 5 weeks after the third infection. The control animals were left uninfected

2.4. Mouse Tissue Preparation and Quantification of Atherosclerosis. Twelve weeks after the first infection with *Cpn* the mice were sacrificed. In deep pentobarbital sodium anaesthesia (i.p. injection of 400 mg/kg pentobarbital sodium) hearts and aortas were perfusion-fixed using 10% buffered formalin administered through the left ventricle. The adequacy of anaesthesia was assessed by pedal withdrawal reflex in hind limbs; mice displaying no locomotor activity were processed. After formalin-perfusion, the upper part of the heart and the descending aorta were dissected. Aortic sinus samples were

also collected for RNA extraction from mice anaesthetized as described above. The basis of the heart was separated from the aorta which was dissected until the iliac bifurcation. The upper part of the hearts was embedded in paraffin and sectioned for morphometric analyses according to the method described by Paigen et al. [35]. From the end of the aortic sinus 10 μm sections were prepared until the point where the valve cusps disappeared and stained with hematoxylin eosin. Images of aortic root sections (8 sections/mouse, every third sections) were acquired with a light microscope (Leitz Optical microscope) and Olympus C-7070 digital compact camera. Percentage length of the plaque-covered perimeter of aorta lumen and percentage of aorta lumen area occupied by plaque were analysed with JMicroVision software. The aortic arch and the adjoining descending aorta were cleared from adjacent tissue and were opened longitudinally. The aortas were laid flat on black plastic surface and pictures of the longitudinally opened vessels were taken applying the same illumination, magnification, and focal distance using a CMOS camera (DCM 510; pixel size: 2.2 μm × 2.2 μm, 2592 × 1944 pixels; 5 Mpixel; Hangzhou Scopetek Opto-Electric Co., Ltd., Hangzhou, Zheijang, China) and the ScopePhoto software (Hangzhou Scopetek Opto-Electric Co., Ltd.) attached to a stereomicroscope (Alpha STO 44, Elektro-Optika Kft., Érd, Hungary). The digital image of the luminal surface was evaluated for the extent of atherosclerosis by tracing and measuring the plaque area and the total luminal surface using JMicroVision software. The percentage of the luminal area covered by plaque was calculated for each aorta sample.

2.5. RNA Extraction and Quantitative Real Time-PCR. Aorta sinus with aortic arch for RNA extraction was collected from mice (in deep pentobarbital sodium anaesthesia as described in the previous paragraph) at the indicated time points after *Cpn* inoculation for one time or three times and pools of 3 samples at each time points were snap-frozen in liquid nitrogen. Aorta samples from noninfected mice were also dissected parallel with the samples collected one week after one infection.

Total RNA was isolated from the pooled aorta samples with RNA extraction kit (Nucleospin RNA XS kit, Macherey-Nagel GmbH, Düren, Germany). Concentration and purity (OD260/280) of RNA was determined by spectrophotometry. The extracted RNA was treated with DNaseI (Sigma, St. Louis, MO, USA). Complementary DNA (cDNA) was synthetized from 1 μg DNase-treated RNA with qScript cDNA Supermix synthesis kit (Quanta Biosciences, Gaithersburg, MD, USA). RNA and cDNA were stored at −80°C until use.

By using cDNA as template qRT-PCR was performed with PerfeCTa SYBR Green Supermix (Quanta) in CFX96 Real Time C1000 Thermal Cycler (BioRad, Hercules, CA, USA). All experiments involved control reactions containing distilled water as template. *Chlamydia* 16SrRNA and mouse β-actin sequences were amplified. The sequences of primers used for RT-PCR were the following: *Cpn* 16S rRNA: 5′-GGCGAAGGCGCTTTTCTAA-3′, 5′-CCAGGGTATCTAATCCTGTTTGCT-3′ [36]; mouse β-actin: 5′-TGGAATCCTGTGGCATCCATGAAA-3′, 5′-TAAAACGCAGCTCAGTAACAGTCCG-3′ [37].

A BLAST search was performed to check the specificity of the product target sequence of the primer sets. The primers were synthesized by Integrated DNA Technologies Inc. (Montreal, Quebec, Canada). The PCR cycles consisted of a 3 min denaturation at 95°C followed by 55 cycles each of 10 s of denaturation at 94°C, 10 s of annealing at 60°C and 10 s of extension at 72°C. The specificity of amplification was confirmed by carrying out a melting curve analysis. The sensitivity of amplification was controlled using standard as described earlier [38]. Amplicon standard was generated by amplifying *Cpn* cDNA with 16S rRNA primers; amplicons were purified with the PCR Clean-Up Kit (GeneElute PCR Clean-Up Kit, Sigma-Aldrich); the DNA concentration was measured with NanoDrop 1000 Spectrophotometer. The copy number was calculated using the following formula: copy number/μl = [6.022 × 1023 (molecules/mole) × DNA concentration (g/μl)]/(number of bases pairs × 660 daltons); and standard curve were generated from 10-fold serial dilutions of the amplicon (from 1000,000 to 1 copies). qPCR analysis of the dilution series showed that the sensitivity threshold of our method was ten 16SrRNA copies.

2.6. ELISA for Detection of Cpn-Specific Antibodies. Plasma samples of mice collected one week after each infection and at the end of the experiment were tested in duplicate for *Cpn*-specific IgG, IgM, and IgA by an in-house developed ELISA test as described earlier [25], where NP-40 treated partially purified *Cpn* and similarly treated Hep-2 mock preparation were used as antigens. Briefly, NUNC Maxisorp ELISA plates were coated with *Cpn* and mock antigen (0.625 μg protein in 50 μl PBS/well), respectively, overnight at 4°C. Blocking was done with 1% skim milk in PBS with 0.05% TWEEN 20 for 1 h. The serum samples were diluted in 0.4% skim milk in PBS with 0.05% TWEEN 20.

Mouse IgG, IgM, and IgA were detected with HRP-anti-mouse IgG (Jackson ImmunoResearch Laboratories West Grove, PA, USA), α-mouse IgA-HRP (Sigma), and anti-mouse IgM μ-chain (ab97260, Abcam, Cambridge, UK) secondary antibodies, respectively. Optical densities (OD-s) detected on *Cpn* antigen were corrected with OD values measured on the control antigen. *Cpn*-specific IgG antibody titres were determined by testing serial 2-fold dilutions of the serum samples on *Cpn* and control ELISA antigen, and reciprocal of the dilution producing OD ≥ 0.1 after correction with OD values measured on control antigen was regarded as titre. Geometric mean of titres of individual serum samples was calculated. For determination of *Cpn*-specific IgM and IgA levels serum samples were tested at 1 : 50 dilution and determined as the measured and corrected OD values.

2.7. Serum Lipoprotein Analysis. Levels of total cholesterol, triglycerides, high-density lipoprotein (HDL), and LDL-cholesterol were determined in plasma samples of mice through a service from the Department of Laboratory Medicine, University of Szeged, Hungary.

2.8. Statistical Analysis. Data are expressed as mean ± SD. Independent-samples t-test was used with SigmaPlot for Windows Version 11.0 software. A P value of less than

0.05 was considered to indicate statistically significant difference.

3. Results

3.1. Infection of ApoB100only/LDLR$^{-/-}$ Mice with Cpn. Mice infected 3 times with *Cpn* showed mild symptoms of a disease as ruffled fur and moderate food consumption, especially during the first week after the first infection. At the time of the first infection half of the mice were given a high-fat/high-cholesterol diet the other half were kept on normal rodent chow. Noninfected mice were kept under similar conditions. All infected mice produced *Cpn*-specific antibodies which were not seen in the noninfected mice. Normal and high-fat/high-cholesterol diet-fed mice produced similar level of *Cpn*-specific IgG antibodies (OD 0.36–0.4 at dilution 1 : 100).

3.2. Repeated Cpn Infection Aggravates Atherosclerosis Development in the Aorta Sinus and in the Descending Aorta of ApoB100only/LDLR$^{-/-}$ Mice Kept on Normal Diet. The mice received the first *Cpn* infection at the age of 8-9 weeks; uninfected mice with same age served as controls. Fed with an atherogenic diet very similar pathology was observed in the aorta sinus of the mice that received three chlamydia infections and in those remaining uninfected. The quantitative evaluation did not disclose significant difference in the length of the plaque-covered perimeter of the lumen (Figure 1(a)) nor in the size of the plaque-occupied area in the aorta lumen (Figure 1(b)). The aorta sections of the normal diet-fed noninfected animals demonstrated very early-stage and small extent of atherosclerosis with a single layer of foam cells. However, in the aorta sections of repeatedly *Cpn*-infected mice, we observed a significant increase in the length of the plaque-covered perimeter of the lumen ($P < 0.05$) (Figure 1(a)) and in the size of the plaque-occupied area in the aorta lumen ($P < 0.05$) (Figure 1(b)) compared with that in the noninfected counterpart in normal diet-fed group.

On the luminal surface of the longitudinally opened descending aorta well discernible plaques could be observed. Small areas corresponding to atherosclerotic alteration were seen in the case of the aorta of the noninfected animals fed with normal diet. The atherosclerosis-affected areas were measured significantly larger in the descending aorta of the infected animals. In the high-fat/high-cholesterol diet-fed animals, significantly increased plaque-covered spots were visible compared to that in the normal diet-fed mice; however, the infection did not enhance the lesion formation in this part of the aorta (Figure 1(c)).

3.3. Viable Cpn Was Detectable in the Aorta of ApoB100only/LDLR$^{-/-}$ Mice. Figure 2(a) shows that the persistence of the bacterium was tested early, that is, one week after the first infection and again four weeks after single infection and at 9-week and 12-week time points after three chlamydial infections by RT-PCR. An equal amount of RNA purified from pooled ascending aorta samples of mice was DNase-treated and then reverse-transcribed and mouse *β-actin* as housekeeping gene was amplified from all samples. One and four weeks after single inoculation the expression of chlamydial 16SrRNA was detectable (Figure 2(b)) with a ~ 1000-fold lower relative expression level at four weeks than at 1-week time point (Figure 2(c)). Five weeks after the third infection one aorta sample of 2 showed metabolically active *Cpn* in the aorta and the relative expression level was similar to that after single infection at 4 weeks (Figure 2(c)). At later time point, our test was not able to detect chlamydial gene expression.

3.4. Infection of ApoB100only/LDLR$^{-/-}$ and ApoE$^{-/-}$ Mice with Cpn Induces Similar Kinetics of Antibody Production. Based on the above results, we aimed at performing a comparative experiment by applying our infection protocol both in ApoB100only/LDLR$^{-/-}$ and in ApoE$^{-/-}$ mice (14-15 weeks of age) while keeping them on a nonatherogenic diet. The humoral immune response induced by the infections was compared by measuring the titre of *Cpn*-specific IgG antibodies (Figure 3(a)) and the level of IgM (Figure 3(b)) and IgA (Figure 3(c)) antibodies one week after all three infections and at the end of the experiment. The level of antibody response did not differ significantly in the two mouse strains. The IgA level tended to be lower in ApoE$^{-/-}$ mice (Figure 3(c)); however, the difference was not significant. Two independent experiments gave similar results.

3.5. The Extent of Atherosclerosis Is Similarly Increased in the Aorta of Cpn-Infected and Normal Diet-Fed ApoB100only/LDLR$^{-/-}$ and ApoE$^{-/-}$ Mice. In normal chow-fed ApoB100only/LDLR$^{-/-}$ mice at the age of 24-25 weeks the lesions consisted of mainly single or multiple layers of macrophage foam cells but some more advanced plaques with cholesterol crystals and necrotic core were also seen. In ApoE$^{-/-}$ mice at same age more numerous advanced lesions with necrotic core and cholesterol cleft were found. In *Cpn*-infected ApoB100only/LDLR$^{-/-}$ mice larger advanced plaques and in infected ApoE$^{-/-}$ mice more plaques with necrotic core and accumulated cholesterol crystals appeared. Representative sections from the experimental groups are shown in Figure 4(a).

The measurements proved that in ApoE$^{-/-}$ mice the atherosclerosis was more pronounced than in ApoB100only/LDLR$^{-/-}$ mice. The difference was seen in respect of the size of plaque-occupied lumen area in the aortic sinus (Figure 4(b)) and the length of the plaque-covered aorta surface in the lumen (Figure 4(c)). Lesions in the descending aorta also were larger in ApoE$^{-/-}$ mice than in ApoB100only/LDLR$^{-/-}$ mice (Figures 4(d) and 4(e)). When the effect of *Cpn* infection was analysed, significant enhancement in the measured values was found. The plaque-covered perimeter of the lumen in the aorta sinus sections (Figure 4(b)), the plaque-occupied lumen area (Figure 4(c)), and the plaque size in the descending aorta (Figure 4(e)) increased 2.08-fold ($P = 0.035$), 1.7-fold ($P = 0.004$), and 2.5-fold ($P = 0.001$), respectively, in ApoB100only/LDLR$^{-/-}$ and 2.04-fold ($P = 0.019$), 1.32-fold ($P = 0.026$), and 2.56-fold ($P = 0.002$), respectively, in ApoE$^{-/-}$ mice.

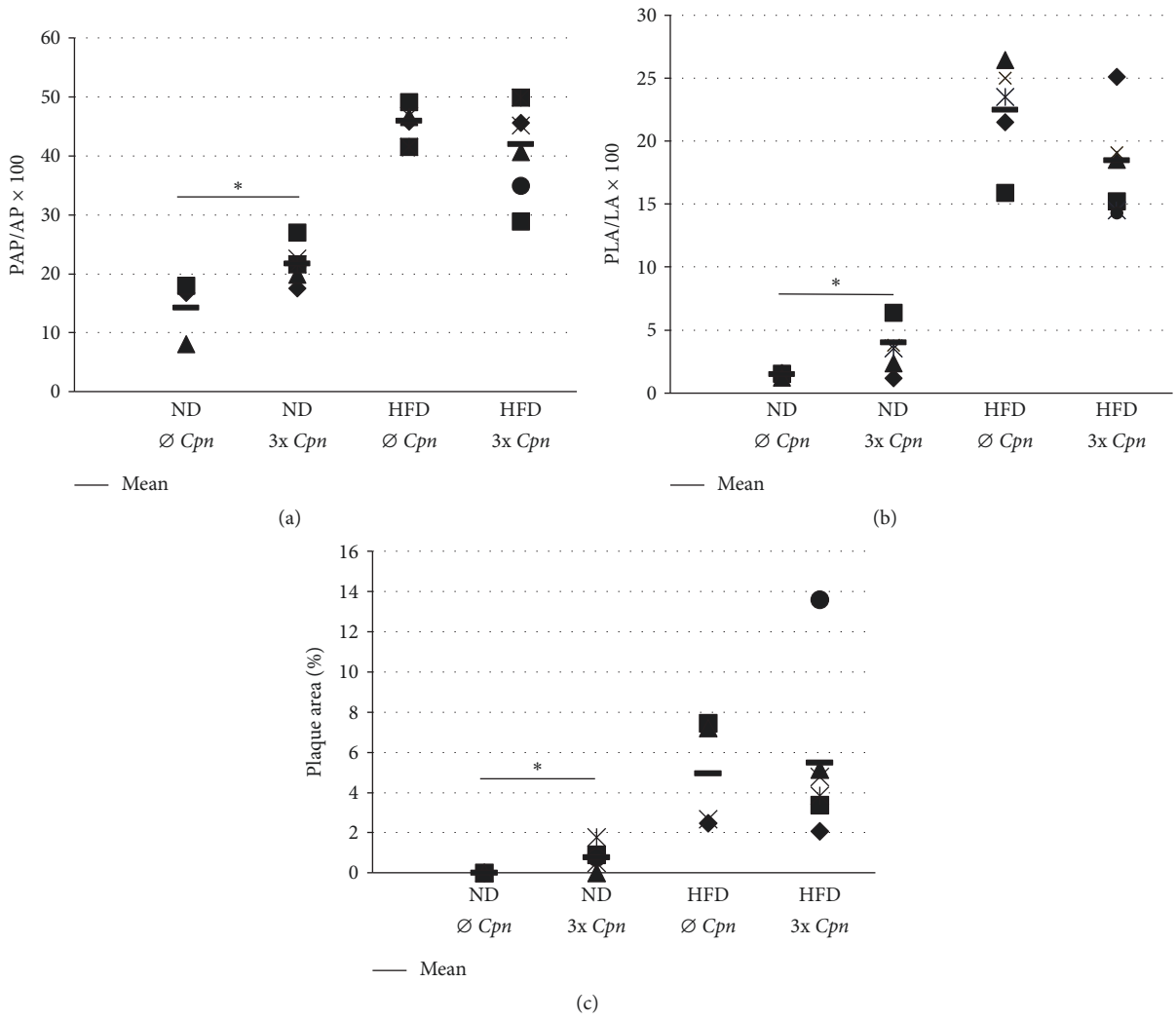

Figure 1: Morphometric analyses of atherosclerotic plaques in ApoB100only/LDLR$^{-/-}$ mice. (a) Measurements for the length of the aortic luminal surface (perimeter) covered by plaque (PAP/AP × 100); (b) percentage of aortic lumen area occupied by plaques (PLA/LA × 100) in 8 cross sections of aortic root from each ApoB100only/LDLR$^{-/-}$ mouse in groups kept on normal diet without *Cpn* infection (number of mice (N) = 6) or infected with *Cpn* 3 times (N = 8) or on high-fat/high-cholesterol diet for 12 weeks without *Cpn* infection (N = 6) or infected with *Cpn* 3 times (N = 8). Average percentage values from individual mice and mean percentages in groups are shown. PAP: plaque-covered aorta perimeter; AP: aorta perimeter; PLA: plaque-occupied lumen area; LA: aorta lumen area. (c) Plaque size was measured in the longitudinally opened descending aorta of each ApoB100only/LDLR$^{-/-}$ mouse in groups kept on normal or high-fat/high-cholesterol diet for 12 weeks without *Cpn* infection or infected with *Cpn* 3 times. The percentage of total aorta area covered by plaques was calculated. Data show the results of one of two independent experiments. For comparison of groups independent-samples t-test was used, $^*P < 0.05$. ND: normal diet; HFD: high-fat/high-cholesterol diet; 3x: three intranasal *Cpn* infections.

3.6. Plasma Lipid Levels in ApoB100only/LDLR$^{-/-}$ and ApoE$^{-/-}$ Mice. Plasma samples of mice were tested for lipid levels. At each tested time point irrespective of the infection status ApoE$^{-/-}$ mice carried a higher level of total cholesterol than the ApoB100only/LDLR$^{-/-}$ mice (Figure 5(a)). In the plasma of uninfected ApoB100only/LDLR$^{-/-}$ mice the triglyceride concentration was elevated compared to that in ApoE$^{-/-}$ mice (Figure 5(b)). Infection one or two times did not cause increase in triglyceride level, but the third *Cpn* inoculation resulted in a significant elevation (P = 0.001) in ApoE$^{-/-}$ mice. In ApoB100only/LDLR$^{-/-}$ mice no infection-related change in triglyceride level was obvious (Figure 5(b)). Plasma concentration of LDL was higher in ApoE$^{-/-}$ mice than in ApoB100only/LDLR$^{-/-}$ mice (Figure 5(c)). Infection-related significant increase in LDL level was associated with the first infection in ApoB100only/LDLR$^{-/-}$ mice only (P = 0.04). HDL plasma concentration was generally higher in ApoB100only/LDLR$^{-/-}$ mice than in ApoE$^{-/-}$ mice and in these mice the concentration decreased by the end of the observation period but remained high in

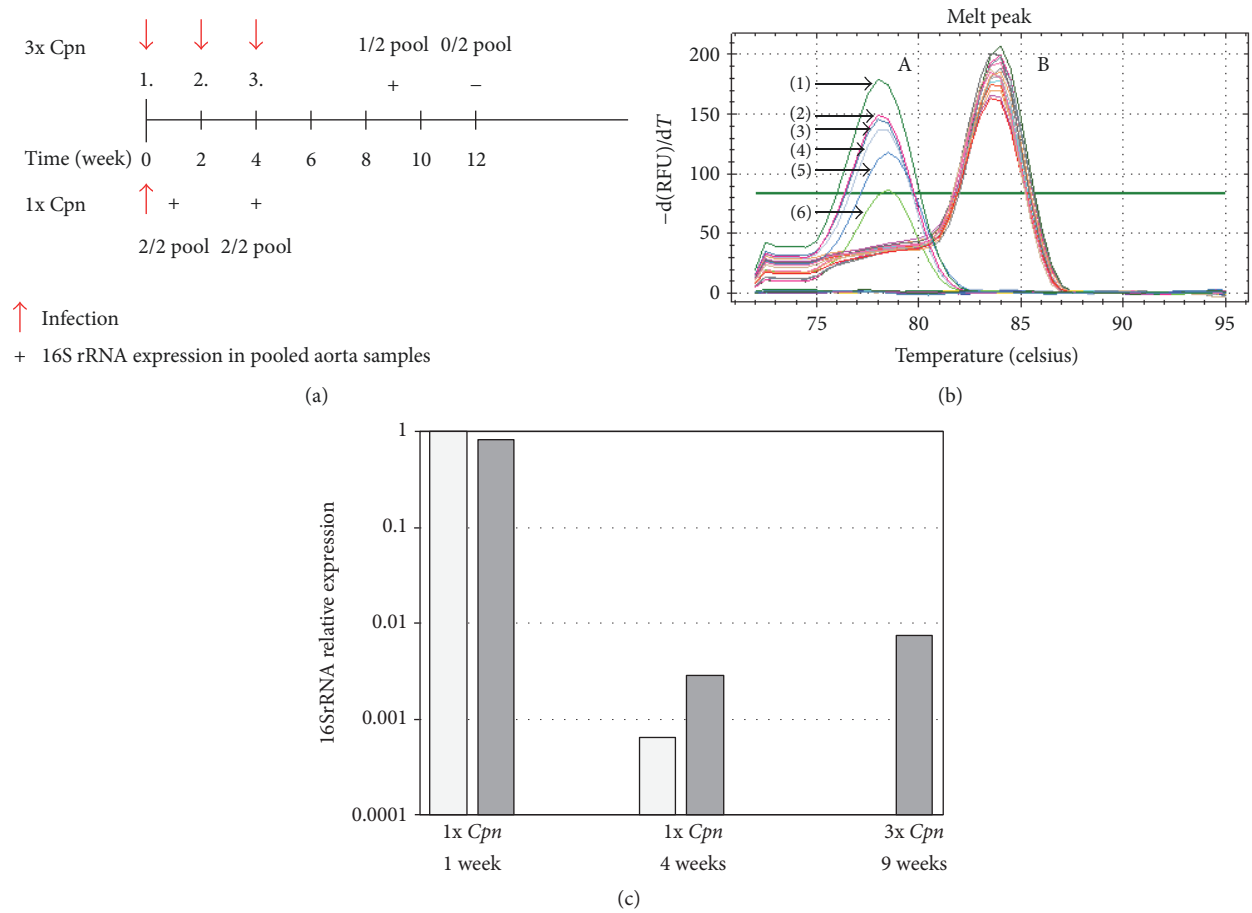

Figure 2: *Chlamydia* RNA in the aorta tissues. (a) Experimental design for *Cpn* infection of ApoB100only/LDLR$^{-/-}$ mice and 16SrRNA transcript detection in pooled aorta samples (two pools of 3 aortas from 6 mice) of one time (1x *Cpn*) and 3 times (3x *Cpn*) *Cpn*-infected and noninfected mice ("+": aorta samples tested positive; "–": aorta samples tested negative for expression of 16SrRNA by qRT-PCR). ((b)A) Identification of the RT-PCR-amplified *Cpn* 16SrRNA cDNA in the aorta of *Cpn*-infected ApoB100only/LDLR$^{-/-}$ mice. Melt curves show *Cpn* 16SrRNA amplicons in (1) *Cpn*-infected McCoy cells (positive control); (2), (3) in aorta samples tested 1 week after single *Cpn* infection; (4) in aorta samples 5 weeks after third *Cpn* infection, (5), (6) in aorta samples 4 weeks after a single *Cpn* infection; ((b)B) β-actin amplicons in all tested aorta samples and *Cpn*-infected McCoy cells. (c) Expression of *Cpn* 16SrRNA normalized to the expression level of mouse β-actin at 1 week after single *Cpn* infection was set as 1 and relative mouse β-actin-normalized *Cpn* 16SrRNA expression level in all pooled aorta samples giving positive 16SrRNA signal was calculated. The measurements were repeated two times with the same results.

ApoB100only/LDLR$^{-/-}$ mice (Figure 5(d)). No infection-associated change in HDL level was detected.

4. Discussion

ApoE$^{-/-}$ mice are widely used as animal models of atherosclerosis; however, the lipoprotein metabolism of this mouse strain is different from that in humans with hypercholesterolemia. ApoE$^{-/-}$ mice accumulate in their plasma large quantities of ApoB48 containing lipoprotein of the very low-density lipoprotein (VLDL) class while humans with atherosclerosis almost always have high level of cholesterol-rich LDL containing ApoB100 [23, 31]. Many publications investigating the relation of *Cpn* with atherosclerosis have used this model to disclose the nature of the association between infection with this pathogen and initiation and/or acceleration of atherosclerosis [28, 39–42]. It has been suggested that *Cpn* infection exacerbates atherosclerosis in conjunction with hyperlipidaemia; however, ApoE deficiency might influence the immune response to this pathogen and provides increased resistance to vascular infection [41]. We aimed at examining the influence of repeated *Cpn* infection on the formation of atherosclerotic plaques in ApoB100only/LDLR$^{-/-}$ mouse strain another model for lipoprotein abnormalities which can be regarded as the most faithful model of human familial hypercholesterolemia [21].

ApoB100only/LDLR$^{-/-}$ mouse strain was created by genetic modification, so that majority of their plasma cholesterol is in the LDL class with ApoB100 and develops atherosclerosis on low-fat, chow diet. First, we wanted to establish that ApoB100only/LDLR$^{-/-}$ mice can serve as a model for investigating the role of *Cpn* in atherosclerosis. Therefore groups of mice were fed with a normal or high-fat/high-cholesterol diet and were repeatedly infected with *Cpn* or left

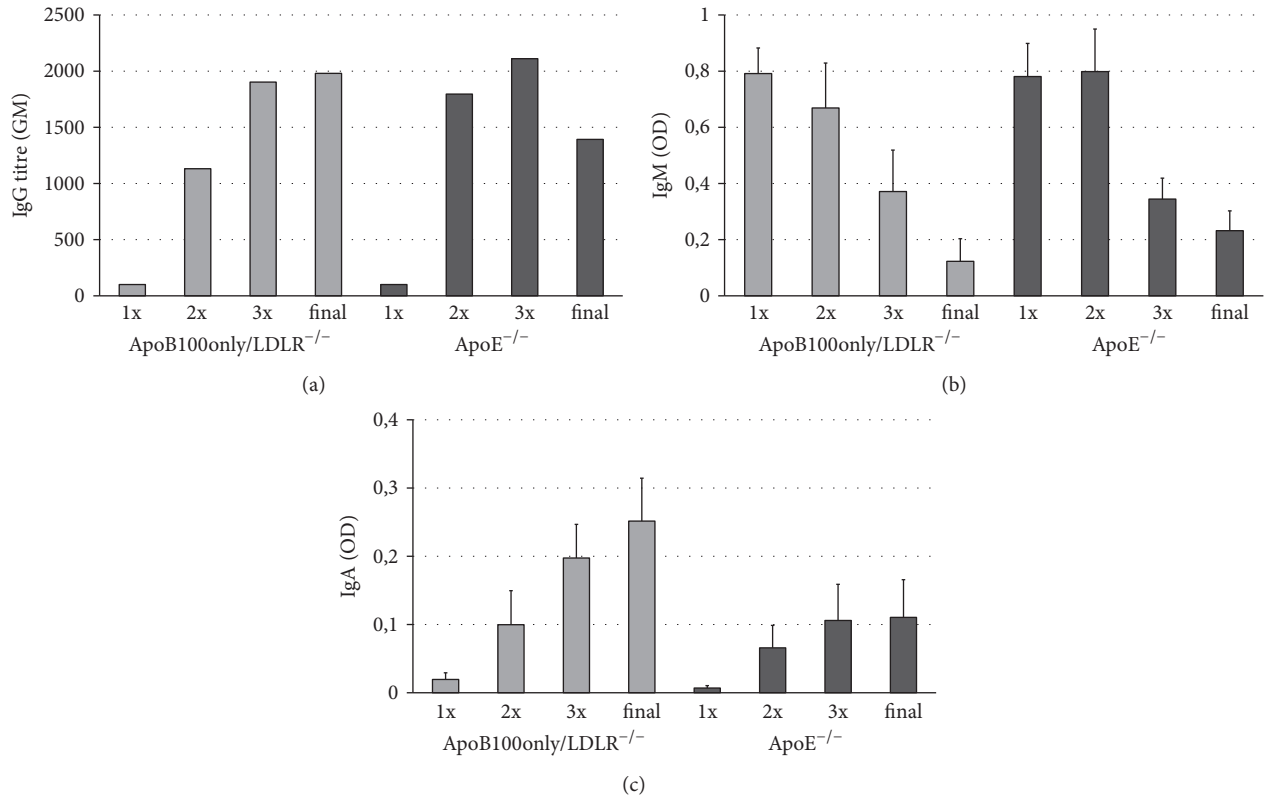

Figure 3: *Cpn*-specific antibodies in the mice. The serum antibody levels were measured in ApoB100only/LDLR$^{-/-}$ and ApoE$^{-/-}$ mice 1 week after first (1x), second (2x), third (3x) *Cpn* infection and at the end of the experiment (week 12) by an in-house ELISA test with *Cpn* antigen. (a) Geometric mean (GM) of IgG titres, reciprocal of dilutions producing OD ≥ 0.1 is shown. (b) For detection of *Cpn*-specific IgM and (c) IgA level in the sera 1 : 50 dilutions of serum samples (ApoB100only/LDLR$^{-/-}$: $N = 7$, ApoE$^{-/-}$ mice: $N = 8$) were tested with the ELISA test. OD values and standard deviations (SD) are shown. Data represent the results of one of two independent experiments.

uninfected, and development of atherosclerosis was followed. As our experiments showed, in ApoB100only/LDLR$^{-/-}$ mice which were fed with normal diet repeated three *Cpn* infections resulted in an enhanced atherosclerosis development in the aortic sinus and the descending aorta. High-fat/high-cholesterol diet-induced enhanced atherosclerosis was not exacerbated by *Cpn* infections. Thus all further experiments were done with mice kept on normal diet. As it is said that *Cpn* acts in cooperation with hyperlipidaemia it seems that the effect of hyperlipidaemia in ApoB100only/LDLR$^{-/-}$ mice can be aggravated by *Cpn* infection but *Cpn* does not exacerbate atherosclerosis further in the presence of high-fat/high-cholesterol diet [43–45]. Nevertheless, the bacterium influenced the course of atherosclerosis development indicating that ApoB100only/LDLR$^{-/-}$ mice are suitable for further research. Our results are consistent with findings of Moazed et al. who described atherosclerosis-accelerating effect of *Cpn* infection in ApoE$^{-/-}$ mice eating regular chow diet [44]. However, atherosclerosis was also exacerbated in ApoE$^{-/-}$ mice kept on high-fat diet by single or 3 repeated *Cpn* infections [39, 46].

We hypothesized that, based on the genetic difference between ApoB100only/LDLR$^{-/-}$ and ApoE$^{-/-}$ mice, features that characterize *Cpn* infection or atherosclerosis may also differ, and therefore we compared the effects of the bacterium in these mouse strains. In our infection model the successful infection was demonstrated by detecting *Cpn*-specific IgG, IgA, and IgM antibodies in the mice throughout the course of the experiment and at the time of sacrifice. When IgG antibody level was compared in ApoB100only/LDLR$^{-/-}$ and ApoE$^{-/-}$ mice, no significant difference was observed. Nazzal et al. [41] reported that ApoE$^{-/-}$ mice produced more *Cpn*-specific antibodies than wild-type mice which was attributed to ApoE deficiency. Our results do not support this suggestion considering that in ApoB100only/LDLR$^{-/-}$ mice repeated *Cpn* infection led to high level of antibody production without the contribution of ApoE deficiency.

Not only was antibody response the sign of infection, but we were able to detect metabolically active *Cpn* in the aorta samples for nine weeks after the first infection. Previous studies demonstrated the presence of *Cpn* in the aorta of repeatedly infected ApoE$^{-/-}$ mice by isolating the bacterium early two weeks after infection. Furthermore, bacterial DNA was amplified by PCR at later time points [47]. As reviewed by Campbell and Rosenfeld [48] several lines of evidence point to the ability of *Cpn* to establish persistent infection *in vivo*. Our results provide additional information about persisting chlamydia as 16SrRNA gene transcripts suggest metabolically

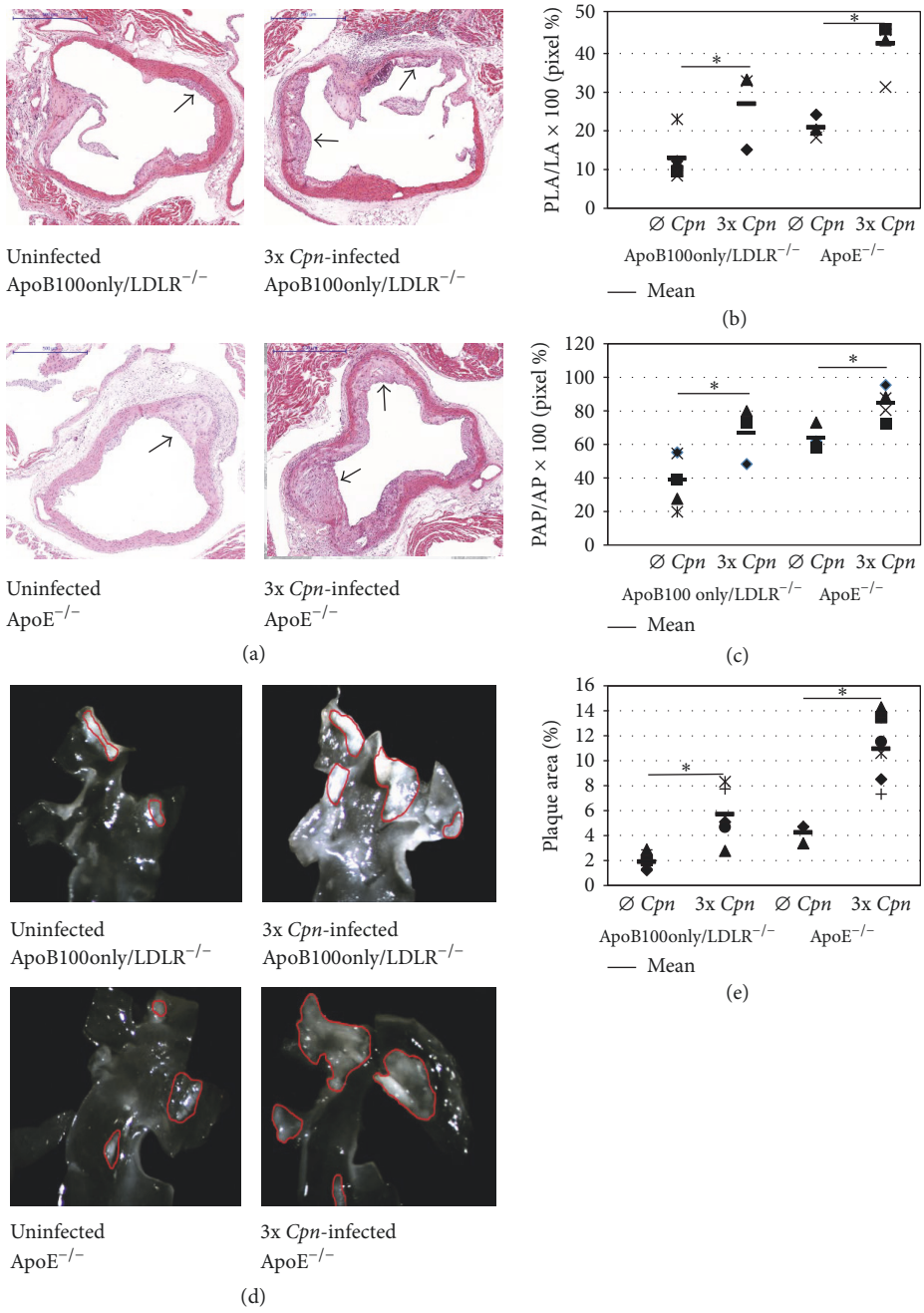

FIGURE 4: Comparative quantitative assessment of atherosclerosis in ApoB100only/LDLR$^{-/-}$ and ApoE$^{-/-}$ mice. Atherosclerosis development was assessed by histological and morphometric analyses in the aorta sinus and descending aorta of ApoB100only/LDLR$^{-/-}$ and ApoE$^{-/-}$ mice without and with 3 *Cpn* infections, 12 weeks after the first infection kept on normal diet. (a) Photo of representative hematoxylin and eosin-stained cross sections of the noninfected and *Cpn*-infected ApoB100only/LDLR$^{-/-}$ mice and noninfected and *Cpn*-infected ApoE$^{-/-}$ mice (scale bar: 500 μm). Arrows point to atherosclerotic lesions. (b) The percentage length of the aortic luminal surface (perimeter) covered by atherosclerotic plaque (PAP/AP × 100); (c) percentage of aortic lumen area occupied by atherosclerotic plaques (PLA/LA × 100) in 8 sections of aortic root from noninfected ($N = 6$), *Cpn*-infected ($N = 7$) ApoB100only/LDLR$^{-/-}$, and noninfected ($N = 6$) and *Cpn*-infected ($N = 8$) ApoE$^{-/-}$ mice. Average percentage values from individual mice and mean percentages in groups are shown. (d) In situ microscopic pictures of en face proximal aorta of noninfected and *Cpn*-infected ApoB100only/LDLR$^{-/-}$ and ApoE$^{-/-}$ mice, respectively. (e) Plaque size was measured on the length of the luminal surface of the descending aorta of 6–8 mice, and the percentage of total aorta area covered by plaques was calculated. Percentage values in individual mice and mean percentages in groups are shown. Data demonstrate the results of one of two independent experiments. For comparison of groups independent-samples t-test was used, $^{*}P < 0.05$. PAP: plaque-covered aorta perimeter; AP: aorta perimeter; PLA: plaque-occupied lumen area; LA: aorta lumen area; 3x: three intranasal *Cpn* infections.

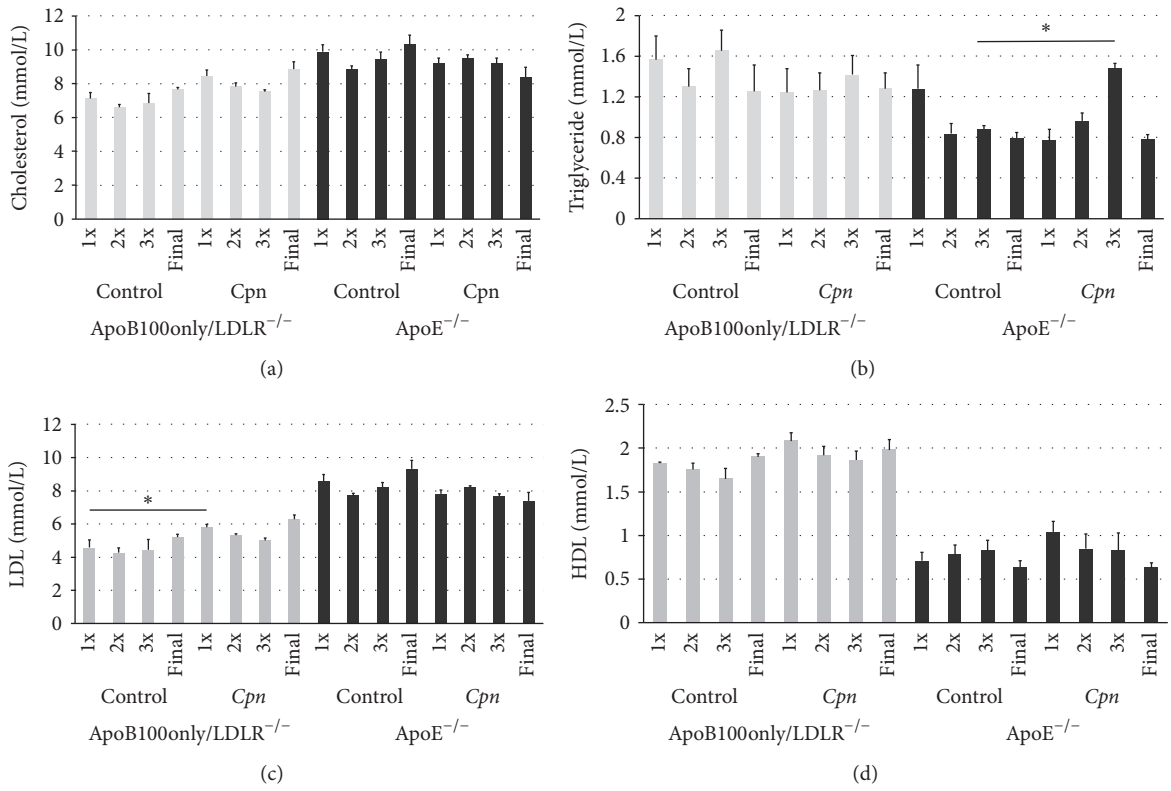

Figure 5: Plasma lipid levels in the mice. Plasma samples of ApoB100only/LDLR$^{-/-}$ and ApoE$^{-/-}$ mice taken at 1 week after the first (1x), second (2x), and third (3x) *Cpn* infection and at the end of the experiment (week 12) and from the noninfected control mice at the same time points were tested for concentration of (a) total cholesterol, (b) triglyceride, (c) LDL, and (d) HDL content. Lipid concentrations are expressed as mmol/L; mean of values measured in individual mouse sera (ApoB100only/LDLR$^{-/-}$ noninfected ($N = 6$), *Cpn*-infected ($N = 7$), and ApoE$^{-/-}$ mice noninfected ($N = 6$), *Cpn*-infected ($N = 8$)), and standard deviations (SD) are shown; independent-samples t-test was used, $^{*}P = 0.01$. The figure demonstrates the results of one of two independent experiments.

active bacteria not only persisting DNA or antigen late after repeated infections. Long-term presence of viable chlamydia in the aorta tissues of some infected mice might contribute to the atherogenic effect of the infection.

In female ApoE$^{-/-}$ mice we have disclosed more advanced atherosclerosis than in ApoB100only/LDLR$^{-/-}$ mice at the same age at the end of the 12-week observation period. Less pronounced difference was disclosed by Powell-Braxton et al. [21]. Nevertheless, in ApoE$^{-/-}$ mice, similar to ApoB100only/LDLR$^{-/-}$ mice, the infection resulted in an enhanced lesion formation without the need of feeding the mice with high-fat diet confirming the results with ApoE$^{-/-}$ mice of Moazed et al. [44].

It has been described that *Cpn* can cause hepatic fatty acid imbalance [49] dysregulation of lipid metabolic genes in the liver [50] and altered macrophage cholesterol homeostasis [51]; however, most of the studies in mice did not detect major changes in plasma lipid profile after *Cpn* infection [34, 39]. Increase in triglyceride concentration after repeated infection of ApoE$^{-/-}$ mice similarly to our results has been noted by Rothstein et al. [33]. The reason of increase in triglyceride level in chronic infection induced by multiple inoculations in ApoE$^{-/-}$ mice may be the absence of ApoE. ApoE is known to provide protection against the inflammation induced by bacterial lipopolysaccharide [52] and the inflammation related change in lipid metabolism [53]. Early increase of LDL level in ApoB100only/LDLR$^{-/-}$ mice after primary infection may also be due to the primary infection caused inflammation [54]. Our findings are concordant with results of a study by Kontula et al. [55] suggesting a significant association between chronic infection with *Cpn* and increased risk of coronary heart disease in patients with familial hypercholesterolemia.

5. Conclusion

In the field of infection-related exacerbation of atherosclerosis, the ApoB100only/LDLR$^{-/-}$ mouse strain has not been utilized. According to our results the infection is followed by long-lasting vascular infection in this mouse strain contributing to the potential direct effect of the infection in the vessel wall. As ApoE deficiency may alter the immune response against *Cpn* infection compared to wild-type mice, ApoB100only/LDLR$^{-/-}$ mice might provide additional information regarding the immune mechanisms participating in

the *Cpn* induced acceleration of atherosclerosis. The results of our experiments further support the proatherogenic role of *Cpn* infection in a model of human familial hypercholesterolemia. As repeated *Cpn* inoculation is able to aggravate lesion development in association with the lipoprotein abnormalities without feeding high-fat/high-cholesterol diet to these mice, we suggest using this mouse strain as an alternative model to investigate the role of infection in atherosclerosis development.

Conflicts of Interest

The authors declare that there are no conflicts of interest regarding the publication of this article.

Acknowledgments

This work was supported by Thrombosis Research Institute, London, UK, and Human Resources Development Operational Programme EFOP-3.6.1-16-2016-00008 [Dezső Péter Virok]. The authors thank Istvánné Lévai for excellent technical assistance and Krisztián Daru for histotechnological work.

References

[1] C. Weber and H. Noels, "Atherosclerosis: current pathogenesis and therapeutic options," *Nature Medicine*, vol. 17, no. 11, pp. 1410–1422, 2011.

[2] D. Lloyd-Jones, R. Adams, M. Carnethon et al., "Heart disease and stroke statistics—2009 update. A report from the American heart association statistics committee and stroke statistics subcommittee," *Circulation*, vol. 119, no. 3, pp. 480–486, 2009.

[3] R. H. Knopp and P. Paramsothy, "Treatment of hypercholesterolemia in patients with metabolic syndrome: How do different statins compare?" *Nature Clinical Practice Endocrinology & Metabolism*, vol. 2, no. 3, pp. 136-137, 2006.

[4] J. F. Bentzon, F. Otsuka, R. Virmani, and E. Falk, "Mechanisms of plaque formation and rupture," *Circulation Research*, vol. 114, no. 12, pp. 1852–1866, 2014.

[5] Pathobiological Determinants of Atherosclerosis in Youth (PDAY) Research Group, "Natural history of aortic and coronary atherosclerotic lesions in youth. Findings from the PDAY Study," *Arteriosclerosis, Thrombosis, and Vascular Biology*, vol. 13, no. 9, pp. 1291–1298, 1993.

[6] P. Libby, P. M. Ridker, and G. K. Hansson, "Inflammation in atherosclerosis: from pathophysiology to practice," *Journal of the American College of Cardiology*, vol. 54, no. 23, pp. 2129–2138, 2009.

[7] A. J. Lusis, "Atherosclerosis," *Nature*, vol. 407, no. 6801, pp. 233–241, 2000.

[8] M. Aikawa, E. Rabkin, S. J. Voglic et al., "Lipid lowering promotes accumulation of mature smooth muscle cells expressing smooth muscle myosin heavy chain isoforms in rabbit atheroma," *Circulation Research*, vol. 83, no. 10, pp. 1015–1026, 1998.

[9] J. B. Muhlestein, B. D. Horne, J. F. Carlquist et al., "Cytomegalovirus seropositivity and C-reactive protein have independent and combined predictive value for mortality in patients with angiographically demonstrated coronary artery disease," *Circulation*, vol. 102, no. 16, pp. 1917–1923, 2000.

[10] T. Kurita-Ochiai, R. Jia, Y. Cai, Y. Yamaguchi, and M. Yamamoto, "Periodontal disease-induced atherosclerosis and oxidative stress," *Antioxid Basel Switz*, vol. 4, no. 3, pp. 577–590, 2015.

[11] M. E. Cabalén, M. F. Cabral, L. M. Sanmarco et al., "Chronic Trypanosoma cruzi infection potentiates adipose tissue macrophage polarization toward an anti-inflammatory M2 phenotype and contributes to diabetes progression in a diet-induced obesity model," *Oncotarget* , vol. 7, no. 12, pp. 13400–13415, 2016.

[12] L. A. Campbell and M. E. Rosenfeld, "Infection and Atherosclerosis Development," *Archives of Medical Research*, vol. 46, no. 5, pp. 339–350, 2015.

[13] C. Watson and N. Alp, "Role of Chlamydia pneumoniae in atherosclerosis," *Clinical Science*, vol. 114, no. 8, pp. 509–531, 2008.

[14] G. Fazio, M. Giovino, A. Gullotti, D. Bacarella, G. Novo, and S. Novo, "Atherosclerosis, inflammation and Chlamydia pneumoniae," *World Journal of Cardiology*, vol. 1, no. 1, pp. 31–40, 2009.

[15] F. Blasi, P. Tarsia, and S. Aliberti, "Chlamydophila pneumoniae," *Clinical Microbiology and Infection*, vol. 15, no. 1, pp. 29–35, 2009.

[16] W. L. Beatty, R. P. Morrison, and G. I. Byrne, "Persistent chlamydiae: from cell culture to a paradigm for chlamydial pathogenesis," *Microbiology and Molecular Biology Reviews*, vol. 58, no. 4, pp. 686–699, 1994.

[17] R. Tewari, V. S. Nijhawan, M. N. Mishra, P. Dudeja, and T. K. Salopal, "Prevalence of helicobacter pylori, cytomegalovirus, and chlamydia pneumonia immunoglobulin seropositivity in coronary artery disease patients and normal individuals in north indian population," *Medical Journal Armed Forces India*, vol. 68, no. 1, pp. 53–57, 2012.

[18] K. Burian, Z. Kis, D. Virok et al., "Independent and joint effects of antibodies to human heat-shock protein 60 and Chlamydia pneumoniae infection in the development of coronary atherosclerosis," *Circulation*, vol. 103, no. 11, pp. 1503–1508, 2001.

[19] J. Jawien, P. Nastalek, R. Korbut, J. Jawień, and P. Nastałek, "Mouse models of experimental atherosclerosis," *Journal of Physiology and Pharmacology*, vol. 55, no. 3, pp. 503–517, 2004.

[20] F. R. Kapourchali, G. Surendiran, L. Chen, E. Uitz, B. Bahadori, and M. H. Moghadasian, "Animal models of atherosclerosis," *World Journal of Clinical Cases*, vol. 2, no. 5, pp. 126–132, 2014.

[21] L. Powell-Braxton, M. Véniant, R. D. Latvala et al., "A mouse model of human familial hypercholesterolemia: markedly elevated low density lipoprotein cholesterol levels and severe atherosclerosis on a low-fat chow diet," *Nature Medicine*, vol. 4, no. 8, pp. 934–938, 1998.

[22] A. S. Plump, J. D. Smith, T. Hayek et al., "Severe hypercholesterolemia and atherosclerosis in apolipoprotein E-deficient mice created by homologous recombination in ES cells," *Cell*, vol. 71, no. 2, pp. 343–353, 1992.

[23] D. J. Rader and G. A. FitzGerald, "State of the art: Atherosclerosis in a limited edition," *Nature Medicine*, vol. 4, no. 8, pp. 899-900, 1998.

[24] Z. P. Yang, C. C. Kuo, and J. Thomas Grayston, "Systemic dissemination of chlamydia pneumoniae following intranasal inoculation in mice," *The Journal of Infectious Diseases*, vol. 171, no. 3, pp. 736–738, 1995.

[25] Z. Kis, K. Burian, B. Treso et al., "Inflammatory- and immune responses in relation to bacterial replication in mice following

re-infections with Chlamydophila pneumoniae," *Inflammation Research*, vol. 57, no. 6, pp. 287–295, 2008.

[26] S. Chen, K. Shimada, W. Zhang, G. Huang, T. R. Crother, and M. Arditi, "IL-17A is proatherogenic in high-fat diet-induced and *Chlamydia pneumoniae* infection-accelerated atherosclerosis in mice," *The Journal of Immunology*, vol. 185, no. 9, pp. 5619–5627, 2010.

[27] L. Liu, H. Hu, H. Ji, A. D. Murdin, G. N. Pierce, and G. Zhong, "Chlamydia pneumoniae infection significantly exacerbates aortic atherosclerosis in an LDLR-/-mouse model within six months," *Molecular and Cellular Biochemistry*, vol. 215, no. 1-2, pp. 123–128, 2000.

[28] E. Blessing, L. A. Campbell, M. E. Rosenfeld, B. Chesebro, and C.-C. Kuo, "A 6 week course of azithromycin treatment has no beneficial effect on atherosclerotic lesion development in apolipoprotein E-deficient mice chronically infected with Chlamydia pneumoniae," *Journal of Antimicrobial Chemotherapy*, vol. 55, no. 6, pp. 1037–1040, 2005.

[29] K. Burián, H. Hegyesi, E. Buzás et al., "Chlamydophila (Chlamydia) pneumoniae induces histidine decarboxylase production in the mouse lung," *Immunology Letters*, vol. 89, no. 2-3, pp. 229–236, 2003.

[30] A. Bogdanov, V. Endrész, S. Urbán et al., "Application of dna chip scanning technology for automatic detection of chlamydia trachomatis and chlamydia pneumoniae inclusions," *Antimicrobial Agents and Chemotherapy*, vol. 58, no. 1, pp. 405–413, 2014.

[31] R. V. Farese Jr., M. M. Véniant, C. M. Cham et al., "Phenotypic analysis of mice expressing exclusively apolipoprotein B48 or apolipoprotein B100," *Proceedings of the National Acadamy of Sciences of the United States of America*, vol. 93, no. 13, pp. 6393–6398, 1996.

[32] D. M. Wuttge, A. Sirsjö, P. Eriksson, and S. Stemme, "Gene expression in atherosclerotic lesion of ApoE deficient mice," *Molecular Medicine*, vol. 7, no. 6, pp. 383–392, 2001.

[33] N. M. Rothstein, T. C. Quinn, G. Madico, C. A. Gaydos, and C. J. Lowenstein, "Effect of azithromycin on murine arteriosclerosis exacerbated by Chlamydia pneumomiae," *The Journal of Infectious Diseases*, vol. 183, no. 2, pp. 232–238, 2001.

[34] L. Erkkilä, K. Laitinen, K. Haasio et al., "Heat shock protein 60 autoimmunity and early lipid lesions in cholesterol-fed C57BL/6JBom mice during Chlamydia pneumoniae infection," *Atherosclerosis*, vol. 177, no. 2, pp. 321–328, 2004.

[35] B. Paigen, A. Morrow, P. A. Holmes, D. Mitchell, and R. A. Williams, "Quantitative assessment of atherosclerotic lesions in mice," *Atherosclerosis*, vol. 68, no. 3, pp. 231–240, 1987.

[36] L. Mannonen, E. Kamping, T. Penttilä, and M. Puolakkainen, "IFN-γ induced persistent Chlamydia pneumoniae infection in HL and Mono Mac 6 cells: characterization by real-time quantitative PCR and culture," *Microbial Pathogenesis*, vol. 36, no. 1, pp. 41–50, 2004.

[37] T. Mosolygó, J. Korcsik, E. P. Balogh et al., "Chlamydophila pneumoniae re-infection triggers the production of IL-17A and IL-17E, important regulators of airway inflammation," *Inflammation Research*, vol. 62, no. 5, pp. 451–460, 2013.

[38] S. Dhanasekaran, T. M. Doherty, and J. Kenneth, "Comparison of different standards for real-time PCR-based absolute quantification," *Journal of Immunological Methods*, vol. 354, no. 1-2, pp. 34–39, 2010.

[39] R. Sorrentino, A. Yilmaz, K. Schubert et al., "A single infection with *Chlamydia pneumoniae* is sufficient to exacerbate atherosclerosis in ApoE deficient mice," *Cellular Immunology*, vol. 294, no. 1, pp. 25–32, 2015.

[40] S. B. Damy, M. L. Higuchi, J. Timenetsky et al., "Mycoplasma pneumoniae and/or Chlamydophila pneumoniae inoculation causing different aggravations in cholesterol-induced atherosclerosis in apoE KO male mice," *BMC Microbiology*, vol. 9, article no. 194, 2009.

[41] D. Nazzal, N. Therville, H. Yacoub-Youssef et al., "Apolipoprotein e-deficient mice develop an anti-chlamydophila pneumoniae T helper 2 response and resist vascular infection," *The Journal of Infectious Diseases*, vol. 202, no. 5, pp. 782–790, 2010.

[42] T. C. Moazed, C.-C. Kuo, J. T. Grayston, and L. A. Campbell, "Murine models of Chlamydia pneumoniae infection and atherosclerosis," *The Journal of Infectious Diseases*, vol. 175, no. 4, pp. 883–890, 1997.

[43] H. Hu, G. N. Pierce, and G. Zhong, "The atherogenic effects of chlamydia are dependent on serum cholesterol and specific to Chlamydia pneumoniae," *The Journal of Clinical Investigation*, vol. 103, no. 5, pp. 747–753, 1999.

[44] T. C. Moazed, L. A. Campbell, M. E. Rosenfeld, J. T. Grayston, and C.-C. Kuo, "Chlamydia pneumoniae infection accelerates the progression of atherosclerosis in apolipoprotein E-deficient mice," *The Journal of Infectious Diseases*, vol. 180, no. 1, pp. 238–241, 1999.

[45] E. Blessing, L. A. Campbell, M. E. Rosenfeld, N. Chough, and C.-C. Kuo, "*Chlamydia pneumoniae* infection accelerates hyperlipidemia induced atherosclerotic lesion development in C57BL/6J mice," *Atherosclerosis*, vol. 158, no. 1, pp. 13–17, 2001.

[46] Y. Naiki, R. Sorrentino, M. H. Wong et al., "TLR/MyD88 and liver X receptor α signaling pathways reciprocally control Chlamydia pneumoniae-induced acceleration of atherosclerosis," *The Journal of Immunology*, vol. 181, no. 10, pp. 7176–7185, 2008.

[47] L. A. Campbell, T. C. Moazed, C.-C. Kuo, and J. T. Grayston, "Preclinical models for Chlamydia pneumoniae and cardiovascular disease: hypercholesterolemic mice," *Clinical Microbiology and Infection*, vol. 4, Suppl 4, pp. S23–S32, 1998.

[48] L. A. Campbell and M. E. Rosenfeld, "Persistent C. pneumoniae infection in atherosclerotic lesions: Rethinking the clinical trials," *Frontiers in Cellular and Infection Microbiology*, vol. 5, Article ID Article 34, 2014.

[49] K. Hyvärinen, A. M. Tuomainen, S. Laitinen et al., "The effect of proatherogenic pathogens on adipose tissue transcriptome and fatty acid distribution in apolipoprotein E-deficient mice," *BMC Genomics*, vol. 14, no. 1, article no. 709, 2013.

[50] A. Marangoni, E. Fiorino, F. Gilardi et al., "Chlamydia pneumoniae acute liver infection affects hepatic cholesterol and triglyceride metabolism in mice," *Atherosclerosis*, vol. 241, no. 2, pp. 471–479, 2015.

[51] A. M. Tuomainen, K. Hyvärinen, P. I. Ehlers et al., "The effect of proatherogenic microbes on macrophage cholesterol homeostasis in apoE-deficient mice," *Microbial Pathogenesis*, vol. 51, no. 3, pp. 217–224, 2011.

[52] M. Van Oosten, P. C. N. Rensen, E. S. Van Amersfoort et al., "Apolipoprotein E protects against bacterial lipopolysaccharide-induced lethality: A new therapeutic approach to treat Gram-negative sepsis," *The Journal of Biological Chemistry*, vol. 276, no. 12, pp. 8820–8824, 2001.

[53] W. Khovidhunkit, M.-S. Kim, R. A. Memon et al., "Effects of infection and inflammation on lipid and lipoprotein

metabolism: mechanisms and consequences to the host," *Journal of Lipid Research*, vol. 45, no. 7, pp. 1169–1196, 2004.

[54] K. R. Feingold, I. Hardardottir, R. Memon et al., "Effect of endotoxin on cholesterol biosynthesis and distribution in serum lipoproteins in Syrian hamsters," *Journal of Lipid Research*, vol. 34, no. 12, pp. 2147–2158, 1993.

[55] K. Kontula, A. Vuorio, H. Turtola, and P. Saikku, "Association of seropositivity for Chlamydia pneumoniae and coronary artery disease in heterozygous familial hypercholesterolaemia," *The Lancet*, vol. 354, no. 9172, pp. 46-47, 1999.

II.

Pathogens and Disease, 76, 2018, fty024

doi: 10.1093/femspd/fty024
Advance Access Publication Date: 16 March 2018
Research Article

RESEARCH ARTICLE

Growth characteristics of *Chlamydia trachomatis* in human intestinal epithelial Caco-2 cells

Ildikó Lantos[1], Dezső P Virok[1], Tímea Mosolygó[1], Zsolt Rázga[2], Katalin Burián[1] and Valéria Endrész[1,*]

[1]Department of Medical Microbiology and Immunobiology, University of Szeged, H-6720, Szeged, Dóm Sq. 10, Hungary and [2]Department of Pathology, University of Szeged, H-6720, Állomás Str. 2, Hungary

*Corresponding author: Department of Medical Microbiology and Immunobiology, University of Szeged, H-6720, Szeged, Dóm Sq. 10, Hungary. Tel: +36-62-545-541; Fax: +36-62-545-113; E-mail: endresz.valeria@med.u-szeged.hu

One sentence summary: Our analyses of growth characteristics of *Chlamydia trachomatis* in intestinal epithelial Caco-2 cells support the possibility of the gastrointestinal tract behaving as a source of reinfection of the urogenital tract.

Editor: Peter Timms

ABSTRACT

Chlamydia trachomatis is an obligate intracellular bacterium causing infections of the eyes, urogenital and respiratory tracts. Asymptomatic, repeat and chronic infections with *C. trachomatis* are common in the urogenital tract potentially causing severe reproductive pathology. Animal models of infection and epidemiological studies suggested the gastrointestinal tract as a reservoir of chlamydiae and as a source of repeat urogenital infections. Thus, we investigated the growth characteristics of *C. trachomatis* in human intestinal epithelial Caco-2 cells and the infection-induced defensin production. Immunofluorescence staining and transmission electron microscopy showed the presence of chlamydial inclusions in the cells. Chlamydial DNA and viable *C. trachomatis* were recovered from Caco-2 cells in similar quantity compared to that detected in the usual *in vitro* host cell of this bacterium. The kinetics of expression of selected *C. trachomatis* genes in Caco-2 cells indicated prolonged replication with persisting high expression level of late genes and of heat shock protein gene *groEL*. Replication of *C. trachomatis* induced moderate level of β-defensin-2 production by Caco-2 cells, which might contribute to avoidance of immune recognition in the intestine. According to our results, Caco-2 cells support *C. trachomatis* replication, suggesting that the gastrointestinal tract is a site of residence for these bacteria.

Keywords: Caco-2; *Chlamydia*; defensin; gastrointestinal tract; gene expression

INTRODUCTION

Chlamydiae are Gram-negative bacteria, obligate, intracellular pathogens that cause different acute and chronic human diseases. *Chlamydia trachomatis* infects the urogenital and ocular mucosa of humans, and it causes the most common sexually transmitted infection and trachoma as well (Mpiga and Ravaoarinoro 2006).

Chlamydiae have a unique developmental cycle involving two main forms. They exist as infective and metabolically inactive elementary bodies (EBs) or as non-infective but metabolically active reticulate bodies (RBs; Bastidas *et al.* 2013).

Several publications have described a third, persistent phase of the chlamydial developmental cycle, in which the RBs are enlarged and pleomorphic in morphologically abnormal inclusions. In persistence, chlamydiae show altered gene expression patterns (Schoborg 2011). The persistent form of *Chlamydia* was induced by interferon-gamma (IFN-γ; Kokab *et al.* 2010), antibiotics (Kintner *et al.* 2014; Phillips-Campbell, Kintner and Schoborg 2014), iron depletion (Mäurer *et al.* 2007), and it could

Received: 16 November 2017; **Accepted:** 15 March 2018

also be induced in different cell types, e.g. in monocytes (Datta *et al.* 2014).

C. trachomatis persistence has been associated with chronic infections (Wyrick 2010).

Animal pathogenic *Chlamydia* species were isolated from various animals, for example, porcines, ruminants and avians, and they were detected in different organs as well as in feces. In most animals, chlamydiae persist in the gastrointestinal (GI) tract and are transmitted via the fecal–oral route (Rank and Yeruva 2014). Oral infection with *C. muridarum* has resulted in a long term, persistent infection of the mouse GI tract (Igietseme, Portis and Perry 2001). The GI tract seems to be an ideal site, in which *Chlamydia* can persist because of a down regulated host immune response. In Caco-2 cells, inclusions have indicated a substantial growth of porcine *C. pecorum* and *C. suis*; therefore, Caco-2 cells can be regarded as suitable hosts for animal *Chlamydia* (Schiller *et al.* 2004).

C. trachomatis urogenital strains have been associated with persistent or recurrent infection of the genital tract in women, the nature of which has not been identified. It has been suggested that genital tract infection can be accompanied by infection of the GI tract either via oral infection or by autoinoculation from genital secretions or during sexual activity (van Liere *et al.* 2014). Anorectal samples taken from both men and women have been tested and found positive for *C. trachomatis* (Bax *et al.* 2011). Studies by Yeruva *et al.* have suggested that reinfection of the genital tract may occur via contamination of the genital tract from the infected GI tract, especially in women (Yeruva *et al.* 2013). Furthermore, *C. trachomatis* might have a role in irritable bowel disease (IBD) as suggested by the detection of *C. trachomatis* antigen in the intestine of IBD patients (Dlugosz *et al.* 2010).

Caco-2 cell line could be a suitable model for the investigation of *Chlamydia* infection in the human GI tract. If chlamydiae can persist in the GI tract, it is of relevance to examine the growth characteristics of human *Chlamydia* in Caco-2 cells, and the induced innate immune response in these cells.

In the colonic mucosa, defensins, and among them human β-defensin (hBD)-2 represent the important effectors of the innate host defenses not only by their microbicidal activity but by providing a link to the adaptive immune system as they attract immature dendritic cells and memory T-cells (Kim 2014).

In this study, we applied several morphological and molecular approaches to investigate the growth characteristics of *C. trachomatis* in the intestinal epithelial cell line Caco-2, and we examined whether *Chlamydia* infection induce hBD-2 production in these cells.

MATERIALS AND METHODS

Cell lines

Caco-2, HeLa 229 and McCoy cells were maintained in minimal essential medium (MEM) with Earle's salts completed with 10% FBS, 2 mmol/liter L-glutamine, 1× nonessential amino acids, 25 μg/mL gentamicin and 0.5 μg/mL fungizone. The cell lines were purchased from American Types Culture Collection (ATCC).

Bacterial strains

Chlamydia trachomatis serovar D, UW-3/CX strain from ATCC was used, and it was propagated in McCoy cell line. The infected cells were purified by density gradient centrifugation, as previously described, with some modification (Sabet, Simmons and Caldwell 1984; Burián *et al.* 2003).

The partially purified and concentrated EBs were aliquoted in sucrose–phosphate–glutamic acid buffer (SPG) and stored at –80°C until use. Infective chlamydiae were quantitated by inoculating 10-fold serial dilutions of the EB-containing preparations onto McCoy cells; the inclusions were detected by indirect immunofluorescent method applying anti-Chlamydia lipopolysaccharide (cLPS) monoclonal antibody (AbD Serotec, Oxford, United Kingdom) and fluorescein isothiocyanate (FITC)-labeled anti-mouse IgG (Sigma-Aldrich, St. Louis, MO, USA). The concentration of infective EBs was expressed as inclusion forming units/mL (IFU/mL).

Bacterial infection

The cells were grown in 6-well (1×10^6 cells/well), 96-well (4×10^4 cells/well), or 24-well culture plates (2.5×10^5 cells/well) with 13 mm glass coverslips. The plates were kept for 1 h at room temperature (RT), and then incubated overnight in 5% CO_2 atmosphere at 37°C to reach 90% confluency. The cells were then infected with *Chlamydia* at a multiplicity of infection (MOI) of 1 or 5 in complete MEM with 0.5% glucose and centrifuged at 800 × *g* for 1 h RT. The medium was replaced in the wells with a cycloheximide-containing one (1 μg/mL). Cycloheximide was not added to the medium of cells in 6-well plates infected for testing defensin secretion or RNA expression analyses. For DNA quantitation, the infected cells in 96-well plates were incubated in cycloheximide-containing medium or cycloheximide-free medium. The culture plates were incubated for different time periods in CO_2 incubator at 37°C.

Assessment of the infectivity of *C. trachomatis* D replicating in Caco-2 or HeLa cells was done by inoculation of the infected cell lysates onto McCoy cells in 24-well plates with glass coverslips. Cell lysates were prepared by scraping the infected cells into the culture medium at each examination time point. After two freeze-thaw cycles and sonication in water bath, the lysates were centrifuged at 800 × *g* for 1 h onto McCoy cells grown in 24-well plates with 13-mm glass coverslips. After 48 h, the cells were fixed with acetone at –20°C for 10 min.

Immunofluorescent staining of infected cells for visualization of inclusions and quantitation of recoverable *Chlamydia*

The staining of *Chlamydia*-infected cells on coverslips was performed via using anti-cLPS and FITC-labeled anti-mouse IgG as secondary antibody. The coverslips were treated with Evan's Blue at RT for 1 min. The chlamydial inclusions were photographed and counted under a fluorescent microscope.

Transmission electron microscopy

The cells were cultured in 6-well plates and infected with *Chlamydia* at an MOI of 1. After 24, 48 and 72 h, the infected cells were washed in plates with 3 mL phosphate buffered saline (PBS) and collected after trypsin treatment. After sedimentation with 400 × *g* for 5 min, the cells were fixed with 2% glutaraldehyde and 1% osmium tetroxide overnight at 4°C. Samples were embedded in Embed 812 (EMS, Hatfield, PA, USA) using a routine transmission electron microscopy (TEM) embedding protocol. Ultrathin sections (70 nm) were cut with an Ultracut S ultra-microtome (Leica, Vienna, Austria). After staining with uranyl acetate and lead citrate, the sections were examined with a Philips CM10

Table 1. Primer sequences used in qRT-PCR analysis.

C. trachomatis target gene	Sequence	PCR product size (bp)
16S rRNA F	5'-CACAAGCAGTGGAGCATGTGGTTT-3'	191
16S rRNA R	5'-ACTAACGATAAGGGTTGCGCTCGT-3'	
euo F	5'-TCCCCGACGCTCTCCTTTCA-3'	263
euo R	5'-CTCGTCAGGCTATCTATGTTGCT-3'	
ftsK F	5' CGGAAGAAAGCAAGCGTTTC 3'	70
ftsK R	5' GGGCTAGATACACGCATGTTTTAAC 3'	
groEL F	5'-TCACTCTAGGGCCTAAAGGACG-3'	115
groEL R	5'-TCATGTTTGTCGGCAAGCTC-3'	
omcB F	5' TGAAGCAGAGTTCGTACGCAGTG 3'	179
omcB R	5' AACGGATCTCTGGACAAGCGCAT 3'	
ompA F	5'-TCGACGGAATTC TGTGGGAAGGTT-3'	171
ompA R	5'-TATCAGTTGTAGGCTTGGCACCCA-3'	
pyk F	5'-GTTGCCAACGCCATTTACGATGGA-3'	81
pyk R	5'-TGCATGTACAGGATGGGCTCCTAA-3'	

electron microscope. Images were acquired by using Olympus Soft Imagine Viewer program.

Chlamydial DNA quantitation

For the quantitative assessment of chlamydial replication, we followed a direct DNA quantitation method described previously (Eszik *et al*. 2016). The cells cultured in 96 or 24-well plates were infected with *Chlamydia*. After 0, 24, 48 and 72 h, the infected cells in 3 parallel wells were washed in the plates twice with 200 μL/well PBS. Then, either 100 or 625 μL Milli-Q water was added to the wells, and the plates were stored at –80°C. Two freeze-thaw cycles were applied to free the DNA from the cells. Thoroughly mixed lysates were used as templates directly for quantitative PCR (qPCR) using SsoFast EvaGreen ®Supermix (BioRad, Hercules, CA, USA). Pyk primers were used for the detection of *C. trachomatis* D genomes (Table 1).

RNA extraction

For the analysis of gene expression, total RNA was extracted from the infected cells in 6-well plates at 2, 24, 48 or 72 h after infection (3 parallel cultures at each time point) with GenElute Mammalian Total RNA Miniprep Kit (Sigma-Aldrich) according to the manufacturer's protocol. Concentration of RNA was determined by spectrophotometry. The extracted RNA was treated with DNase I (Sigma-Aldrich). cDNA was synthetized from DNase-treated RNA with qScript cDNA Supermix synthesis kit (Quanta Biosciences, Gaithersburg, MD, USA). RNA and cDNA were stored at –80°C until use.

Quantitative RT-PCR

By using cDNA as template, quantitative real-time polymerase chain reaction (qRT-PCR) was performed with PerfeCTa SYBR Green Supermix (Quanta) in CFX96 Real Time C1000 Thermal Cycler (Bio-Rad). 16S rRNA was used as the internal standard for counting the relative expression of *Chlamydia* genes as this gene was previously shown to be an accurate normalizing gene for gene expression analysis in *C. trachomatis* (Borges *et al*. 2010). The relative expression of *euo*, *groEL, ftsK, omcB, ompA* and *pyk* transcripts of *C. trachomatis* was evaluated. The sequences of all primers used for RT-PCR are shown in Table 1. All primers were synthetized by Integrated DNA Technologies Inc. (Montreal, Quebec, Canada). The PCR cycles consisted of a 3-min denaturation at 95°C followed by 55 cycles of 10 s of denaturation at 94°C; 10 s of annealing at 61.5°C for *16S rRNA*, *groEL, omcB, ompA*, *pyk*, 54°C for *ftsK* and 10 s of extension at 72°C. The samples were tested in triplicates, and no-template controls with distilled water were run in each case. The melt curve analysis was performed to prove the specificity of the amplification.

The relative gene expression levels (RQ) were given by calculating the delta-delta Ct ($\Delta\Delta$Ct) value. The lowest cycle number, at which the various transcripts were detectable, referred to as Ct, was compared with that of the 16S rRNA, and the difference was referred to as ΔCt (Borges *et al*. 2010). The relative expression level was given as $2^{-(\Delta\Delta Ct)}$, where $\Delta\Delta Ct = \Delta Ct$ for the experimental sample minus ΔCt for the control sample at 2 h.

Enzyme-linked immunosorbent assay (ELISA) for detection of hBD-2

The supernatant of the infected cells from 3 parallel wells from 24-well plates were harvested at different time points post infection. For the detection of hBD-2 production, the supernatants of the cells were tested by using hBD-2 ELISA kit (Alpha Diagnostic, San Antonio, TX, USA). The level of the hBD-2 (12.5–200 pg/mL detection range) was determined according to the manufacturer's instructions. The supernatant of Caco-2 cells treated with heated (1 h, 56°C) overnight culture of *Escherichia coli* Nissle 1917 strain (MOI of 100), a potent inducer of HBD-2, was used as positive control.

Statistical analysis

Data are expressed as mean ± SD. Independent-samples t-test was used with SigmaPlot for Windows Version 11.0 software. A *P* value of less than 0.05 was considered to indicate statistically significant difference.

RESULTS

Detection of *Chlamydia* growth by immunofluorescence staining in Caco-2 and conventional host cells

After indirect immunofluorescence staining with anti-cLPS antibody, inclusions of *C. trachomatis* were seen in Caco-2 and HeLa cells. The detection of the inclusions suggested ongoing replication in both cell types; however, the morphology of the inclusions demonstrated different growth kinetics in the different cell types. *C. trachomatis* D formed compact inclusions in Caco-2 cells with cLPS appearing in the cell membrane (Fig. 1A), and HeLa cells showed inclusions with dense core and expanding cLPS signal at 24 h post-infection (Fig. 1B); at 48 h in Caco-2 cells (Fig. 1C), the inclusions grew larger but in the permissive HeLa cells expanding fluorescing areas had shown the final stage of replication cycle by this time (Fig. 1D).

Transmission electron microscopy of *Chlamydia*-infected Caco-2 and conventional host cells

With TEM, *C. trachomatis* D inclusions were observed both in Caco-2 (Fig. 2A, B) and HeLa (Fig. 2C, D) cells. The developmental stage of the bacteria in the inclusions at 48 h post-infection was rather heterogeneous in Caco-2 cells; however, in HeLa cells fully developed inclusions with numerous EBs were seen.

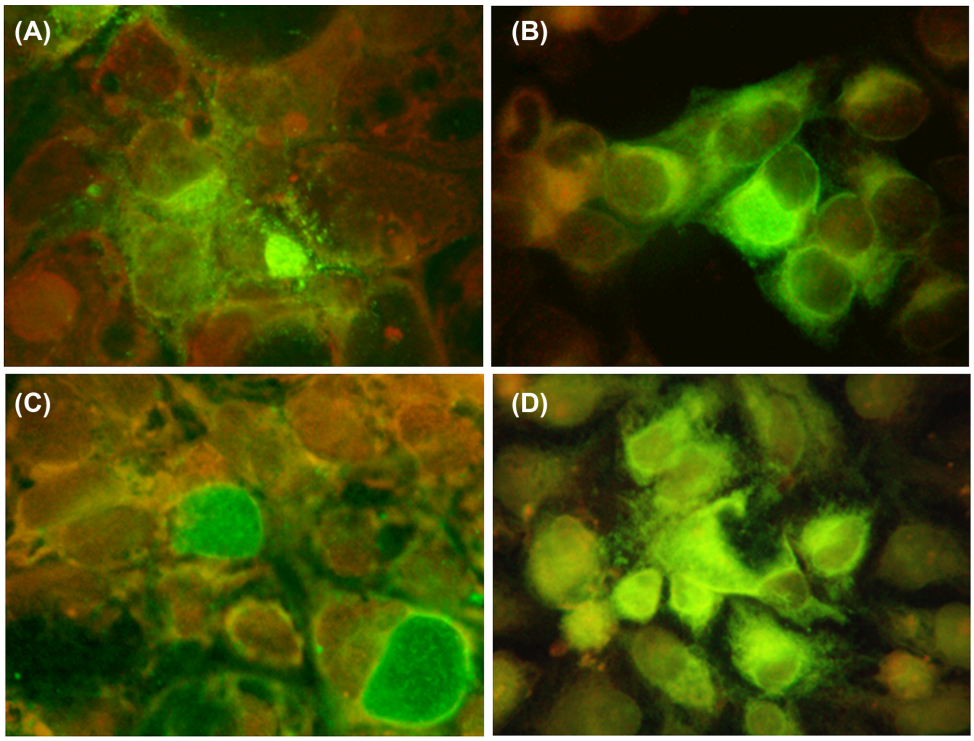

Figure 1. Immunofluorescence-stained inclusions of *C. trachomatis* D in Caco-2 and HeLa cells. The cells were grown on 13-mm coverslips, and the monolayers were infected at an MOI of 1. *Chlamydia trachomatis* D-infected Caco-2 cells were incubated for 24 h (**A**) or for 48 h (**C**), and *C. trachomatis*-infected HeLa cells were incubated for 24 h (**B**) and for 48 h (**D**). After the indicated times, the cells were stained by indirect immunofluorescence using anti-cLPS antibody and FITC-labeled anti-mouse IgG secondary antibody. Pictures were acquired by a digital camera attached to a fluorescence microscope using 625-fold magnification.

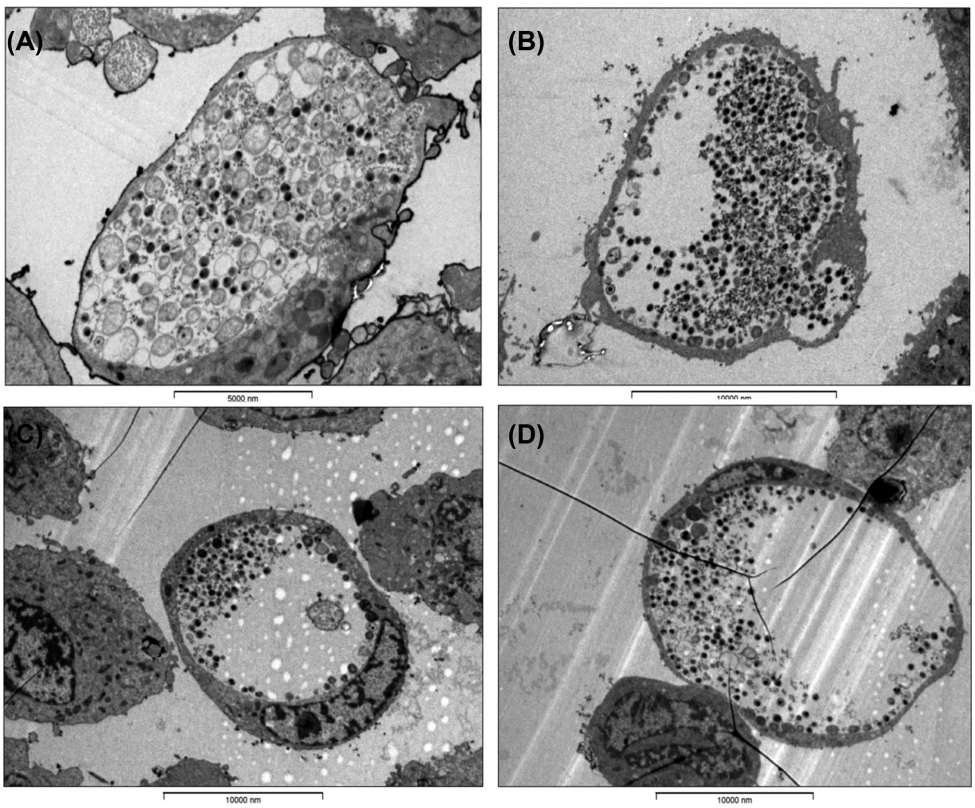

Figure 2. TEM images of *C. trachomatis* D inclusions in infected cells. Cells grown in 6-well plates were infected with chlamydiae at an MOI of 1. At the indicated time points after infection, the cells were fixed and processed for electron microscopy. Chlamydial inclusions in (**A**, **B**) *C. trachomatis* serovar D-infected Caco-2 cells 48 h post-infection; (**C**, **D**) *C. trachomatis* D-infected HeLa cells 48 h post-infection. Magnification is shown by the scale bars.

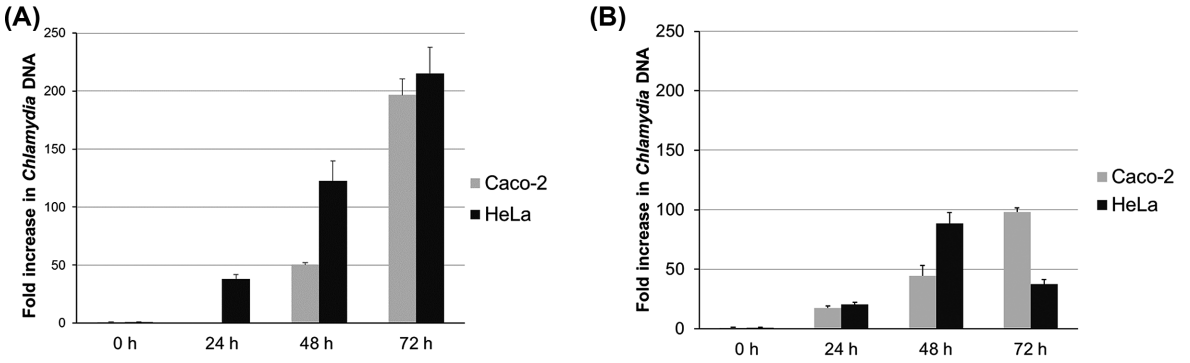

Figure 3. Analysis of *C. trachomatis* D growth based on the quantitation of chlamydial DNA by qPCR in *Chlamydia*-infected cells. Caco-2 and HeLa cells were infected in 96-well plates at an MOI of 5 in a medium with cycloheximide or without cycloheximide; direct detection of *Chlamydia* genes in the lysate of infected cells was done at 0, 24, 48 and 72 h post-infection. Increase in the quantity of chlamydial DNA was compared to the quantities detected at 0 h of infection. (**A**) Increase in the amount of *C. trachomatis* D *pyk* gene in the presence of cycloheximide, and (**B**) in the absence of cycloheximide. The mean of fold change in 3 parallel cultures and SD is shown. The data represent the results of one of three independent experiments.

Chlamydia genome accumulation in Caco-2 and conventional host cells

The quantitative features of *Chlamydia* replication in the intestinal epithelial cells in comparison with that in conventional host cells were investigated with a novel DNA quantitation method (Eszik *et al.* 2016). We followed the accumulation of *Chlamydia* genomes during a 3-day culture period in Caco-2 and in HeLa cells. The lysates of infected cells were used as templates, and the quantity of chlamydial genomes was estimated with qPCR at different time points after infection. Fold increase in the amount of *pyk* gene of *C. trachomatis* was calculated in comparison with the amount detected at 0 h of infection. *C. trachomatis* growth seemed unrestricted in Caco-2 cells, *Chlamydia* genomes propagated to similar amount by 72 h as in HeLa cells (Fig. 3A). As suggested by the microscopic findings, the kinetics of replication followed a slower course in Caco-2 cells. In cycloheximide-free conditions, the yield was lower in Caco-2 cells and in HeLa cells too (Fig. 3B). In HeLa cells the replication peaked at 48 h and declined thereafter; the latter was not seen in Caco-2 cells. In Caco-2 cells, the effect of cycloheximide did not cause any major change in the course of the replication opposite to that in HeLa cells.

Production of infective *Chlamydia* progeny in Caco-2 and conventional host cells

In order to see whether the production of infective chlamydiae paralleled DNA accumulation, the infected cells were collected together with their supernatant, and the recoverable viable *C. trachomatis* bacteria were quantitated by inoculation of the sonicated cells in their media onto McCoy cells. Infective chlamydiae were recoverable showing that a full replication cycle takes place in Caco-2 cell line. The growth of *C. trachomatis* was somewhat delayed in Caco-2 cells, but at 72 h post-infection, similar amount of *C. trachomatis* was cultured from Caco-2 cells to that from HeLa cells (Fig. 4).

Transcript patterns for selected *Chlamydia* genes during infection of Caco-2 and conventional host cells

As the kinetics of *C. trachomatis* replication exhibited difference in Caco-2 cells compared to that in HeLa cells, we investigated the expression of selected *Chlamydia* genes during a 3-day period. Intrinsic characteristics of the intestinal epithelial cells as

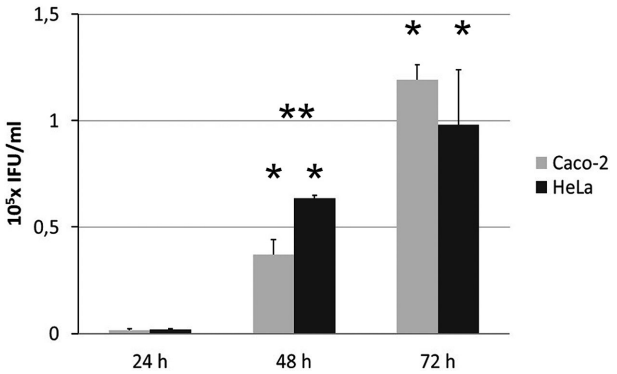

Figure 4. Kinetics of replication of *C. trachomatis* D in Caco-2 cells and in the conventional host cells as assayed by quantitation of recoverable infective bacteria. Lysates of *C. trachomatis*-infected (MOI 5) Caco-2 and HeLa cells in their supernatants were collected at different time points after infection, and they were inoculated onto McCoy cells grown on cover slips. After 48 h incubation, the inclusions were visualized by immunofluorescence staining. The mean of titers expressed as IFU/mL in 3 parallel cultures and SDs are shown. The single asterisk (*) shows statistically significant differences between IFU values in the same cell type at different time points; the double asterisk (**) indicates statistically significant difference between values measured in supernatants of different cell types: $P < 0.05$. The data represent the results of one of three independent experiments.

growth environment could be reflected in a change of gene expression pattern of chlamydiae. The relative gene expression levels normalized to 16S rRNA expression are shown in Fig 5. At 24 h post-infection, the earliest time point evaluated, the relative expression of the early cluster gene *euo* (Fig. 5A) was at much lower level in HeLa cells than in Caco-2 cells, and it increased at later time points, when the replication was already at lower rate. After 24 h, *euo* expression level moved to the opposite direction in Caco-2 cells in parallel with the continued replication.

The relative expression of *pyk*, *ompA*, *ftsK* and *omcB* (Fig. 5) genes of *C. trachomatis* D followed similar trends in both examined cell lines, but the relative expression persisted at higher levels in Caco-2 cells than in HeLa cells. After 24 h, the level of *pyk* gene expression decreased gradually over time at similar rates (Fig. 5B) in both examined cell lines. The highest level of *ompA* gene expression was observed at 24 h and persisted at high level for a longer time in Caco-2 than in HeLa cells (Fig. 5E). The highest level of *ftsK* gene expression was observed at 24 h after infection, at the time of frequent cytokinesis, and it remained at high level in Caco-2 cells at later time points too (Fig. 5D).

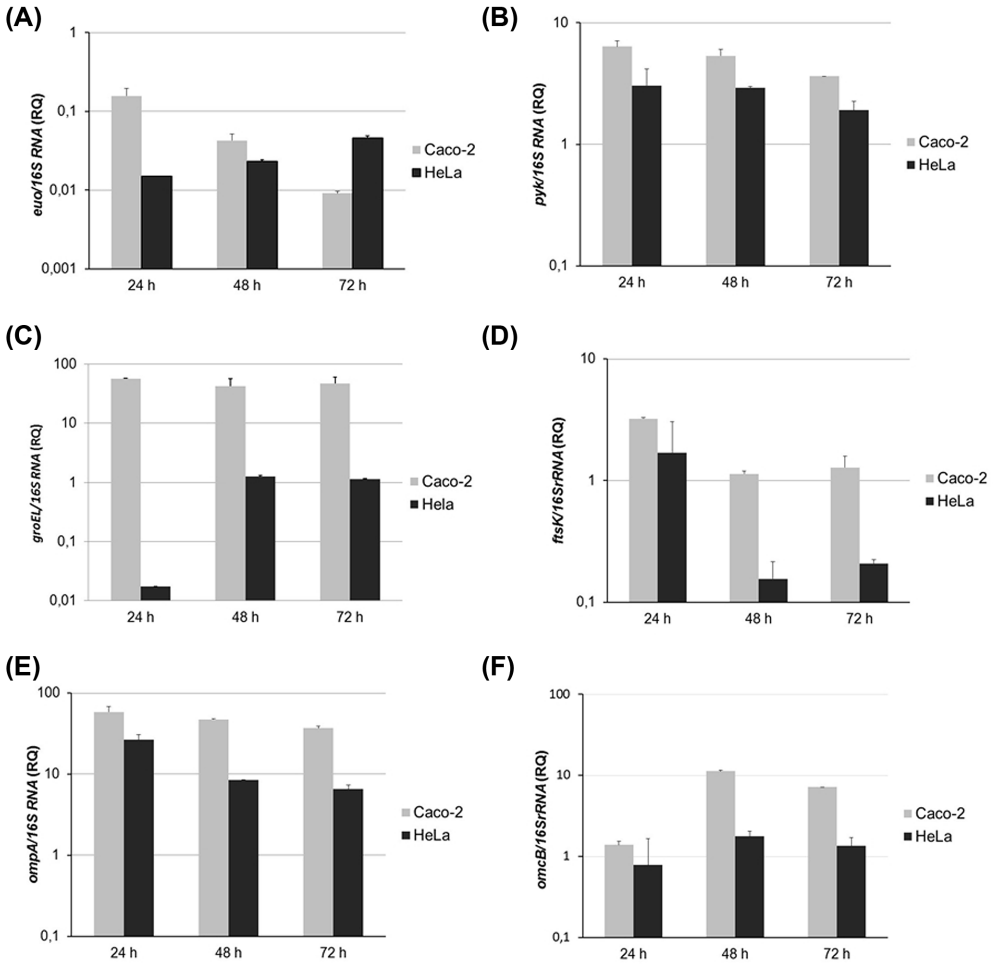

(G)

Gene	Caco-2/HeLa		
	24 h	48 h	72 h
euo	10,46	1,85	0,20
ftsK	1,90	7,32	6,16
groEL	3285,74	33,97	42,02
pyk	2,09	1,83	1,90
ompA	2,20	5,59	5,67
omcB	1,77	6,37	5,33

4000	10	2	0,1

Figure 5. The time course of relative expression of different *C. trachomatis* D genes in Caco-2 cells and in conventional permissive HeLa cells. cDNA was prepared from Caco-2 and HeLa cells at different time points (24, 48 and 72 h) after infection with *C. trachomatis* D at an MOI of 5 in 6-well plates in a medium without cycloheximide. Real time qRT-PCR for quantitation of relative expression of (**A**) *euo*, (**B**) *pyk*, (**C**) *groEL*, (**D**) *ftsK*, (**E**) *ompA* and (**F**) *omcB* genes was performed; the expression levels were normalized to *16S rRNA* gene expression. The fold change in relative expression levels is shown (RQ). The data represent the mean values and SD measured in three parallel samples of one of two independent experiments. (**G**) Calculated ratios of relative gene expression values detected in Caco-2 cells versus in HeLa cells are shown. A bar indicating the color scale for calculated differences is given: boxes with different shades of red through white color denote increased expression; green colored boxes denote decreased expression.

The expression of the late gene *omcB* peaked at 48 h post-infection with again a higher level in Caco-2 cells than in HeLa cells (Fig. 5F).

Constantly, high relative amount of *groEL* transcripts was observed in Caco-2 cells, including the earliest time point tested at 24 h (Fig. 5C). An increased relative high rate of expression of *groEL* gene occurred only from 48 h post-infection in HeLa cells. Further analysis and summary of the above data are shown in Fig. 5G on the ratios of gene expression values seen in Caco-2 cells versus that in HeLa cells. These data demonstrate the delayed and prolonged replication cycle in Caco-2 cells with higher *euo* expression at early time point (24 h) and decreased *euo*

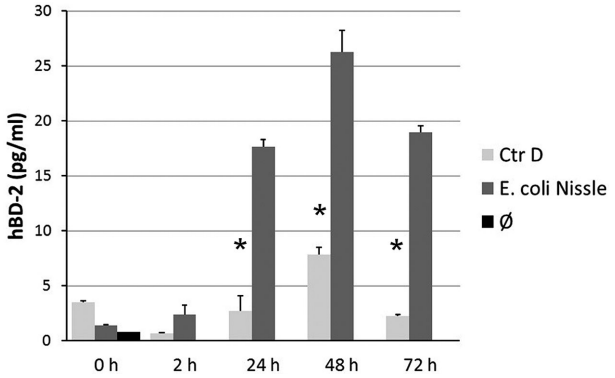

Figure 6. hBD-2 production by Caco-2 cells in response to *Chlamydia* infection. The supernatants of non-infected cells (ø) and the cells infected with *C. trachomatis* D (Ctr D) at an MOI of 5 or treated with heat-treated *E. coli* Nissle strain in 24-well plates were harvested at different time points post-infection. For the detection of hBD-2 production, the supernatants of the cells were tested by hBD-2 specific ELISA. The mean concentration values in three parallel cultures and SDs are shown. The asterisk (*) shows statistically significant differences between values measured in the supernatant of *Chlamydia*-infected cells and values measured in supernatants of *E. coli* Nissle-treated cells; $P < 0.05$.

expression at late time point (72 h), with higher cytokinesis related (*ftsK*) and membrane protein gene (*ompA, omcB*) expressions at later time points in Caco-2 cells. An outstanding *groEL* gene transcription, especially at 24 h post-infection in Caco-2 cells, is detectable.

HBD-2 inducing capability of *C. trachomatis* in Caco-2 cells

Since Caco-2 cells are intestinal mucosal epithelial cells, and this cell type has an important role as a physiological barrier for pathogens in the colon, and hBD-2 is induced by microbial molecules, it was investigated whether *C. trachomatis* was able to induce production of this antimicrobial peptide by Caco-2 cells. By hBD-2 ELISA, hBD-2 protein was detectable in high levels in the supernatant of Nissle-stimulated control Caco-2 cultures with a peak at 48 h post-treatment (Fig. 6). *C. trachomatis* D-infected cells showed similar time course of hBD-2 release, however at a significantly lower level than in the case of stimulation with *E. coli* Nissle.

DISCUSSION

In this study, we investigated the morphological and molecular features of *C. trachomatis* infection in Caco-2 human intestinal cells. We selected this cell line for our investigation because it shows the characteristics of enterocytes, and in recent publications, the hypothesis of chlamydial persistence in the GI tract and the infected GI tract behaving as a source of genital tract reinfection has been proposed (Bavoil *et al.* 2017). Furthermore, *C. trachomatis* has been implicated in GI tract pathologies. As hBD-2 is produced by epithelial cells in the GI tract in response to infection as part of the innate defense (Cobo and Chadee 2013), we tested the defensin inducing capability of *Chlamydia* in Caco-2 cells.

C. trachomatis D inclusions in Caco-2 cells visualized by immunofluorescence staining and TEM suggested similar but prolonged replication cycle of this *Chlamydia* strain compared to that in HeLa cells. The slower accumulation of chlamydiae was also detectable by finding lower amount of genomes and infective chlamydiae at 48 h post-infection in Caco-2 cells. However, by 72 h post-infection, the values had reflected similar level of chlamydial reproduction in the two cell lines. These results allow us to conclude that for this human genital *Chlamydia* strain, Caco-2 cells provide a growth-conducive environment. In case, the growth medium of the host cells is supplemented with cycloheximide, *Chlamydia* replication cycle occurs in optimal conditions, where the host cell protein synthesis has less influence on the bacterial growth. When cycloheximide was omitted from the medium, chlamydial genome accumulation reached a lower level and suffered early decline in HeLa cells, but this phenomenon was not as pronounced in Caco-2 cells. Gene expression analyses were done in the absence of cycloheximide, when the natural cellular environment would prevail.

It has been described that chlamydial developmental cycle is regulated at transcriptional level (Nicholson *et al.* 2003). The change in the transcription profile has been demonstrated in *in vitro* models, where different stimuli (IFN-γ, penicillin) induced a persistent phase of chlamydiae. Certain cell types proved to be non-permissive for normal *Chlamydia* growth, and the transcription pattern suggested a persistent form of infection in these cells (Gérard *et al.* 1998). Since the growth kinetics in Caco-2 cells was found different from that in the optimal *in vitro* host cell line, we aimed to examine the expression of *C. trachomatis* genes in Caco-2 cells and compared it to that in HeLa cells. The expression level of selected chlamydial genes representing early (*euo*), mid-cycle (*ompA, groEL, pyk*) and late stage (*omcB*) replication cycles, and cell division related *ftsK* gene were analyzed and was normalized to the expression level of *16S rRNA* gene. As the *eou* gene products were described as suppressors of the late genes (Rosario and Tan 2012; Rosario, Hanson and Tan 2014), decreased expression of this gene could explain the higher expression level of *omcB* gene encoding the membrane protein of EBs (Cobo and Chadee 2013) in Caco-2 cells, even at later time points during the infection. As EUO protein binding to *ftsK* promoter has been detected earlier (Rosario and Tan 2012), the persisting high level of the cytokinesis related *ftsK* gene might be associated with this decreased *euo* expression in Caco-2 cells. Transcripts from the *ftsK* gene required for cytokinesis were detectable at a relatively high level during the first day of *C. trachomatis* growth, when bacterial division occurs at the highest rate. It seems that cytokinesis dropped earlier in HeLa cells than in Caco-2 cells. The expression of the ATP synthesis-related *pyk* gene of *C. trachomatis* declined in HeLa cells after 48 h. It occurred synchronously with the decrease in the amount of the chlamydial chromosome detected in this cell line. In concordance, longer high level of *pyk* expression paralleled a more extended genome accumulation in Caco-2 cells. The tendency of the change in *ompA* gene expression level was similar in both cell lines. *pyk* and *ompA* genes are regarded as genes of the mid-cycle (Nicholson *et al.* 2003), when RBs accumulate and EBs start to be formed. The *groEL* gene of *C. trachomatis*, a heat shock protein 60 (GroEL-1) encoding gene was highly upregulated throughout the observation period in Caco-2 cells. A stress response related increase in the production of GroEL-1 has been described for *C. trachomatis* (Gérard *et al.* 2004). Our results suggest that replication of *C. trachomatis* in Caco-2 cells evoked a certain stress response by the bacteria.

It has been suggested that in the male and female reproductive tracts, small antibacterial molecules may contribute to a sustained inflammatory response (Redgrove and McLaughlin 2014), or they may control inflammatory and adaptive immune response (Hemshekhar, Anaparti and Mookherjee 2016). According to Niyonsaba *et al.* (Niyonsaba, Ogawa and Nagaoka 2004), hBD-2 can be regarded as a potent chemoattractant of

neutrophils. Increased hBD-2 expression could contribute to host defense by recruiting neutrophils. The role of hBDs in the attraction of immature dendritic cells and memory T cells to the site of microbial invasion (Yang *et al.* 1999) has been described. Expression of hBD has been reported in women with *C. trachomatis* positive cervicovaginal samples, albeit at a significantly lower level than in non-infected controls (Noda-Nicolau *et al.* 2017). In our experiments with Caco-2 cell line, *C. trachomatis* infection induced the production of hBD-2 at a moderate level compared to the effect of a strong inducer, the *E. coli* Nissle strain. In a murine model of *C. muridarum* infection, oral application of the bacterium resulted in long carriage and a lack of inflammatory response in the large intestine; however, the infection of the genital tract was cleared after a short period and following inflammation at the infection site (Igietseme, Portis and Perry 2001). The low level of hBD-2 production by the *Chlamydia*-infected Caco-2 cell line might be a sign of suppressed innate immune response, and potentially, a subsequently suppressed adaptive response as well.

In conclusion, Caco-2 cell line representing the epithelial cell lining in the large intestine seems to be a sufficiently permissive host cell for *C. trachomatis*, which primarily infects the genital tract, thus allowing these bacteria to survive at this body site. Together with the low hBD-2 inducing capacity, *C. trachomatis* might be able to replicate there without provoking an inflammatory response. These results seem to support the theory that the GI tract could serve as a site of extra genital survival of chlamydiae, and it could potentially serve as a source of reinfection in the genital tract, especially in women. Our data have relevance to the published data on high co-occurrence of urogenital *Chlamydia* infection with anorectal infection in women (van Liere *et al.* 2014). Our data are also in concordance with the previously published data that more infected men are detected among homosexuals when rectal samples were taken (Bax *et al.* 2011).

Conflicts of interest. None declared.

REFERENCES

Bastidas RJ, Elwell CA, Engel JN *et al.* Chlamydial intracellular survival strategies. *CSH Perspect Med* 2013;**3**:a010256.

Bavoil PM, Marques PX, Brotman R *et al.* Does active oral sex contribute to female infertility? *J Infect Dis* 8 2017;**216**:932–5. DOI: 10.1093/infdis/jix419.

Bax CJ, Quint KD, Peters RPH *et al.* Analyses of multiple-site and concurrent *Chlamydia trachomatis* serovar infections, and serovar tissue tropism for urogenital versus rectal specimens in male and female patients. *Sex Transm Infect* 2011;**87**:503–7.

Borges V, Ferreira R, Nunes A *et al.* Normalization strategies for real-time expression data in *Chlamydia trachomatis*. *J Microbiol Methods* 2010;**82**:256–64.

Burián K, Hegyesi H, Buzás E *et al.* Chlamydophila (*Chlamydia*) pneumoniae induces histidine decarboxylase production in the mouse lung. *Immunol Lett* 2003;**89**:229–36.

Datta B, Njau F, Thalmann J *et al.* Differential infection outcome of *Chlamydia trachomatis* in human blood monocytes and monocyte-derived dendritic cells. *BMC Microbiol* 2014;**14**:209.

Dlugosz A, Törnblom H, Mohammadian G *et al.* *Chlamydia trachomatis* antigens in enteroendocrine cells and macrophages of the small bowel in patients with severe irritable bowel syndrome. *BMC Gastroenterol* 2010;**10**:19.

Cobo ER, Chadee K. Antimicrobial human β-defensins in the colon and their role in infectious and non-infectious diseases. *Pathogens* 2013;**2**:177–92.

Eszik I, Lantos I, Önder K *et al.* High dynamic range detection of *Chlamydia trachomatis* growth by direct quantitative PCR of the infected cells. *J Microbiol Methods* 2016;**120**:15–22.

Gérard HC, Köhler L, Branigan PJ *et al.* Viability and gene expression in *Chlamydia trachomatis* during persistent infection of cultured human monocytes. *Med Microbiol Immunol (Berl)* 1998;**187**:115–20.

Gérard HC, Whittum-Hudson JA, Schumacher HR *et al.* Differential expression of three *Chlamydia trachomatis* hsp60-encoding genes in active vs. persistent infections. *Microb Pathogenesis* 2004;**36**:35–9.

Hemshekhar M, Anaparti V, Mookherjee N. Functions of cationic host defense peptides in immunity. *Pharmaceuticals* 2016;**9**:E40. DOI: 10.3390/ph9030040.

Igietseme JU, Portis JL, Perry LL. Inflammation and clearance of *Chlamydia trachomatis* in enteric and nonenteric mucosae. *Infect Immun* 2001;**69**:1832–40.

Kim JM. Antimicrobial proteins in intestine and inflammatory bowel diseases. *Intest Res* 2014;**12**:20–33.

Kintner J, Lajoie D, Hall J *et al.* Commonly prescribed Î²-lactam antibiotics induce *C. trachomatis* persistence/stress in culture at physiologically relevant concentrations. *Front Cell Infect Mi* 2014;**4**:44.

Kokab A, Jennings R, Eley A *et al.* Analysis of modulated gene expression in a model of Interferon-gamma-induced persistence of *Chlamydia trachomatis* in HEp-2 cells. *Microb Pathogenesis* 2010;**49**:217–25.

van Liere GAFS, Hoebe CJPA, Wolffs PFG *et al.* High co-occurrence of anorectal chlamydia with urogenital chlamydia in women visiting an STI clinic revealed by routine universal testing in an observational study; a recommendation towards a better anorectal chlamydia control in women. *BMC Infect Dis* 2014;**14**:274.

Mäurer AP, Mehlitz A, Mollenkopf HJ *et al.* Gene expression profiles of *Chlamydophila pneumoniae* during the developmental cycle and iron depletion mediated persistence. *PLoS Pathog* 2007;**3**:e83.

Mpiga P, Ravaoarinoro M. *Chlamydia trachomatis* persistence: an update. *Microbiol Res* 2006;**161**:9–19.

Nicholson TL, Olinger L, Chong K *et al.* Global stage-specific gene regulation during the developmental cycle of *Chlamydia trachomatis*. *J Bacteriol* 2003;**185**:3179–89.

Niyonsaba F, Ogawa H, Nagaoka I. Human beta-defensin-2 functions as a chemotactic agent for tumour necrosis factor-alpha-treated human neutrophils. *Immunology* 2004;**111**:273–81.

Noda-Nicolau NM, Bastos LB, Bolpetti AN *et al.* Cervicovaginal levels of human β-Defensin 1, 2, 3, and 4 of Reproductive-Aged Women With Chlamydia trachomatis Infection. *J Low Genit Tract Di* 2017;**21**:189–92.

Phillips-Campbell R, Kintner J, Schoborg RV. Induction of the *Chlamydia muridarum* stress/persistence response increases azithromycin treatment failure in a murine model of infection. *Antimicrob Agents Ch* 2014;**58**:1782–4.

Rank RG, Yeruva L. Hidden in plain sight: chlamydial gastrointestinal infection and its relevance to persistence in human genital infection. *Infect Immun* 2014;**82**:1362–71.

Redgrove KA, McLaughlin EA. The role of the immune response in *Chlamydia trachomatis* infection of the male genital tract: a double-edged sword. *Front Immunol* 2014;**5**:534.

Rosario CJ, Hanson BR, Tan M. The transcriptional repressor EUO regulates both subsets of *Chlamydia* late genes. *Mol Microbiol* 2014;**94**:888–97.

Rosario CJ, Tan M. The early gene product EUO is a transcriptional repressor that selectively regulates promot-

ers of *Chlamydia* late genes. *Mol Microbiol* 2012;**84**:1097–107.

Sabet SF, Simmons J, Caldwell HD. Enhancement of *Chlamydia trachomatis* infectious progeny by cultivation of HeLa 229 cells treated with DEAE-dextran and cycloheximide. *J Clin Microbiol* 1984;**20**:217–22.

Schiller I, Schifferli A, Gysling P *et al*. Growth characteristics of porcine chlamydial strains in different cell culture systems and comparison with ovine and avian chlamydial strains. *Vet J* 2004;**168**:74–80.

Schoborg RV. *Chlamydia* persistence – a tool to dissect *Chlamydia*–host interactions. *Microbes Infect* 2011;**13**:649–62.

Wyrick PB. *Chlamydia trachomatis* persistence in vitro: an overview. *J Infect Dis* 2010;**201**:88–95.

Yang D, Chertov O, Bykovskaia SN *et al*. β-defensins: linking innate and adaptive immunity through dendritic and T Cell CCR6. *Science* 1999;**286**:525–8.

Yeruva L, Spencer N, Bowlin AK *et al*. Chlamydial infection of the gastrointestinal tract: a reservoir for persistent infection. *Pathog Dis* 2013;**68**:88–95.